
SIMULATIONS USING FINITE ELEMENT ANALYSIS

6.1 INTRODUCTION

Chapter 5 introduced the main features that govern the bridge behaviour when it is traversed by a truck. However, only a few degrees of freedom were considered and the influence of three-dimensional effects was neglected. In order to cover for more realistic models, this chapter describes the interaction of complex truck and bridge structures through a finite element technique. The structures are subdivided into a finite number of simple elements (such as plates, beams, bars, springs, masses, etc.), and the complex differential equations are then solved for the simple elements. Assemblage of the elements into a global matrix transforms the problem from a differential equations formulation over a continuum to a linear algebra problem.

Vehicles and bridges have been modelled with the general-purpose finite element analysis package MSC/NASTRAN for Windows¹⁸ (1999), which provides the capability for performing statics, normal modes and transient dynamic response (Cifuentes 1989a). NASTRAN (**N**ASA **S**tructural **A**nalysis) initiated the implementation of the finite element method on computers under a project by the National Aeronautics and Space Administration (NASA) in the 1960's (Schaeffer 1977).

The author has developed a C++ program that derives the interaction forces for any arbitrary planar or spatial bridge and vehicle finite element models. This code incorporates the road surface profile and it is implemented using a set of auxiliary functions to enforce the compatibility conditions at the bridge/vehicle interface. The speed of the vehicles, their initial position, path on the bridge and road irregularities can be easily modified in the program input. Simultaneous traffic events running in the same or different lanes, in the same or opposite directions and singularities such as a bump at any location can also be specified. Different bridge/truck models and results of simulations are introduced at the end of this chapter. This data will be used for testing B-WIM algorithms in Chapter 9.

6.2 TECHNIQUE FOR DETERMINATION OF BRIDGE-VEHICLE DYNAMIC INTERACTION

The load imposed by a truck crossing a bridge is an enforced motion transient problem. MSC/NASTRAN has the ability to perform enforced motion analysis by placing extremely large masses or inertias to obtain the desired motion at selected locations (MSC/NASTRAN 1997d). Extremely large forces are applied to the large masses to cause the desired motion histories. However, this method has traditionally been prone to numerical error if the large masses are too large or too small (Flanigan 1994) and it is inadequate for the bridge-vehicle interaction problem. Accordingly, the author uses an alternative approach based on a Lagrange technique that eliminates the need for large masses (Cifuentes 1989b, Baumgärtner 1999). The Lagrange Multiplier formulation allows for the representation of the compatibility condition at the bridge/vehicle interface through a set of auxiliary functions. Accordingly, software has been developed to generate an entry into the assembled stiffness matrix of the vehicle-bridge system. This entry allows for the definition of the forces acting on the bridge due to the moving wheels. A compatibility condition between the vertical displacement of the wheel and the bridge at the contact point is also established.

6.2.1 Equations of Motion and Compatibility

Cifuentes (1989b) gives an introduction to the problem of solving for the motion of a single circular mass moving at constant speed on a one-dimensional bridge model. This section extends the solution to allow for the presence of multiple masses travelling in given paths at different speeds. If the bridge structure along a mass path is divided into $(N-1)$ finite elements, coordinates x_1, x_2, \dots, x_N are adopted for the N nodes. The variables defining the behaviour of the bridge are:

$z(x, t)$: vertical deflection of the bridge in position x at time t ,

$z_i = z_i(t)$: deflection of node i at time t ,

$\mathbf{q} = \mathbf{q}(t)$: rotation of node i at time t ,

$\ddot{z}_i = \ddot{z}_i(t)$: acceleration of vertical displacement in node i at time t ,

$\ddot{\mathbf{q}}_i = \ddot{\mathbf{q}}_i(t)$: acceleration of rotation in node i at time t .

The one-dimensional problem for a single mass is represented in Figure 6.1.

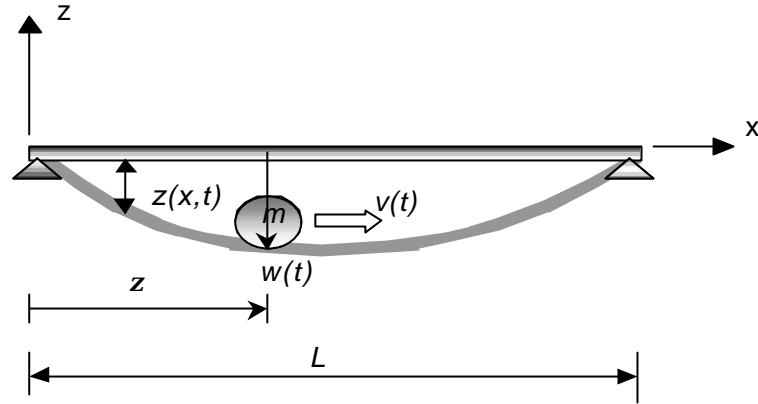


Figure 6.1 – Structure traversed by a mass m with velocity $v(t)$

The variables defining the behaviour of a series of moving masses j (one per wheel or one per axle in a 3D or 2D problem respectively) are:

$v_j = v_j(t)$: time-dependent velocity of the vehicle (defined by the user). If there are different vehicles, v_j might be different for each vehicle.

m_j : mass of wheel j (defined by the user),

$w_j = w_j(t) = z(\mathbf{z}_j, t)$: vertical displacement of wheel j measured with respect to the horizontal axis (the bridge geometry is assumed to be in a horizontal plane before deformation),

$R_j = R_j(t)$: Interaction force at contact point of wheel j ,

$\mathbf{z}_j = \mathbf{z}_j(t)$: Distance x travelled on the bridge by moving wheel j at time t .

The variable \mathbf{z}_j denoting position of mass j on the bridge at time t can be defined as a function of the velocity input $v_j(t)$ as:

$$\mathbf{z}_j = \int_{t_j}^t v_j(t) dt = \sum_{t=t_j}^t v_j(t) \Delta t \quad 0 \leq \mathbf{z}_j \leq L \quad (6.1)$$

where time t_j is the instant at which mass j enters the bridge and L is the bridge length.

The equation of motion of the bridge finite element model can be written as:

$$\begin{bmatrix} m_{11} & m_{12} & \cdot & \cdot & \cdot & \cdot \\ m_{21} & m_{22} & \cdot & \cdot & \cdot & \cdot \\ \cdot & \cdot & \cdot & \cdot & \cdot & \cdot \\ \cdot & \cdot & \cdot & m_{2N-1,2N-1} & m_{2N-1,2N} & \cdot \\ \cdot & \cdot & \cdot & m_{2N,2N-1} & m_{2N,2N} & \cdot \end{bmatrix} \begin{Bmatrix} \ddot{z}_1 \\ \ddot{\mathbf{q}}_1 \\ \cdot \\ \ddot{z}_N \\ \ddot{\mathbf{q}}_N \end{Bmatrix} + \begin{bmatrix} k_{11} & k_{12} & \cdot & \cdot & \cdot & \cdot \\ k_{21} & k_{22} & \cdot & \cdot & \cdot & \cdot \\ \cdot & \cdot & \cdot & \cdot & \cdot & \cdot \\ \cdot & \cdot & \cdot & k_{2N-1,2N-1} & k_{2N-1,2N} & \cdot \\ \cdot & \cdot & \cdot & k_{2N,2N-1} & k_{2N,2N} & \cdot \end{bmatrix} \begin{Bmatrix} z_1 \\ \mathbf{q}_1 \\ \cdot \\ z_N \\ \mathbf{q}_N \end{Bmatrix} = \begin{Bmatrix} f_1 \\ M_1 \\ \cdot \\ f_N \\ M_N \end{Bmatrix} \quad (6.2)$$

where $[m]$ is the mass matrix of the finite element model and $[k]$ is the stiffness matrix, representing the dynamic characteristics of the bridge model. $\{z\}$ is a vector containing the displacements of the nodes and $\{\ddot{z}\}$ their acceleration at time t . Vector $\{f\}$ represents the force $f_i(t)$ and moment $M_i(t)$ acting on node i at a certain time due to the moving loads.

A compatibility condition between the vertical displacement $w_j(t)$ of each mass j and the bridge at the contact point must be established at any time t . For this purpose a set of auxiliary functions $A_{ij}(t)$ and $B_{ij}(t)$ are defined for every mass j , and the compatibility condition at the contact point of mass j is formulated as (Cifuentes 1989b):

$$w_j(t) = z(\mathbf{z}_p, t) = \sum_{i=1}^N A_{ij}(t) z_i(t) + \sum_{i=1}^N B_{ij}(t) \mathbf{q}_i(t) \quad ; \quad j=1,2, \dots, p \quad (6.3)$$

where $z_i(t)$ and $\mathbf{q}(t)$ are the displacement and rotation at each node i , N the total number of bridge nodes, p total number of moving loads, and $A_{ij}(t)$ and $B_{ij}(t)$ auxiliary functions for load j . $A_{ij}(t)$ and $B_{ij}(t)$ can adopt different values in each node i at each instant t . Equations 6.4 and 6.5 define these functions:

$$A_{ij}(t) = \begin{cases} 1 - 3 \left[\frac{(t - t_{1,j} - t_{i,j})}{(t_{i+1,j} - t_{i,j})} \right]^2 + 2 \left[\frac{(t - t_{1,j} - t_{i,j})}{(t_{i+1,j} - t_{i,j})} \right]^3 & \text{for } t_{i,j} \leq t \leq t_{i+1,j} \\ 1 - 3 \left[\frac{(t_{i,j} - (t - t_{1,j}))}{(t_{i,j} - t_{i-1,j})} \right]^2 + 2 \left[\frac{(t_{i,j} - (t - t_{1,j}))}{(t_{i,j} - t_{i-1,j})} \right]^3 & \text{for } t_{i-1,j} \leq t \leq t_{i,j} \\ 0 & \text{otherwise} \end{cases} \quad i=1,2,\dots,N; \quad j=1,2,\dots,p \quad (6.4)$$

$$B_{ij}(t) = \begin{cases} \left[-\frac{((t-t_{1,j})-t_{i,j})}{2(t_{i+1,j}-t_{i,j})} + \frac{((t-t_{1,j})-t_{i,j})^2}{2(t_{i+1,j}-t_{i,j})^2} \right] [x_{i+1}-x_i] & \text{for } t_{i,j} \leq t \leq t_{i+1,j} \\ \left[-\frac{(t_{i,j}-(t-t_{1,j}))}{2(t_{i,j}-t_{i-1,j})} + \frac{(t_{i,j}-(t-t_{1,j}))^2}{2(t_{i,j}-t_{i-1,j})^2} \right] [x_i-x_{i-1}] & \text{for } t_{i-1,j} \leq t \leq t_{i,j} \\ 0 & \text{otherwise} \end{cases} \quad i=1,2,\dots,N; \quad j=1,2,\dots,p \quad (6.5)$$

where t_{ij} is the time that moving mass j takes between the origin and the bridge node i . t_{1j} is the travelling time of mass j from the original position to the first node at the bridge.

The shape of these auxiliary functions is shown in Figure 6.2. They have zero value out of the interval between adjacent nodes.

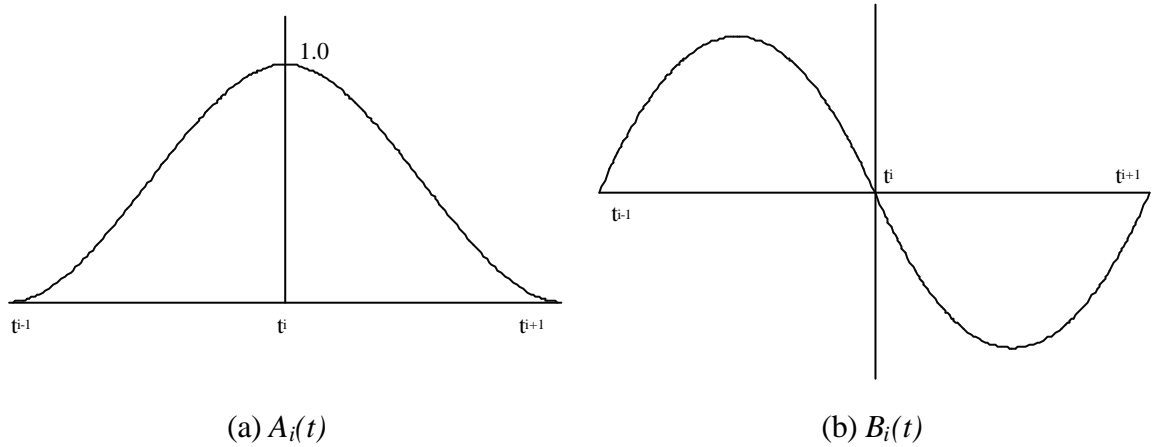


Figure 6.2 – Auxiliary Functions

The temporal variable t_{ij} can be determined numerically from the knowledge of velocity $v_j(t)$ and the geometry of the finite element model such that:

$$\sum_{t=0}^{t_{ij}} v_j(t) \Delta t = x_i + x_j + x_0 \quad (6.6)$$

where $v_j(t)$ is the velocity function (same function for all masses j in a vehicle), x_i the coordinate of the node number i related to the bridge start, x_j the longitudinal spacing between the contact point corresponding to the first mass and the contact point of the j^{th}

mass and x_0 is the length of the bridge approach. So, $A_{ij}(t)$ and $B_{ij}(t)$ are completely defined once $v_j(t)$, approach length, axle spacings and the coordinates of the bridge nodes are known. Each axle takes a different time to reach the same node and each wheel of the same axle follows a different path on the bridge. Thus, auxiliary functions change at each mass j and time t .

According to Cifuentes (1989b), the interaction force $R_j(t)$ between a moving circular mass m_j and the bridge structure contains the following terms:

- Inertial force, due to vertical motion of the mass $= -m_j \left[\frac{\partial^2 z(x,t)}{\partial t^2} \right]_{(x_j,t)}$,
- Coriolis force, due to relative motion between the bridge and the load $= -2m_j v_j \left[\frac{\partial^2 z(x,t)}{\partial x \partial t} \right]_{(x_j,t)}$,
- Centripetal force, due to circular motion following the deformed shape of the bridge, acting towards the centre of the mass $= -m_j v_j^2 \left[\frac{\partial^2 z(x,t)}{\partial x^2} \right]_{(x_j,t)}$,
- Weight, due to gravity force $= -m_j g$.

Hence the interaction force can be defined as:

$$R_j = -m_j \{ \ddot{z} + 2v_j \dot{z}' + v_j^2 z'' + g \} \mathbf{d}(x - \mathbf{x}_j) \quad (6.7)$$

where $\ddot{z} = \left[\frac{\partial^2 z(x,t)}{\partial t^2} \right]_{(x_j,t)}$, $\dot{z}' = \left[\frac{\partial^2 z(x,t)}{\partial x \partial t} \right]_{(x_j,t)}$, $z'' = \left[\frac{\partial^2 z(x,t)}{\partial x^2} \right]_{(x_j,t)}$ and \mathbf{d} is the Dirac

function. If $x \neq \mathbf{z}_j$, $R_j = 0$, where \mathbf{z}_j is the distance travelled by the mass j as defined in Equation 6.1.

By combination of Equations 6.3 and 6.7, this interaction force R_j between the bridge and the j^{th} mass can also be expressed as:

$$R_j = -m_j \ddot{w}_j - m_j g - m_j [2v_j \dot{z}' + v_j^2 z''] \quad (6.8)$$

And using the Lagrange multiplier functions:

$$R_j = -m_j \ddot{w}_j - m_j g - m_j \sum_i A_i [2v_{ij} \dot{z}'_i + v_{ij}^2 z''_i] \quad (6.9)$$

where $v_{ij} = v_j(t_i)$, that is, velocity of mass m_j when it reaches node i .

By re-ordering terms:

$$m_j \ddot{w}_j + R_j = -m_j g - m_j \sum_i A_i [2v_{ij} \dot{z}'_i + v_{ij}^2 z''_i] \quad (6.10)$$

The roughness of the pavement surface $r(x)$ can be imported into Equation (6.10) by taking into account that vertical displacement of the mass m_j will be equal to the vertical deformation of the beam minus the depth of the irregularities at the same location. This gives:

$$m_j \ddot{w} + R_j = -m_j g - m_j \sum_i A_i [2v_{ij} \dot{z}'_i + v_{ij}^2 z''_i + v_{ij}^2 r_i''] \quad (6.11)$$

An initial deflected shape can be introduced in the same way. Therefore, the force $f_{ij}(t)$ and the moment $M_{ij}(t)$ due to a mass j , acting on bridge node i at time t can be expressed using the auxiliary functions as (Cifuentes 1989b):

$$f_{ij}(t) = A_{ij}(t) R_j \quad (6.12)$$

and

$$M_{ij}(t) = B_{ij}(t) R_j \quad (6.13)$$

Equation 6.14 defines the total force $f_i(t)$ and moment $M_i(t)$ acting on a bridge node i at time t due to p different masses:

$$\begin{Bmatrix} f_1 \\ M_1 \\ f_2 \\ M_2 \\ \vdots \\ f_N \\ M_N \end{Bmatrix} = \begin{Bmatrix} A_{11} \\ B_{11} \\ A_{21} \\ B_{21} \\ \vdots \\ A_{N1} \\ B_{N1} \end{Bmatrix} R_1 + \dots + \begin{Bmatrix} A_{1p} \\ B_{1p} \\ A_{2p} \\ B_{2p} \\ \vdots \\ A_{Np} \\ B_{Np} \end{Bmatrix} R_p \quad (6.14)$$

Finally, the equations of motion of the complete moving load plus finite element model are given by:

$$\begin{bmatrix} m_{11} \frac{\partial^2}{\partial t} + k_{11} & m_{12} \frac{\partial^2}{\partial t} + k_{12} & \dots & \dots & 0 & 0 & 0 & \dots & 0 & 0 \\ m_{21} \frac{\partial^2}{\partial t} + k_{21} & m_{22} \frac{\partial^2}{\partial t} + k_{22} & \dots & \dots & 0 & 0 & 0 & \dots & 0 & 0 \\ \dots & \dots & \dots & \dots & \dots & \dots & \dots & \dots & \dots & \dots \\ \dots & \dots & \dots & m_{2N-1,2N-1} \frac{\partial^2}{\partial t} + k_{2N-1,2N-1} & m_{2N-1,2N} \frac{\partial^2}{\partial t} + k_{2N-1,2N} & 0 & 0 & \dots & 0 & 0 \\ \dots & \dots & \dots & m_{2N,2N-1} \frac{\partial^2}{\partial t} + k_{2N,2N-1} & m_{2N,2N} \frac{\partial^2}{\partial t} + k_{2N,2N} & 0 & 0 & \dots & 0 & 0 \\ 0 & 0 & \dots & 0 & 0 & m_1 \frac{\partial^2}{\partial t} & 1 & \dots & 0 & 0 \\ 0 & 0 & \dots & 0 & 0 & 1 & 0 & \dots & 0 & 0 \\ \dots & \dots & \dots & \dots & \dots & \dots & \dots & \dots & \dots & \dots \\ 0 & 0 & \dots & 0 & 0 & 0 & 0 & \dots & m_p \frac{\partial^2}{\partial t} & 1 \\ 0 & 0 & \dots & 0 & 0 & 0 & 0 & \dots & 1 & 0 \end{bmatrix} \begin{Bmatrix} z_1 \\ \mathbf{q} \\ z_N \\ \mathbf{q}_N \\ w_1 \\ R_1 \\ \dots \\ w_p \\ R_p \end{Bmatrix} = \begin{Bmatrix} \sum_{j=1}^r A_{1j} R_j \\ \sum_{j=1}^r B_{1j} R_j \\ \dots \\ \sum_{j=1}^r A_{Nj} R_j \\ \sum_{j=1}^r B_{Nj} R_j \\ -m_l g + c_1 \\ \sum_{i=1}^N [A_{i1} z_i + B_{i1} \mathbf{q}] \\ \dots \\ -m_p g + c_p \\ \sum_{i=1}^N [A_{ip} z_i + B_{ip} \mathbf{q}] \end{Bmatrix} \quad (6.15)$$

where the last $(2p)$ rows represent the equations of motion of each moving mass and the compatibility condition between deflections of the moving masses and the bridge. In these rows of the global load vector, the parameter c_j is given by:

$$c_j = -\sum_{i=1}^N \frac{2v_{ij} m_j}{x_i - x_{i-1}} \dot{z}_{ij} A_{ij} + \sum_{i=1}^N \frac{2v_{ij} m_j}{x_i - x_{i-1}} \dot{z}_{i-1j} A_{ij} + \sum_{i=1}^N \frac{v_{ij}^2 m_j}{x_i - x_{i-1}} \mathbf{q}_{ij} A_{ij} + \sum_{i=1}^N \frac{v_{ij}^2 m_j}{x_i - x_{i-1}} \mathbf{q}_{i-1j} A_{ij} \quad j=1, \dots, p \quad (6.16)$$

The following finite differences approximations might be necessary to calculate c_j :

$$\dot{z}_i' = \frac{\dot{z}_i - \dot{z}_{i-1}}{x_i - x_{i-1}} \quad (6.17)$$

$$z_i'' = \frac{-\mathbf{q}_i + \mathbf{q}_{i-1}}{x_i - x_{i-1}} \quad (6.18)$$

where $z_i' = -\mathbf{q}_i$.

When the simulation of a truck travelling over a bridge is implemented in the following section, this term c is ignored. Centripetal and Coriolis forces are not taken into account as most of the vehicle mass (except wheel mass) is not under circular motion and the vehicle speeds are relatively small.

6.2.2 Derivation of NASTRAN Input Code

The program generates an entry into the assembled stiffness matrix of the vehicle-bridge system as shown in Equation 6.15. The interaction forces F_j at the contact point of each wheel j on the bridge are defined as in Equation 6.14. The global stiffness matrix and the forcing vector is adapted to NASTRAN code in this section. In order to obtain the desired results, two sections must be manipulated in NASTRAN: The Case Control and the Bulk Data Sections.

1) The Case Control Section has several basic functions:

- Selects loads and constraints.
- Requests printing, plotting and/or typing of input and output data.
- Defines the subcase structure for the analysis.

2) The Bulk Data section contains entries that specify model geometry, element connectivity, element and material properties, constraints (boundary conditions) and loads. Some entries, such as loads and constraints, are selected by an appropriate Case Control command. Entries are prepared in either fixed or free field format.

A description of the code implementation is given in the following paragraphs. An example of these entries can be found in Appendix F. The whole process involved in the simulation of a truck over a bridge when using NASTRAN will be explained in Section 6.3.

Bulk Data Section

NASTRAN capability to define scalar degrees of freedom is used to define 2 scalar points, one to represent the displacement of the moving mass, w , and another to represent the interaction force F between the bridge and the mass. These scalar points are defined with the instruction SPOINT. The *bulk.dat* file to include in the NASTRAN analysis has a format of 10 fields of 8 characters each (small field format). Details about the format can be found in MSC/NASTRAN V70.5 Quick Reference Guide (1998).

In the case of two moving masses, the data format is illustrated in Figure 6.3.

SPOINT	400000								
SPOINT	401000								
SPOINT	500000								
SPOINT	501000								

Figure 6.3 – Data format for two moving masses

where the scalar points 500000 and 501000 represent the displacements w_1 and w_2 , and 400000 and 401000 are the interaction forces, F_1 and F_2 , for each moving load.

NASTRAN capability to input entries to the assembled stiffness matrix of the system is used to add 2 rows and columns per mass corresponding to (w, F) and (F, w) . These lines are added with the instruction DMIG. DMIG defines direct input matrices related to grid points. The matrix is defined by a single header entry and one or more column entries. Only one header entry is required. A column entry is required for each column with nonzero elements. The header and columns of this instruction have the format illustrated in Figure 6.4. The parameters are identified in Table 6.1.

DMIG	Name	“0”	IFO	TIN	TOUT	Polar		NCOL	
DMIG	Name	GJ	CJ		G1	C1	A1	B1	
	G2	C2	A1	B2	-etc.-				

Figure 6.4 – Header and columns for DMIG entry

Table 6.1 – Parameters used for DMIG entry (see Figure 6.4)

Field	Contents
Name	Name of the matrix
IFO	Form of the matrix input. IFO = 6 (symmetric) must be specified for matrices selected by the K2GG Case Control command.
TIN	Type of matrix being input (Integer): 1 = Real, single precision (One field is used per element), 2 = Real, double precision (One field is used per element), ...
TOUT	Type of matrix that will be created (Integer): 0 = Set by precision system cell (Default), 1 = Real, single precision, 2 = Real, double precision, ...
Polar	Input format of Ai, Bi. (Integer = blank or 0 indicates real, imaginary format; Integer >0 indicates amplitude, phase format.)
NCOL	Number of columns in a rectangular matrix. Used only for IFO=9. (Integer > 0)
GJ	Grid point identification number for column index. (Integer > 0)
CJ	Component number for grid point GJ (0<Integer<=6).
Gi	Grid point identification number for row index. (Integer > 0)
Ci	Component number for Gi for a grid point. (0<CJ<=6)
Ai, Bi	Real and Imaginary parts of a matrix element. If the matrix is real (TIN = 1 or 2), then Bi must be blank. (Real)

Matrices defined with this entry may be used in dynamics by selection in the Case Control with $K2GG = name$. This matrix is added to the structural matrix before constraints are applied. Each non-null column is started with a GJ, CJ pair. The entries for each row of that column follows. Only nonzero terms need be entered.

A matrix called *STIF* is defined in the line illustrated in Figure 6.5.

DMIG	STIF	0	6	1	1				
------	------	---	---	---	---	--	--	--	--

Figure 6.5 – Definition of STIF

In the case of two moving masses, the additional values are illustrated in Figure 6.6:

DMIG	STIF	400000			400000		0		
DMIG	STIF	401000			401000		0		
DMIG	STIF	500000			500000		1		
DMIG	STIF	501000			501000		1		

(a) Main diagonal values

DMIG	STIF	300000	3		400000		1		
DMIG	STIF	301000	3		401000		1		

(b) Off-diagonal values

Figure 6.6 – Adding of elements to the stiffness matrix

Another 2 sets of scalar points per moving load are used to define the auxiliary functions. The first moving load will consist of scalar points 100001 , 100002 , $100000+N$ to represent auxiliary functions $A_{i1}(t)$, and a set 200001 , 200002 , ..., $200000+N$ to represent auxiliary functions $B_{i1}(t)$. In the case of a second moving load, 101001 , 101002 , $101000+N$ represent $A_{i2}(t)$ and 200001 , 200002 , ..., $200000+N$ represent auxiliary functions $B_{i2}(t)$. Thus, if there are 4 nodes in each load path ($N=4$), the entry will be as illustrated in Figure 6.7(a). Unit stiffness is associated to each of these points (see Figure 6.7(b)).

SPOINT	100001	THRU	100004						
SPOINT	101001	THRU	101004						
SPOINT	200001	THRU	200004						
SPOINT	201001	THRU	201004						

(a) Specification of scalar points representing auxiliary functions

DMIG	STIF	100001			100001		1		
=	=	*1	=	=	*1	=	=		
2									
DMIG	STIF	101001			101001		1		
=	=	*1	=	=	*1	=	=		
2									
DMIG	STIF	200001			200001		1		
=	=	*1	=	=	*1	=	=		
2									
DMIG	STIF	201001			201001		1		
=	=	*1	=	=	*1	=	=		
2									

(b) Unit stiffness for each point

Figure 6.7 – Entry for four nodes in each load path

Then, auxiliary functions $A_{i1}(t)$ are applied to scalar points $100000+i$ ($i=1,2,...N$) and auxiliary functions $B_{i1}(t)$ to scalar points $200000+i$ ($i=1,2,...N$). $A_{i1}(t)$ and $B_{i1}(t)$ are

completely defined from the knowledge of $v_j(t)$ and the coordinates of the bridge nodes. The same applies to the scalar points and auxiliary functions corresponding to other moving masses.

The auxiliary functions and the excitation forces to be applied to the structure are established with the instructions DAREA and TLOAD2. The format of these 2 instructions is defined in Figure 6.8.

DAREA	SID	P1	C1	A1	P2	C2	A2		
-------	-----	----	----	----	----	----	----	--	--

Figure 6.8 - Columns for DAREA entry

Table 6.2 – Parameters used for DAREA entry (see Figure 6.8)

Field	Contents
SID	Identification number (Integer > 0)
Pi	Grid point identification number. (Integer > 0)
Ci	Component number (Integer 1 through 6 for grid point; 0 or blank for scalar point)
Ai	Scale factor. (Real)

DAREA define scale factors for dynamic loads and used in conjunction with TLOAD entries (see Figure 6.9).

TLOAD2	SID	DAREA	DELAY	TYPE	T1	T2	F	P	
	C	B							

Figure 6.9 - Columns for TLOAD2 entry

TLOAD2 represents a transient dynamic load $P(t)$ such that:

$$\{P(t)\} = \begin{cases} 0 & \text{for } t < (T1 + \tau) \text{ or } t > (T2 + \tau) \\ A\tilde{\tau}^B e^{C\tau} \cos(2\pi F\tilde{\tau} + P) & \text{for } (T1 + \tau) \leq t \leq (T2 + \tau) \end{cases} \quad (6.19)$$

where $\tilde{\tau} = t - T1 - \tau$.

Table 6.3 - Parameters used for TLOAD2 entry (see Figure 6.9)

Field	Contents
SID	Set identification number. (Integer >0)
DAREA	Identification number of DAREA entry set that defines A. (Integer > 0)
DELAY	Identification number of DELAY entry set that defines τ (Integer ≥ 0 or blank)
TYPE	Defines the nature of the dynamic excitation. (Integer 0 (Force or Moment), 1, 2, 3)
T1	Time constant. (Real ≥ 0.0)
T2	Time constant. (Real; T2>T1)
F	Frequency in cycles per unit time. (Real ≥ 0.0 ; Default=0.0)
P	Phase angle in degrees. (Real; Default=0.0)
C	Exponential coefficient. (Real; Default=0.0)
B	Growth coefficient. (Real; Default=0.0)

The implementation of auxiliary functions $A_i(t)$ is shown in the following example. If each node is spaced 0.5 m from the following one, and the speed of the moving mass is constant and equal to 20 m/s, times t_i to reach each node i will be given as shown in Table 6.4.

Table 6.4 – Times t_i to reach each node

Node ID (identification number)	10	11	12	13	14
Coordinate (x_i)	0.0	0.5	1.0	1.5	2.0
Time (t_i)	0.0	0.025	0.05	0.075	0.1

The three constants “1”, “ $-3/(t_{i+1}-t_i)^2$ ” and “ $2/(t_{i+1}-t_i)^3$ ” in the expression of $A_i(t)$ (Equation 6.4) can be represented with scalar factors. In the example above, as all nodes are equally spaced, $t_i - t_{i-1} = t_{i+1} - t_i = 0.025$, and $-3/(t_{i+1}-t_i)^2 = -4800$, $2/(t_{i+1}-t_i)^3 = 128000$. In the case of the first node of the path, only the part of Equation 6.4 corresponding to the interval $t_i \leq t \leq t_{i+1}$ is necessary, while for the last node, the part corresponding to the interval $t_{i-1} \leq t \leq t_i$ is the one to be used. For any node i different from these initial and final nodes, there will exist 2 definitions of the auxiliary function: One for the time that the load is preceding the node ($t < t_i$), and another for the time the load has passed the node ($t > t_i$) as given in Equation 6.4 (Scalar factors will have the same absolute values in both intervals, but the signs change for some terms to guarantee TLOAD2 is correctly related to t).

Once scalar factors have been defined and associated to a scalar point, it is necessary to define their relation with t . The output shown in Figure 6.10 corresponds to the path of the first moving load for an approach length of 10 m (at 20 m/s, earliest interaction force will act at 0.5 s). The same procedure applies to other moving loads and paths.

DAREA	100001	100001		1					
TLOAD2	100001	100001		0	0.5	0.525	0	0	
	0	0							
DAREA	110001	100001		-4800					
TLOAD2	110001	110001		0	0.5	0.525	0	0	
	0	2							
DAREA	120001	100001		128000					
TLOAD2	120001	120001		0	0.5	0.525	0	0	
	0	3							
DAREA	100002	100002		1					
TLOAD2	100002	100002		0	0.525	0.55	0	0	
	0	0							
DAREA	110002	100002		-4799.98					
TLOAD2	110002	110002		0	0.525	0.55	0	0	
	0	2							
DAREA	120002	100002		127999					
TLOAD2	120002	120002		0	0.525	0.55	0	0	
	0	3							
DAREA	130002	100002		4800.01					
TLOAD2	130002	130002		0	0.5	0.525	0	0	
	0	2							
DAREA	140002	100002		-128000					
TLOAD2	140002	140002		0	0.5	0.525	0	0	
	0	3							
DAREA	100003	100003		1					
TLOAD2	100003	100003		0	0.55	0.575	0	0	
	0	0							
DAREA	110003	100003		-4800					
TLOAD2	110003	110003		0	0.55	0.575	0	0	
	0	2							
DAREA	120003	100003		128000					
TLOAD2	120003	120003		0	0.55	0.575	0	0	
	0	3							
DAREA	130003	100003		4799.99					
TLOAD2	130003	130003		0	0.525	0.55	0	0	
	0	2							
DAREA	140003	100003		-127999					
TLOAD2	140003	140003		0	0.525	0.55	0	0	
	0	3							
DAREA	130004	100004		4800.01					
TLOAD2	130004	130004		0	0.55	0.575	0	0	
	0	2							
DAREA	140004	100004		-128000					
TLOAD2	140004	140004		0	0.55	0.575	0	0	
	0	3							

Figure 6.10 – Values of auxiliary function $A_i(t)$ for first moving load

The auxiliary functions $B_i(t)$ given in Equation 6.5 are expressed in a similar way. The elements “ $-1/[2(t_i - t_{i-1})][x_i - x_{i-1}]$ ” and “ $1/[2(t_i - t_{i-1})^2][x_i - x_{i-1}]$ ” in the expression of $B_i(t)$ can be represented with scalar factors. In the example above, as all nodes are equally spaced and velocity is constant, $t_i - t_{i-1} = 0.025$ and $(x_i - x_{i-1}) = 0.5$ for every node, $-1/[2(t_i - t_{i-1})][x_i - x_{i-1}] = -10.0$ and $1/[2(t_i - t_{i-1})^2][x_i - x_{i-1}] = 400.0$. As before, once the scalar factors have been defined and associated to a scalar point, it is necessary to define their relation with t through TLOAD2. The output for the first two nodes of the wheel path and the first moving load are shown in Figure 6.11.

DAREA	200001	200001		-10					
TLOAD2	200001	200001		0	0.5	0.525	0	0	
	0	1							
DAREA	210001	200001		400.001					
TLOAD2	210001	210001		0	0.5	0.525	0	0	
	0	2							
DAREA	200002	200002		-9.99998					
TLOAD2	200002	200002		0	0.525	0.55	0	0	
	0	1							
DAREA	210002	200002		399.999					
TLOAD2	210002	210002		0	0.525	0.55	0	0	
	0	2							
DAREA	220002	200002		10					
TLOAD2	220002	220002		0	0.5	0.525	0	0	
	0	1							
DAREA	230002	200002		-400					
TLOAD2	230002	230002		0	0.5	0.525	0	0	
	0	2							

Figure 6.11 – Values of auxiliary function $B_i(t)$ for first moving load

NASTRAN allows the definition of non-linear transient forcing functions through the instruction NONLIN2. This instruction defines the force to be applied to the node F_i as a function of a scalar S multiplied by the displacement of scalar p and velocity of a node q as $F_i = SX_p X_q$. The instruction has the format shown in Figure 6.12 and Table 6.5.

NOLIN2	SID	GI	CI	S	GJ	CJ	GK	CK	
--------	-----	----	----	---	----	----	----	----	--

Figure 6.12 – Columns for NOLIN2 entry

Table 6.5 – Parameters used for NOLIN2 entry

Field	Contents
SID	Non-linear load set identification number (Integer > 0)
GI	Grid or scalar point identification number at which non-linear load is to be applied (Integer > 0)
CI	Component number for GI. (Integer 1 through 6 for grid point; 0 or blank for scalar point)
S	Scale factor. (Real)
GJ, GK	Grid or scalar point identification number (Integer >0)
CJ, CK	Component number for GJ, GK (1 Integer 6 for grid, and Blank or zero for scalar point if displacements) (11 Integer 16 for grid, and 10 for scalar point if velocity)

These non-linear loads must be selected with the Case Control command, **NONLINEAR=SID**.

The forces $A_i F$ and $B_i F$ acting on the bridge nodes (Equation 6.14) are implemented as shown in Equation 6.20.

$$\begin{Bmatrix} A_1 F \\ B_1 F \\ A_2 F \\ B_2 F \\ \vdots \\ A_N F \\ B_N F \\ \vdots \end{Bmatrix} = \begin{Bmatrix} X_{100001} X_F \\ X_{200001} X_F \\ X_{100002} X_F \\ X_{200002} X_F \\ \vdots \\ X_{100000+N} X_F \\ X_{200000+N} X_F \\ \vdots \end{Bmatrix} \quad (6.20)$$

where $X_{100000+i}$ is displacement associated with scalar point $(100000+i)$ ($A_i(t)$), $X_{200000+i}$ is displacement associated with scalar point $(200000+i)$ ($B_i(t)$), and X_F is displacement associated with scalar point F (Interaction force defined by 400000). For example, if two masses and four nodes (ID node numbers 10,11,12 and 13 for the path of one mass and 20, 21, 22 and 23 for the other mass), these forces are expressed in NASTRAN code as illustrated in Figure 6.13.

NOLIN2	2	400000		1	100002		11	3	
NOLIN2	2	400000		1	100003		12	3	
NOLIN2	2	401000		1	101002		21	3	
NOLIN2	2	401000		1	101003		22	3	
NOLIN2	2	400000		1	200001		10	5	
NOLIN2	2	400000		1	200002		11	5	
NOLIN2	2	400000		1	200003		12	5	
NOLIN2	2	400000		1	200004		13	5	
NOLIN2	2	401000		1	201001		20	5	
NOLIN2	2	401000		1	201002		21	5	
NOLIN2	2	401000		1	201003		22	5	
NOLIN2	2	401000		1	201004		23	5	

NOLIN2	2	11	3	-1	100002		400000		
NOLIN2	2	12	3	-1	100003		400000		
NOLIN2	2	21	3	-1	101002		401000		
NOLIN2	2	22	3	-1	101003		401000		
NOLIN2	2	10	5	-1	200001		400000		
NOLIN2	2	11	5	-1	200002		400000		
NOLIN2	2	12	5	-1	200003		400000		
NOLIN2	2	13	5	-1	200004		400000		
NOLIN2	2	20	5	-1	201001		401000		
NOLIN2	2	21	5	-1	201002		401000		
NOLIN2	2	22	5	-1	201003		401000		
NOLIN2	2	23	5	-1	201004		401000		

Figure 6.13 – Definition of forces acting on the bridge nodes

The instruction *NONLINEAR* = 2 should be added at the beginning of file *caseco.dat* to be included in NASTRAN analysis with the output queries. The term “ $\sum_i A_i(t)z_i(t) + \sum_i B_i(t)\mathbf{q}_i(t)$ ” corresponding to the compatibility forcing term in the stiffness matrix can also be implemented with the instruction NOLIN2 as illustrated in Figure 6.14.

NOLIN2	2	500000		1	100002		11	3	
NOLIN2	2	500000		1	100003		12	3	
NOLIN2	2	501000		1	101002		21	3	
NOLIN2	2	501000		1	101003		22	3	
NOLIN2	2	500000		1	200001		10	5	
NOLIN2	2	500000		1	200002		11	5	
NOLIN2	2	500000		1	200003		12	5	
NOLIN2	2	500000		1	200004		13	5	
NOLIN2	2	501000		1	201001		20	5	
NOLIN2	2	501000		1	201002		21	5	
NOLIN2	2	501000		1	201003		22	5	
NOLIN2	2	501000		1	201004		23	5	

Figure 6.14 – Definition of compatibility condition

The term $-mg$, though constant with t , can be regarded as a time-dependent term and modelled using DAREA and TLOAD2. If the moving load is located on a node i , the load will be $-mg$. If the moving load is between node i and node $(i+1)$, the load will be distributed between adjacent nodes as follows:

$$\begin{aligned} \text{For } x_i \leq \mathbf{x} \leq x_{i+1} \quad & \text{Load at node } i = -mg (x_{i+1} - \mathbf{x}) / (x_{i+1} - x_i) \\ & \text{Load at node } (i+1) = -mg(\mathbf{x} - x_i) / (x_{i+1} - x_i) \end{aligned} \quad (6.21)$$

If speed is assumed to be constant along an element,

$$\begin{aligned} \text{For } t_i \leq t \leq t_{i+1} \quad & \text{Load at node } i = -mg (t_{i+1} - t) / (t_{i+1} - t_i) \\ & \text{Load at node } i+1 = -mg(t - t_i) / (t_{i+1} - t_i) \end{aligned} \quad (6.22)$$

This can also be expressed as:

$$\begin{aligned} \text{For } t_i \leq t \leq t_{i+1} \quad & \text{Load at node } i = -mg [1 - (t - t_i) / (t_{i+1} - t_i)] \\ & \text{Load at node } i+1 = -mg(t - t_i) / (t_{i+1} - t_i) \end{aligned} \quad (6.23)$$

This is implemented by defining scalar factors $-mg/(t_{i+1} - t_i)$. In the example implemented in this section, $(t_{i+1} - t_i) = 0.025$ is the same for any node i , and if $m = 101.98 \text{ kg}$, then, $g = 9.806$, “ $-mg=1000$ ” and “ $-mg/(t_{i+1} - t_i) = -40000.0$ ”. The *bulk.dat* representation of gravity forces due to the first moving mass moving along the bridge path from ID node 10 to 14 is represented in Figure 6.15.

DAREA	10	10	3	1000					
TLOAD2	10	10		0	0.5	0.525	0	0	
	0	0							
DAREA	10010	10	3	-40000					
TLOAD2	10010	10010		0	0.5	0.525	0	0	
	0	1							
DAREA	11	11	3	40000					
TLOAD2	11	11		0	0.5	0.55	0	0	
	0	1							
DAREA	10011	11	3	-79999.8					
TLOAD2	10011	10011		0	0.525	0.55	0	0	
	0	1							
DAREA	12	12	3	40000					
TLOAD2	12	12		0	0.525	0.575	0	0	
	0	1							
DAREA	10012	12	3	-80000					
TLOAD2	10012	10012		0	0.55	0.575	0	0	
	0	1							
DAREA	13	13	3	40000					
TLOAD2	13	13		0	0.55	0.575	0	0	
	0	1							

Figure 6.15 – Definition of gravity forces

The forces due to the road profile are imposed on scalar points defining the interaction force F (this is, 400000, 401000, etc.). If the power spectral density function defining the road profile is divided into 100 frequency intervals, it will be necessary to define 100 values for each moving load. If there are 4 moving loads and 100 frequency intervals, there will be 400 DAREA and TLOAD2 instructions. These forces will be present all along the time the analysis takes place. The height of the road irregularities is given by (see Section 5.4):

$$x(t) = \sum_{n=1}^N \sqrt{4S(\mathbf{w}_n)} \Delta \mathbf{w} \cos(\mathbf{w}_n t - \mathbf{q}_n) \quad (6.24)$$

The correspondence with the parameters defining TLOAD2 is:

- \mathbf{t} = blank.; $TI = 0$,
- $T2$ = approach_time + time_crossing_bridge + free_vibration_time,
- $A = \sqrt{4S(\mathbf{w}_n)} \Delta \mathbf{w}$ (defined by DAREA),
- $P = -\mathbf{q}_i$ where \mathbf{q}_i in degrees is generated randomly,
- $F = \mathbf{w}$ is temporal frequency in Hz.

Figure 6.16 shows a few frequency components of a road profile.

DAREA	310000	400000		0.0016					
TLOAD2	310000	310000		0	0	7.075	1	99.2744	
	0	0							
DAREA	310001	400000		0.00135					
TLOAD2	310001	310001		0	0	7.075	1.19	264.129	
	0	0							
DAREA	310002	400000		0.00116					
TLOAD2	310002	310002		0	0	7.075	1.38	53.8938	
	0	0							
DAREA	310003	400000		0.00102					
TLOAD2	310003	310003		0	0	7.075	1.57	32.8363	
	0	0							
DAREA	310004	400000		0.00091					
TLOAD2	310004	310004		0	0	7.075	1.76	0.30802	
	0	0							

Figure 6.16 – Definition of road profile

In the same way, a bump can be defined at a certain location by its wavelength and height. In the example illustrated in Figure 6.17, a 10 cm amplitude and 1 m length sinus wave is modelled 10 m prior to the bridge.

DAREA	350000	400000		0.1					
TLOAD2	350000	350000		0	0	0.05	10	0	
	0	0							
DAREA	351000	401000		0.1					
TLOAD2	351000	351000		0	0	0.05	10	0	
	0	0							

Figure 6.17 – Definition of a bump

A particular shape (i.e. a measured road profile) can be approximated by a combination of different sine functions. Finally, the instruction DLOAD defines the dynamic loading condition for the transient response problem as a linear combination of the sets defined via TLOAD2 entries. This is illustrated in Figure 6.18 and Table 6.6

DLOAD	SID	S	S1	L1	S2	L2	S3	L3	
	S4	L4	-etc.-						

(a) Format of DLOAD entry

Figure 6.18 (continued on following page)

DLOAD	999	1	1	100001	1	110001	1	120001	
	1	100002	1	110002	1	120002	1	130002	
	1	140002	1	100003	1	110003	1	120003	
	1	130003	1	140003	1	130004	1	140004	
	1	101001	1	111001	1	121001	1	101002	
	1	111002	1	121002	1	131002	1	141002	
	1	101003	1	111003	1	121003	1	131003	
	1	141003	1	131004	1	141004	1	200001	
	1	210001	1	200002	1	210002	1	220002	
	1	230002	1	200003	1	210003	1	220003	

(b) Implementation

Figure 6.18 – Definition of interaction forces

Table 6.6 – Parameters used for DLOAD entry (see Figure 6.18(a))

Field	Contents
SID	Load set identification number (Integer >0)
S	Scale factor (Real)
Si	Scale factor (Real)
Li	Load set identification numbers of TLOAD2 entries (Integer >0)

Dynamic load sets must be selected in the Case Control Section with $DLOAD = SID$. This will be explained in Section 6.3. Appendix F contains listings of *bulk.dat* files for different vehicle and bridge input parameters.

Caseco Control Section

An example of *caseco.dat* file used for dynamic analysis is presented in Table 6.7 where displacement, velocity and acceleration at nodes 10,11,12,13, displacements at nodes 300000,301000, and strain at elements 1,2,3,4 are required. *K2GG* selects a direct input stiffness matrix. *STIF* is the name of a matrix that is input on the Bulk Data Entry. Another line to include in *caseco.dat* is *PARAM, COUPMASS, 1* that requests the generation of coupled rather than lumped mass matrices for elements with coupled mass capabilities. *SORT1* presents the output as a tabular listing of elements for each time. Other output forms can be found in MSc/NASTRAN Quick Reference Guide (1998).

Table 6.7 – Example of Caseco.dat file

```
$ Input Specification
DLOAD=1
NONLINEAR=2
K2GG=STIF
PARAM,COUPMASS,1
$ SET- Definition of points and elements where output is required
SET 1 = 10,11,12,13
SET 2 = 1,2,3,4
SET 3 = 300000, 301000
$ Output Specification
DISPLACEMENT(SORT1) = 1,3
VELOCITY(SORT1,RALL) = 1
ACCELERATION(SORT1) = 1
STRAIN(SORT1,RALL) = 2
```

6.3 IMPLEMENTATION IN NASTRAN

This section explains the overall procedure to carry out a simulation in a NASTRAN environment. It can be summarised in the following steps:

- [1] Creation of bridge model (*bridge.mod* file) and analysis of the model (*bridge.dat* file).
- [2] Creation of truck model (*truck.mod* file).
- [3] Static analysis of the truck model to obtain the reactions due to self-weight.
- [4] Import analysis of the bridge model (*bridge.dat* file) into truck model (*truck.mod* file), saving combined system as a new file (*system.mod*).
- [5] Edit input dynamic interaction file (*nasbti1.txt*) and specify:
 - Static axle weights
 - Speed
 - Axle spacings
 - Wheel path on the bridge
 - Road profile

- [6] Generate *bulk.dat* file by running *nasbti.exe*. The information required by *nasbti.exe* to perform calculations is taken from *input.txt*. The input code contained in *bulk.dat* was explained in Section 6.2.2 and more examples are given in Appendix F.
- [7] Edit *caseco.dat* file to specify which output results are required.
- [8] Open *system.mod* file, create dynamic load, time transient
- [9] Export model analysis to a file (i.e. *test.dat*), Advanced Analysis, include *caseco.dat* and *bulk.dat*. Exit and Save.
- [10] Open *test.dat*, change $D = 1$ to $D = 999$ and precede line *Loadset = 1* by \$.
- [11] Run *nastranw.exe* on *test.dat* to generate *test.f04* and *test.f06* files. *Test.f06* is the file containing the output results required in *caseco.dat*.
- [12] Run *Convnas.exe* to convert sequential output *test.f06* into an output in columns that can be easily opened in Excel or other worksheet software. The information to be extracted from *test.f06* must be specified in *convnas.txt*

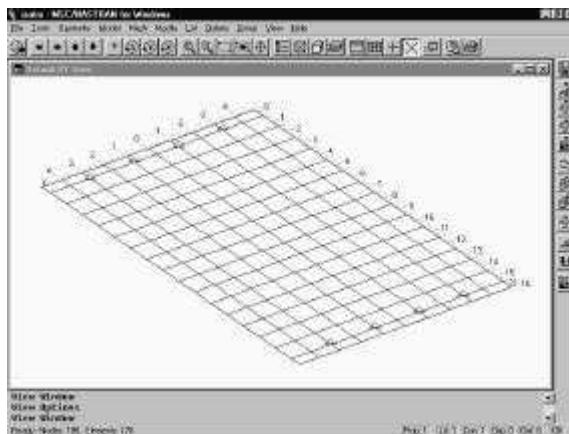
These steps are explained in further detail in the following sections.

Bridge finite element model

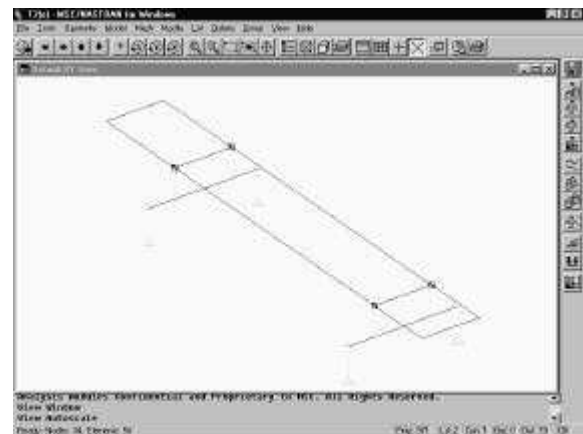
The creation of a bridge model (*bridge.mod* file) and analysis of the model (*bridg000.dat* file) are discussed in this section. This analysis can be static or dynamic. The objective is the generation of a *.*dat* file that contains all the information relating to bridge material, properties, nodes, elements and constraints (MSc/NASTRAN 1997a, 1997b). When building this model (Figure 6.19(a)), a list of nodes should be defined along the wheel path on the structure. There are two aspects to this model that require further consideration:

- The identification of the number and spacing of the nodes corresponding to each wheel path.
- The identification of the numbers of the elements/nodes for which response (strains, displacements, forces, etc.) are to be generated.

Specific bridge models will be introduced in Section 6.5.



(a) Bridge model



(b) Truck Model

Figure 6.19 – Finite Element models

Truck model

The truck is designed and saved in another file (*truck.mod*) independent from the bridge model. When the truck model is created (Figure 6.19(b)), its materials, properties, nodes and elements should have a different identification number from those used in the bridge model defined previously. Otherwise, error messages will be reported when combining both models.

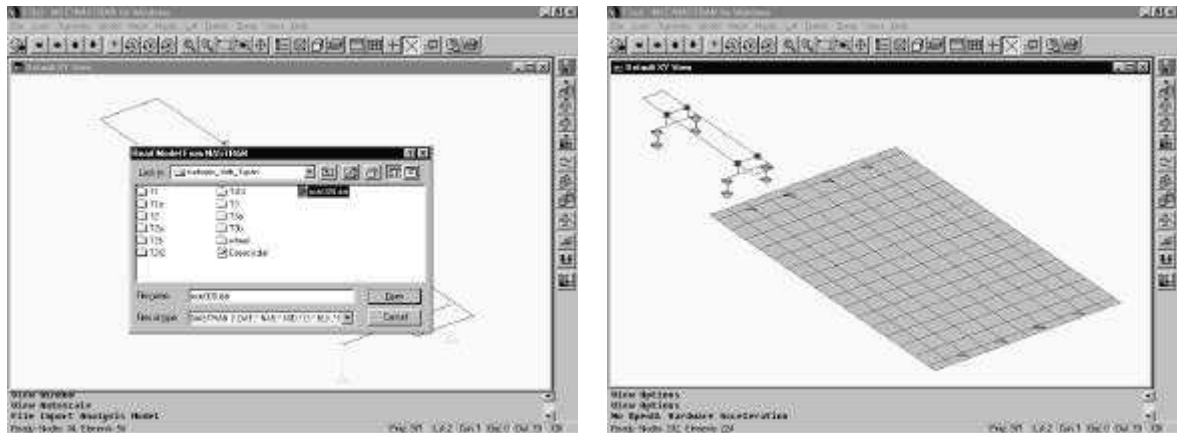
In order to apply forces to the contact points of the truck with the ground, these nodes must have a predetermined numbering identified by the interaction program (Section 6.2.2). Hence, the contact points located on the inner side of the bridge are even numbers of thousands starting at 300000 for the first axle, 302000 for the 2nd axle and so on, while the contact points in the outer side are odd numbers of thousands starting at 301000, 303000, etc. If there were a second vehicle, the contact points of this vehicle would have identification numbers starting at 600000 at the steering wheel side and 601000 at the other side. Some details on the elements composing a truck model were given in Chapter 5. Section 6.4 will describe the truck models used for NASTRAN theoretical simulations.

Determination of static axle weights

A static analysis of the truck model must be carried out to obtain the reactions due to the self-weight. It is necessary to check that the wheel-ground points of contact are restrained in the x , y and z directions, so we can get the vertical reactions due to gravity. NASTRAN has an option for imposing body loading of this type (MSc/NASTRAN 1997a, 1997b).

Bridge-truck combined model

The file containing the truck model is opened (*truck.mod*). The information on the bridge data (*bridg000.dat*) is imported into the truck model (Figure 6.20(a)). Then, the combined system shown in Figure 6.20(b) is saved as a new file (i.e. *system.mod*). At the wheel-ground contact points the truck should be restrained in the x and y direction (only vertical deformation in z direction is allowed).



(a) Import of bridge data

(b) Combined system

Figure 6.20 – Creation of combined finite element model

Edit input file

The input text file (*nasbti1.txt*) contains the number of vehicle events and, for each vehicle:

- Static axle weights,
- Speed as a function of time,
- Axle spacings,
- Wheel path on the bridge,
- Road profile.

An executable file (*input.exe*) allows the generation of *nasbti1.txt* through the computer screen (i.e. this program will fill up node numbers and spacings of the wheel path into *nasbti1.txt* automatically if they follow a consecutive order or pattern). The header of the file contains information on truck characteristics (Figure 6.21(a)). The definition of the wheel path is illustrated in Figure 6.21(b). This path is defined by the identification number for different nodes on the bridge followed by the total distance travelled by the wheel up to that node. Finally information on road profile is given (Figure 6.21(c)). The characteristics

of a second vehicle would follow the ones of a first vehicle in the same way. *Nasbti1.txt* has a special format to be read by *nasbti.exe*, an executable file that produces *bulk.dat*. Though *nasbti1.txt* is a text file that can be filled in directly (Each line contains information on a different input parameter), *input.exe* guarantees the correct format of *nasbti1.txt*.

```

Nasbti1.txt - WinPad
File Edit View Insert Format Help
[Icons]
Analysis_type:(1)1-B_or_(3)3-D
3
Total_Number_vehicles
1
Number_axles
2
Axle_spacing_from_first_axle:
0
5
Wheel_loads_right_side[Nw]:
2000
3000
Wheel_loads_left_side[Nwl]:
2000
3000
Number_speed_points
2
Time_speed_relationship(sec-m/s)
0
20
20
20
Total_Number_Nodes_Each_Path:
5

```

(a) Information on truck characteristics

```

Nasbti1.txt - WinPad
File Edit View Insert Format Help
[Icons]
Total_Number_Nodes_Each_Path:
5
Nodes_Id_coordinates_right_path
34
0
35
0.5
36
1
37
1.5
38
2
Nodes_Id_coordinates_left_path
64
0
65
0.5
66
1
67
1.5
68
2

```

(b) Information on bridge path

```

Nasbti1.txt - WinPad
File Edit View Insert Format Help
[Icons]
2
Nodes_Id_coordinates_left_path
64
0
65
0.5
66
1
67
1.5
68
2
Approach_Length(m):
10
Road_Profile_Type: (1)Theoretical,(3)Smooth
1
Geometric_mean_spatial_Frequency(a)
1.0e-05
Minimum_frequency(Hz):
1
Maximum_frequency(Hz):
20
Number_frequencies:
100

```

(c) Information on road profile

Figure 6.21 - Input file, *nasbti1.txt*, for generation of *bulk.dat*

Generation of Bulk file

Run *nasbti.exe* to generate *bulk.dat* file (Section 6.2.2). *Nasbti.exe* takes as reference the input data in *nasbti1.txt*. *Bulk.dat* contains the interaction forces applied to the structure at each instant in time. These applied forces are based on the theoretical background described in 6.2.1. Depending on how *nasbti.exe* has been compiled, static response can be obtained, special support conditions (such as fixed) can be specified, bumps can be prescribed at the desired positions and/or road profile can be output to a text file.

Output request

Edit *caseco.dat* file to choose those elements and the type of bridge response that is required. The lines starting with a \$ sign are ignored by NASTRAN. The first three lines are caseco control commands for dynamic analysis (MSC/NASTRAN 1997c), and the following lines specify the output request (MSC/NASTRAN 1998). Figure 6.22 shows an example of *caseco.dat* file.

```

NONLINEAR=2
K2GG=STIF
PARAM,COUPMASS,1
$ Sets containing ID for nodes/elements
$SET 1 = 300000,301000,185
SET 2 = 4,5,10,12
$ Type of Request
$DISPLACEMENT(SORT1) = 1
$VELOCITY(SORT1) = 1
$ACCELERATION(SORT1) = 1
$LOAD(SORT1) = 1
$SPCFORCE(SORT1) = 1
$MPCFORCE(SORT1) = 1
$FORCE(SORT1) = 1
$STRESS(SORT1) = 2
$STRAIN(SORT1) = 2

```

Figure 6. 22 – Output Request

Dynamic Transient Analysis

Open *system.mod* file and create a time transient dynamic load (Figure 6.23(a)) as specified by MSc/NASTRAN (1997a, 1997b). A direct numerical method is chosen for the transient response analysis. This method performs a numerical integration on the complete coupled equations of motion (unlike the modal method). The structural response is solved at discrete times, typically with a fixed integration time step. A central finite difference representation for the velocity and acceleration is used at discrete times, and the applied force is averaged over three adjacent time steps. The following features are defined on the Load Set Options for Dynamic Analysis Dialog Box (Figure 6.23(b)):

- Total number of steps, time per step and output interval.

The time per step depends on the characteristics of the problem (generally 0.001).

The total number of steps depends on the length to be recorded and vehicle speed. If speed is constant, $Total_number_steps = Total_length / (speed * time_per_step)$

Some extra steps might be taken into account to study the free vibration of the bridge.

The output time interval depends on the frequency desired for the output results. For example, if the solution is performed every 0.001 seconds, the results can be output every fifth step or every 0.005 seconds.

- Damping

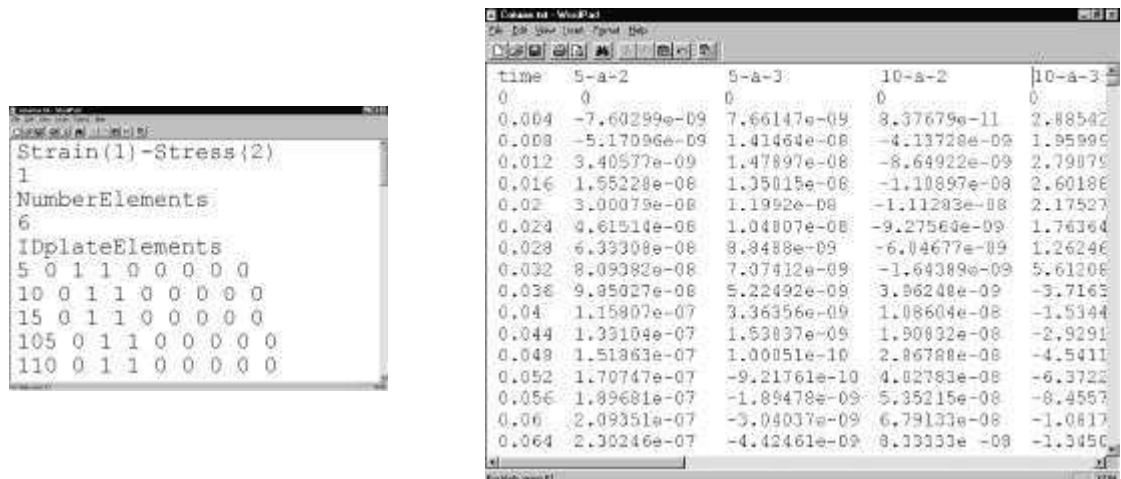
Damping represents the dissipation energy characteristics of the structure and it can be implemented in different ways (MSC/NASTRAN 1997c). Structural damping has been commonly used.

Run solver

Run *nastranw.exe* on *test.dat* which will generate *test.f04* and *test.f06* files (Figure 6.24(b)). *Test.f06* contains all information requested on *caseco.dat*. It also reports on any errors which have taken place during the execution of the simulation.

Output in columns

The results provided by NASTRAN in *test.f06* (Figure 6.24(b)) are difficult to manipulate. A program was written to display the information of *test.f06* in a column output (*column.txt*). This program, *convnas.exe*, reads from *convnas.txt* the identities of the elements to be extracted in *test.f06* and the type of request (i.e., longitudinal and transverse bending strain can be obtained by specifying 01100000. These numbers correspond to eight different types of strain output that NASTRAN gives. Only those positions marked with a 1 are extracted in columns). Figure 6.25 shows examples of *convnas.txt* and *column.txt* files respectively.



time	5-a-2	5-a-3	10-a-2	10-a-3
0	0	0	0	0
0.004	-7.60299e-09	7.66147e-09	8.37679e-11	2.88542
0.008	-5.17096e-09	1.41464e-08	-4.13728e-09	1.95995
0.012	3.40577e-09	1.47897e-08	-8.64922e-09	2.79079
0.016	1.55228e-08	1.35015e-08	-1.10897e-08	2.60186
0.02	3.00079e-08	1.1992e-08	-1.11203e-08	2.17527
0.024	4.61514e-08	1.04807e-08	-9.27564e-09	1.76364
0.028	6.33308e-08	8.8488e-09	-6.04677e-09	1.26246
0.032	8.09382e-08	7.07412e-09	-1.64389e-09	5.61208
0.036	9.95027e-08	5.22492e-09	3.86240e-09	-3.7163
0.04	1.15807e-07	3.36356e-09	1.08604e-08	-1.5344
0.044	1.33104e-07	1.53837e-09	1.90832e-08	-2.9291
0.048	1.51863e-07	1.00051e-10	2.86788e-08	-4.5411
0.052	1.70747e-07	-9.21761e-10	4.02783e-08	-6.3722
0.056	1.89681e-07	-1.89478e-09	5.35215e-08	-8.4557
0.06	2.09351e-07	-3.04037e-09	6.79137e-08	-1.0817
0.064	2.30246e-07	-4.42461e-09	8.13333e-08	-1.3456

(a) *convnas.txt*

(b) *column.txt*

Figure 6.25 – Input and output file for a final tabular display

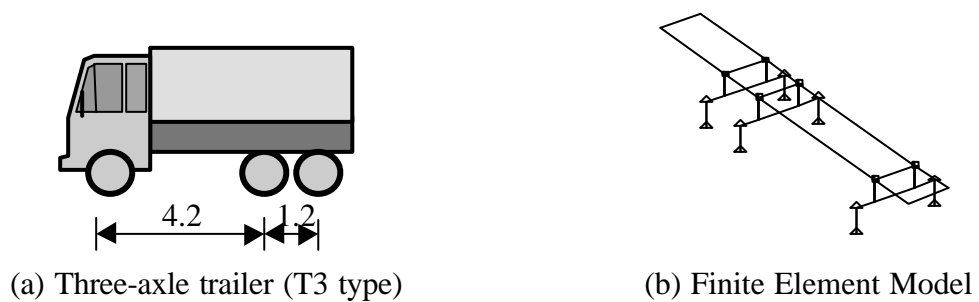
Summarising, once the bridge and truck finite element models have been created, the files involved in the rest of the simulation process are as shown in Table 6.8.

Table 6.8 –Dynamic Interaction Files

<i>Executable file</i>	<i>Input File</i>	<i>Output file</i>
Generation of bridge data	<i>Bridge.mod</i>	<i>Bridge000.dat</i>
Creation of interaction model	<i>Truck.mod</i> <i>Bridge000.dat</i>	<i>System.mod</i>
<i>Input.exe</i>	screen	<i>Nasbti.txt</i>
<i>Nasbti.exe</i>	<i>Nasbti.txt</i>	<i>Bulk.dat</i>
Export input file for simulation	<i>System.mod</i> <i>Caseco.dat</i> <i>Bulk.dat</i>	<i>test.dat</i>
<i>Nastranw.exe</i>	<i>Test.dat</i>	<i>Test.f04</i> <i>Test.f06</i>
<i>Convnas.exe</i>	<i>Convnas.txt</i> <i>Test.f06</i>	<i>column.txt</i>

6.4 TRUCK MODELS

Only rigid frame structures have been modelled spatially, i.e., types T2 and T3 illustrated in Figures 6.26 and 6.27 respectively.

**Figure 6.26** – Two-axle truck**Figure 6.27** – Three-axle truck

The elements of a two-axle truck are represented in Figure 6.28. Friction elements are not part of this modelling, though their influence in dynamic wheel forces could be significant.

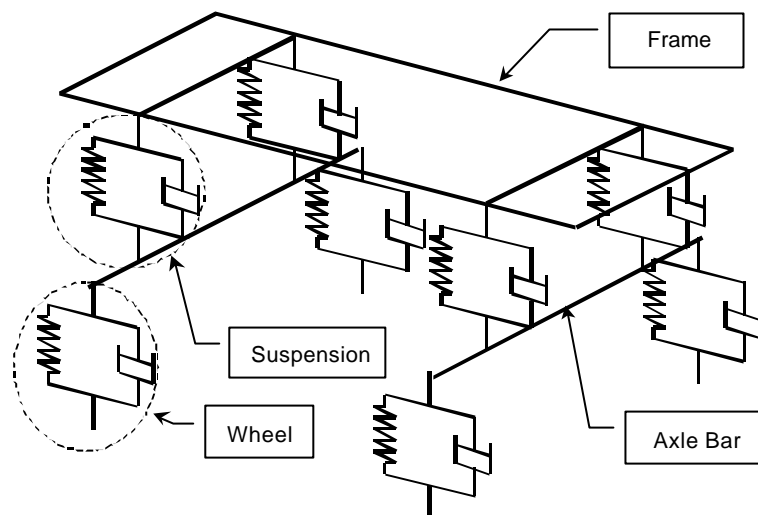


Figure 6.28 – Finite Element Two-Axle Truck Model

Table 6.9 gives the mechanical characteristics used in the design of both trucks. The data for the two-axle truck has been taken from manufacturers (Kirkegaard et al. 1997). The parameters of the three-axle truck have been obtained from experimental studies carried out in Munich (Baumgärtner 1998, Lutzenberger & Baumgärtner 1999) on a Finnish instrumented truck (Huhtala 1999). Details on this truck will be given in Chapter 8. Values are similar for both trucks, except for damping (The Danish model used friction elements in addition to dampers, but these elements have not been included).

Table 6.9 – Suspension and tyre properties

Truck Type	Spring (10 ⁶ N*m)				Damping (10 ³ Ns/m)			Axle mass (kg)		Mass moment of Inertia (kgm ²)	
	Tire		Suspension		Suspension	Tire					
	Front Axle	Rear axles	Front Axle	Rear axles		Front Axle	Rear axles	Front Axle	Rear axle	Front Axle	Rear axles
2-axle	1.0	2.0	1.8	0.3	5.0	3.0	3.0	700	1300	600	1000
3-axle	1.0	2.1	0.21	0.8	55.	40.	80.	343	1343	972.5	972.5

The axle spacing for the two-axle truck is 5 m. The three-axle truck has a rear tandem and the axle spacings are 4.2 m between the first and second axle and 1.2 m for the last two axles. Three different loading conditions and three speeds (55, 70 and 85 km/h) have been used for each truck configuration. Static weights of the two test vehicles are given in Table 6.10.

Table 6.10 – Static weights (kN)

Vehicle Type	1 st Axle	2 nd Axle	3 rd Axle	GVW
T2(Lightly loaded)	55.703	71.195	-	126.897
T2(Half-Loaded)	69.660	87.899	-	157.559
T2(Heavily loaded)	83.904	104.945	-	188.849
T3(Lightly loaded)	59.279	92.818	63.647	215.744
T3(Half-Loaded)	75.226	115.785	77.973	268.985
T3(Heavily Loaded)	91.174	138.752	92.298	322.224

The main modes of vibration of the two-axle truck are represented in Figure 6.29.

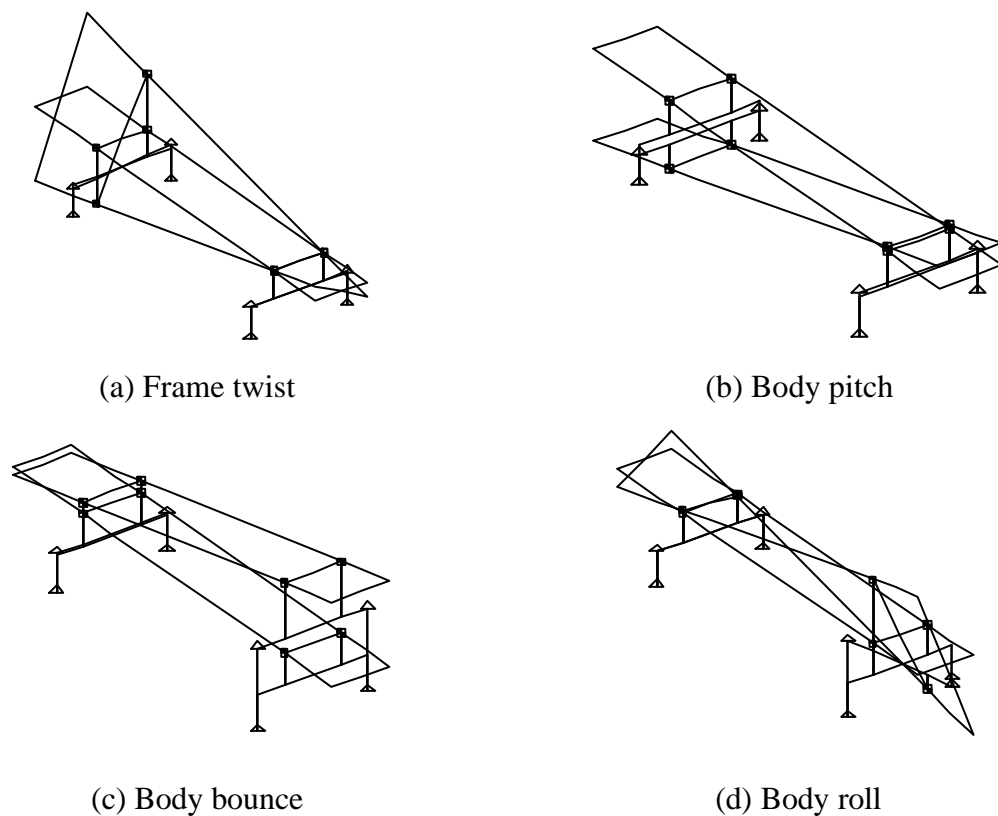
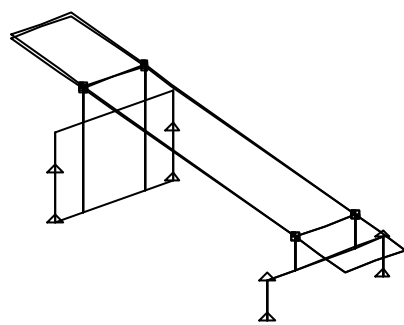
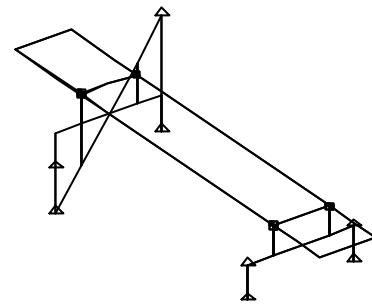


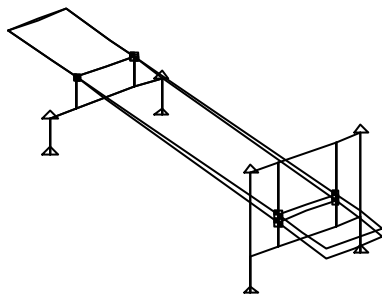
Figure 6.29 (continued on following page)



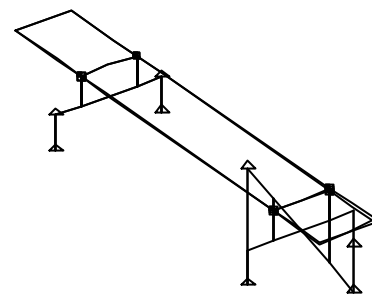
(e) Rear axle hop



(f) Rear axle roll



(g) Front axle hop



(h) Front axle roll

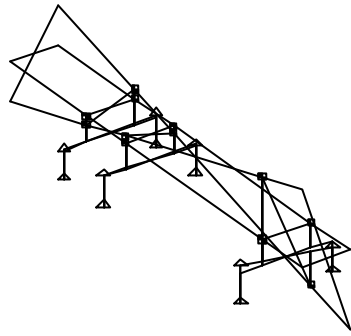
Figure 6.29 – Modes of vibration of a Two-Axle Truck

These modes of vibration are associated with a frequency given in Table 6.11. These frequencies change depending on the truck weight (Table 6.10) and they allow the assessment of the dynamic interaction with the supporting bridge. As the natural frequencies of the bridge and vehicle get closer, the dynamic response increases.

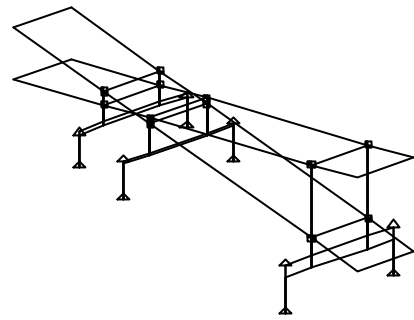
Table 6.11 – Main frequencies of vibration of the two-axle truck (Hz)

Truck load	Frame Twist	Body			Axle Hop		Axle Roll	
		Pitch	Bounce	Roll	Rear	Front	Rear	Front
Light	1.05	1.40	2.35	2.54	9.48	13.49	14.59	15.65
Half	0.99	1.23	2.08	2.37	9.47	13.49	14.51	15.63
Heavy	0.94	1.11	1.89	2.23	9.47	13.49	14.46	15.62

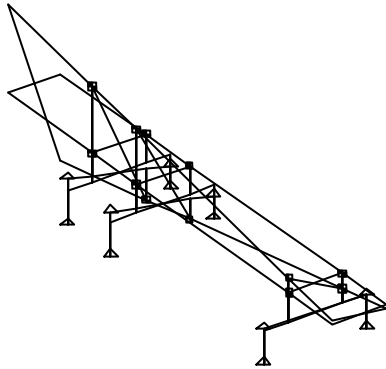
In the same way, Figure 6.30 shows modes of vibration corresponding to the three-axle truck.



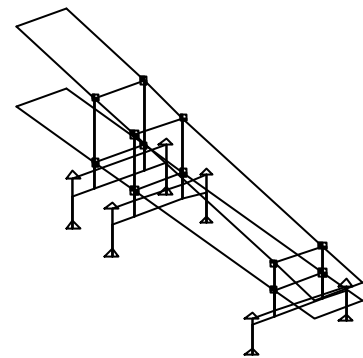
(a) Frame Twist



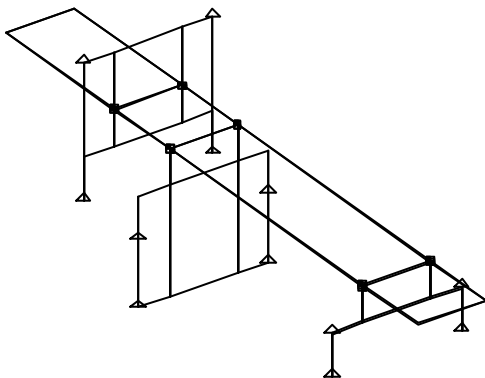
(b) Body Pitch



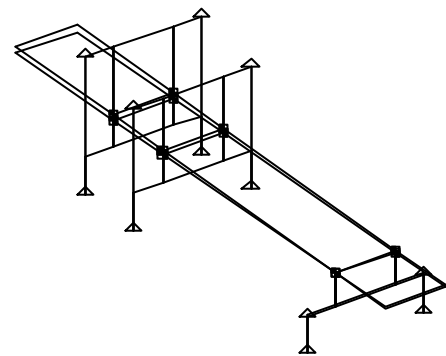
(c) Body roll



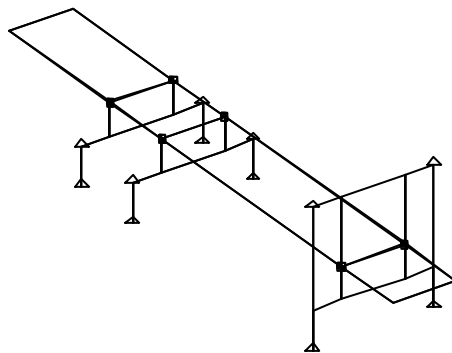
(d) Body bounce



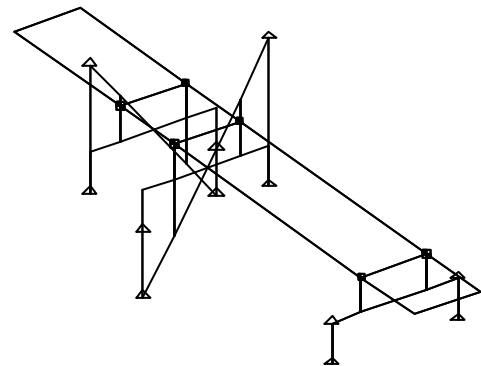
(e) 2nd and 3rd axle hop (out of phase)



(f) 2nd and 3rd axle hop (in phase)



(g) First axle hop



(h) 2nd and 3rd axle roll (out of phase)

Figure 6.30 (continued on following page)

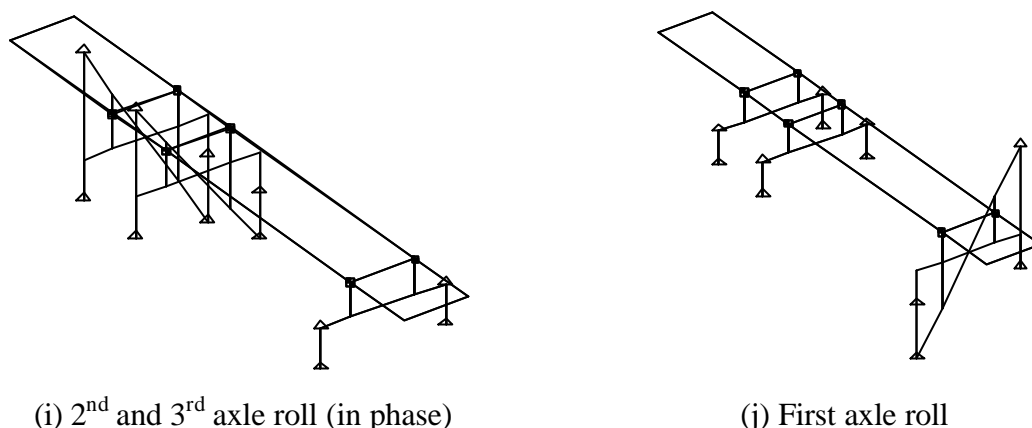


Figure 6.30 – Modes of vibration of a Three-Axle Truck

Table 6.12 shows the frequencies of vibration for different weights (Table 6.10) of the three-axle truck.

Table 6.12 – Main Modes of Vibration of the Three-Axle Truck (Hz)

Truck load	Frame Twist	Body			Tandem Hop		Tandem Roll		Front axle	
		Pitch	Roll	Bounce	Out of phase	In phase	Out of phase	In Phase	Hop	Roll
Light	0.82	1.02	1.58	2.01	9.90	9.97	13.25	13.26	11.08	15.51
Half	0.76	0.90	1.48	1.77	9.90	9.96	13.25	13.26	11.08	15.51
Heavy	0.71	0.81	1.39	1.60	9.90	9.94	13.25	13.26	11.08	15.51

6.5 BRIDGE MODELS

In some cases, bridge decks can be idealised as plate elements with thickness and density properties that match the mass per unit length and inertia of the real bridge in the longitudinal and transverse direction. However, if distribution of mass is not uniform in both directions and very accurate results are required, a 3-D bridge model will be necessary. Simulations of single and simultaneous traffic events (Figures 6.31(a) and 6.31(b)) have been performed on a range of bridge forms to determine their suitability for B-WIM purposes. The results obtained are typically strains in elements, which are easily measurable in the field (Section 4.2). A single span isotropic slab, two-span isotropic slab, slab with edge cantilever, voided slab, beam and slab, skew and cellular bridges are tested. These models follow the guidelines proposed in the examples by O'Brien and Keogh (1999). Typical properties of reinforced/prestressed concrete have been chosen for the

bridge material. Bridge damping is considered to be 5% and the road condition is considered to be ‘good’ (Wong 1993) in all cases.

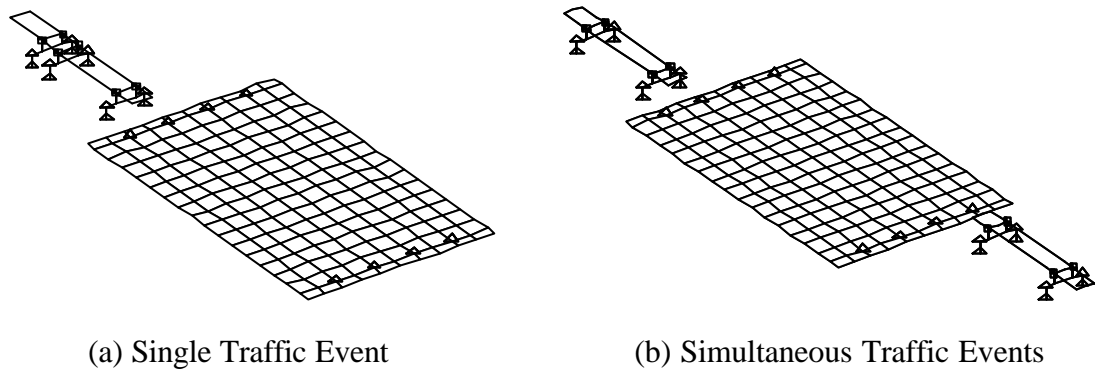
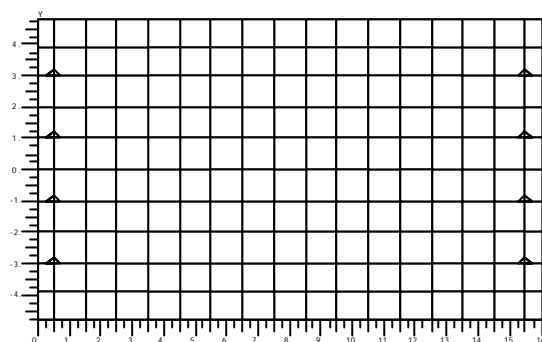


Figure 6.31 – Finite Element Simulations

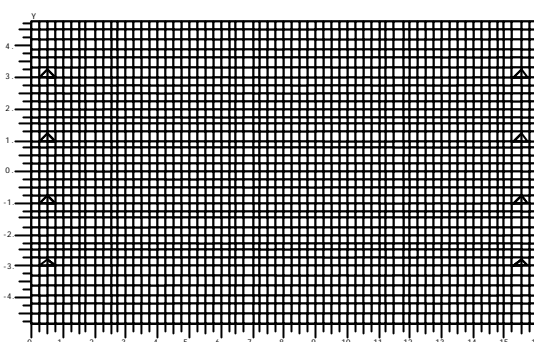
Static, eigenvalue and transient response analysis are necessary for a better understanding of the models and to ensure an accurate dynamic response. A static analysis is useful to determine influence lines at different locations. As seen in Section 3.5.1, accurate influence lines are very important in B-WIM systems. Though experimental influence lines can be obtained, they are limited to a reduced number of runs/trucks/sensors and a theoretical model can supply additional information on the accuracy in other situations. The natural frequencies and mode shapes are an indication of how the bridge will respond to a dynamic excitation. The bridge will then naturally vibrate at these frequencies.

6.5.1 Single Span Isotropic Slab

A slab deck behaves like a flat plate that is structurally continuous for the transfer of moments and torsions in all directions within the plane of the plate. Figure 6.32(a) shows a layout of the slab example (dimensions in m). Traffic direction is parallel to the x -axis. The deck is supported on four bearings at each end. The deck has a uniform rectangular cross-section of 0.6 m depth. It is built of prestressed concrete, 2500 kg/m³ unit weight, 35×10^6 kN/m² modulus of elasticity and 0.15 Poisson’s ratio. These general characteristics will be used in other models unless otherwise specified.



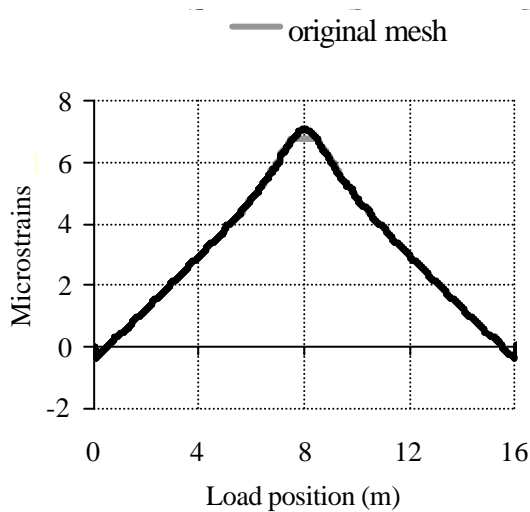
(a) Original Mesh



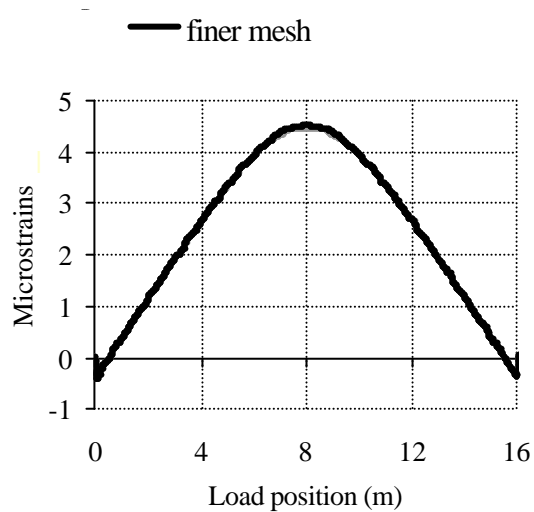
(b) Finer Mesh

Figure 6.32 – Plan view of slab finite element model

Influence lines due to a unit axle load travelling along the slow lane are represented in Figure 6.33. Two different types of mesh are compared: one based on plate elements 1 m long (Figure 6.32(a)) and another based on plate elements 0.5 m long. The difference in strain response is not significant.

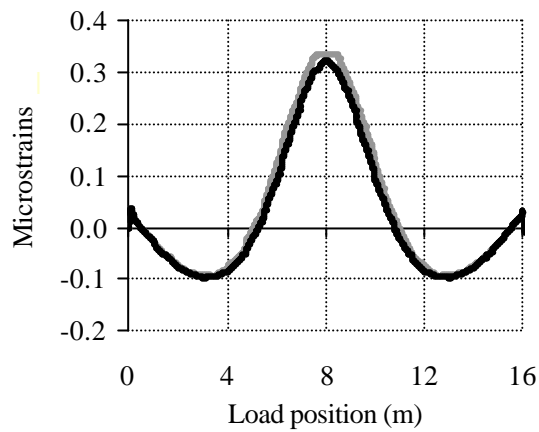


(a) Longitudinal strain, slow lane

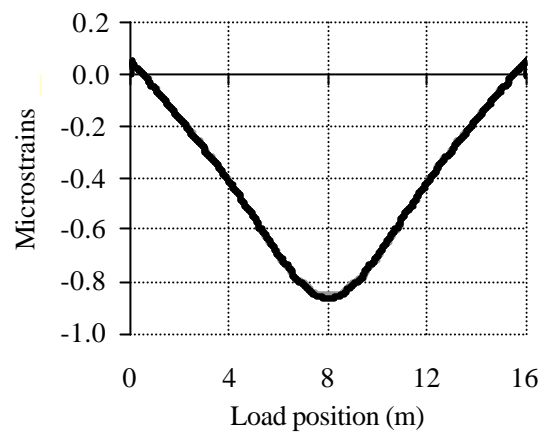


(b) Longitudinal strain, fast lane

Figure 6.33 (continued on following page)



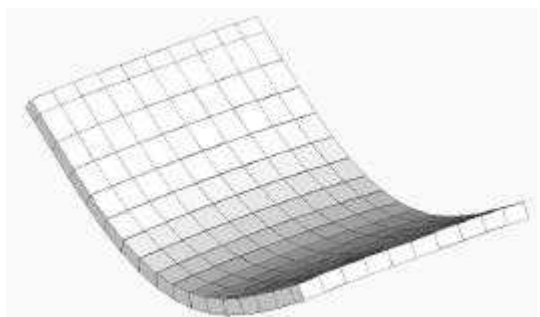
(a) Transverse strain, slow lane



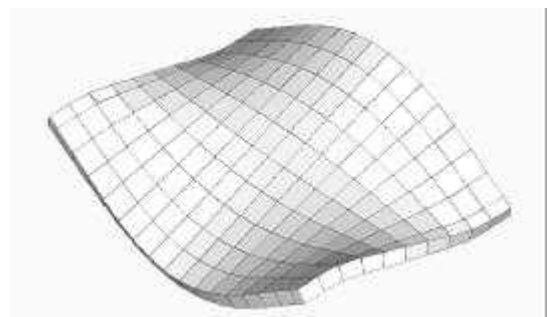
(b) Transverse strain, fast lane

Figure 6.33 - Influence line of strain at midspan (longitudinal distance of the sensor from start of the bridge: 8 m; transverse offset from bridge centreline: 2.5 m)

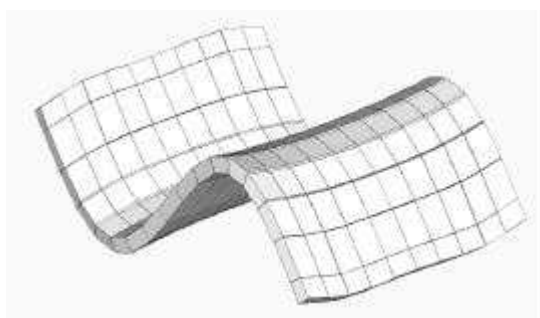
The main modes of vibration of the bridge are represented in Figure 6.34.



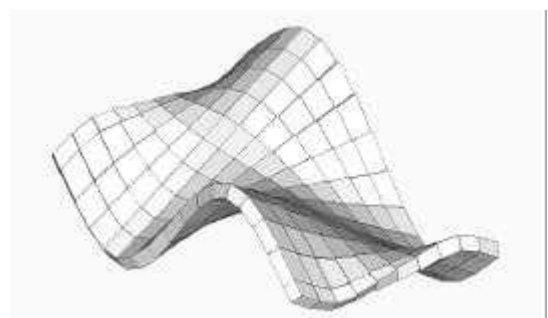
(a) 1st Mode (4.51 Hz)



(b) 2nd Mode (10.4 Hz)

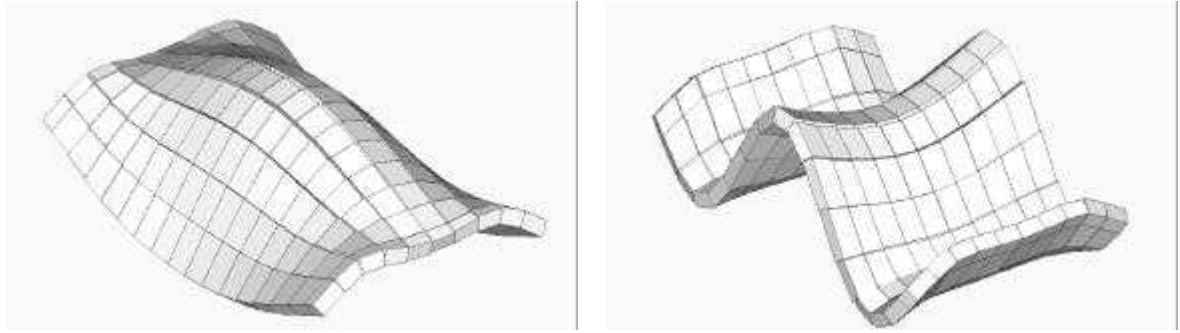


(c) 3rd Mode (17.84 Hz)



(d) 4th Mode (25.03 Hz)

Figure 6.34 (continued on following page)

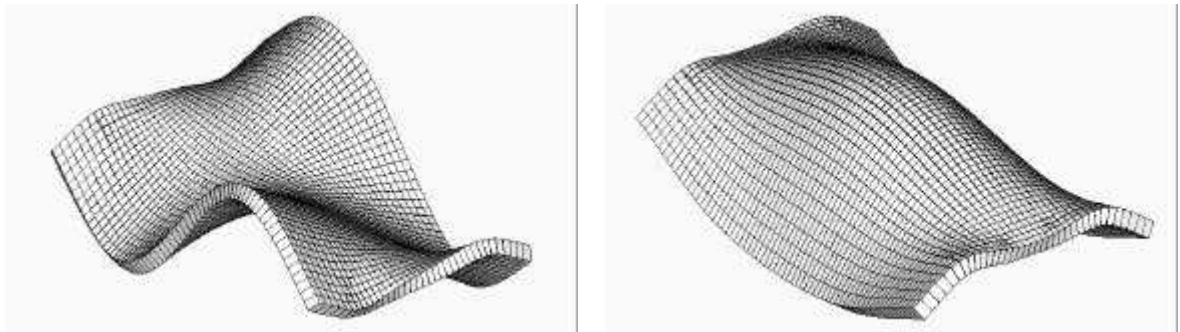


(e) 5th Mode (29.94 Hz)

(f) 6th Mode (39.46 Hz)

Figure 6.34 – Modes of vibration of the slab

A finer model with elements 0.25 m long (Figure 6.32(b)) was also built to compare differences in results. The natural frequencies with the finer model are: 4.51, 10.55, 17.85, 25.50, 30.87 and 39.49 Hz. They are very close to the original model. The biggest difference in natural frequencies are for the 4th and 5th torsional mode shapes, which are represented in Figure 6.35 (compare to Figure 6.34(d) and (e)).



(a) 4th Mode Shape (25.50 Hz)

(b) 5th Mode Shape (30.87 Hz)

Figure 6.35 – Modes of vibration with a finer mesh

A simulation of a three-axle truck (22 t) travelling along the slow lane is also carried out in both meshes. The output is very similar regardless of the mesh as shown in Figure 6.36. Accordingly, it is decided that elements 1 m long achieve enough accuracy for the purpose of simulations, saving memory space and running time.

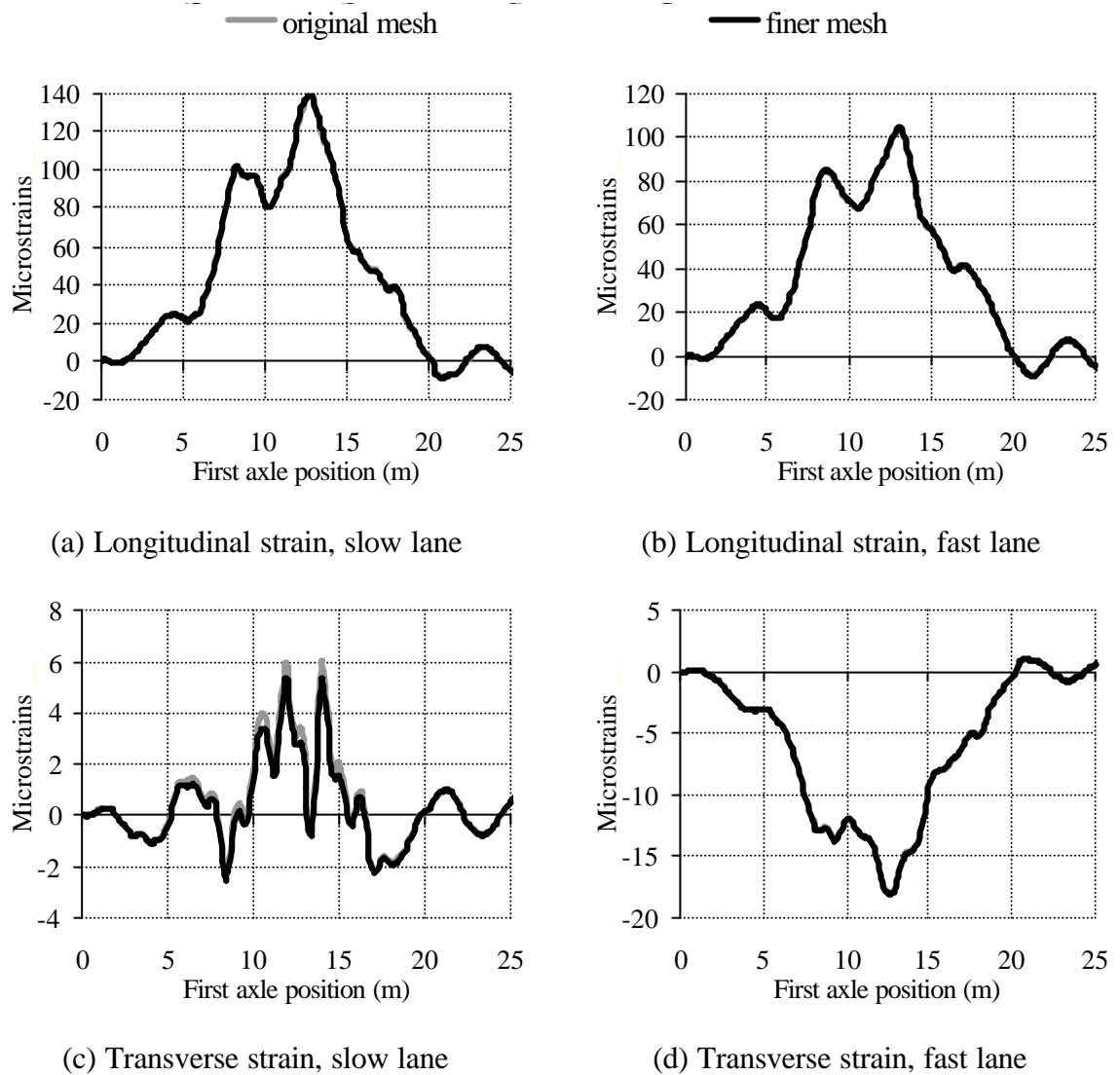


Figure 6.36 - Total strain caused by a 3-axle vehicle travelling at 70 km/h (longitudinal distance of the sensor from start of the bridge: 8 m; transverse location from bridge centreline: 2.5 m)

The results of strains at midspan for different transverse locations when the heaviest two-axle truck travels over the bridge at 85 km/h are illustrated in Figure 6.37. The truck wheels are located at 1 and 3 m from the centreline and the maximum longitudinal strain takes place at 3.5 m from it (Figure 6.37(a)). Longitudinal strain decreases as measurements take place towards the fast lane. Maximum transverse strain occurs in the fast lane, at the location furthest from the truck position and it decreases as measurements move towards the slow lane (Figure 6.37(d)).

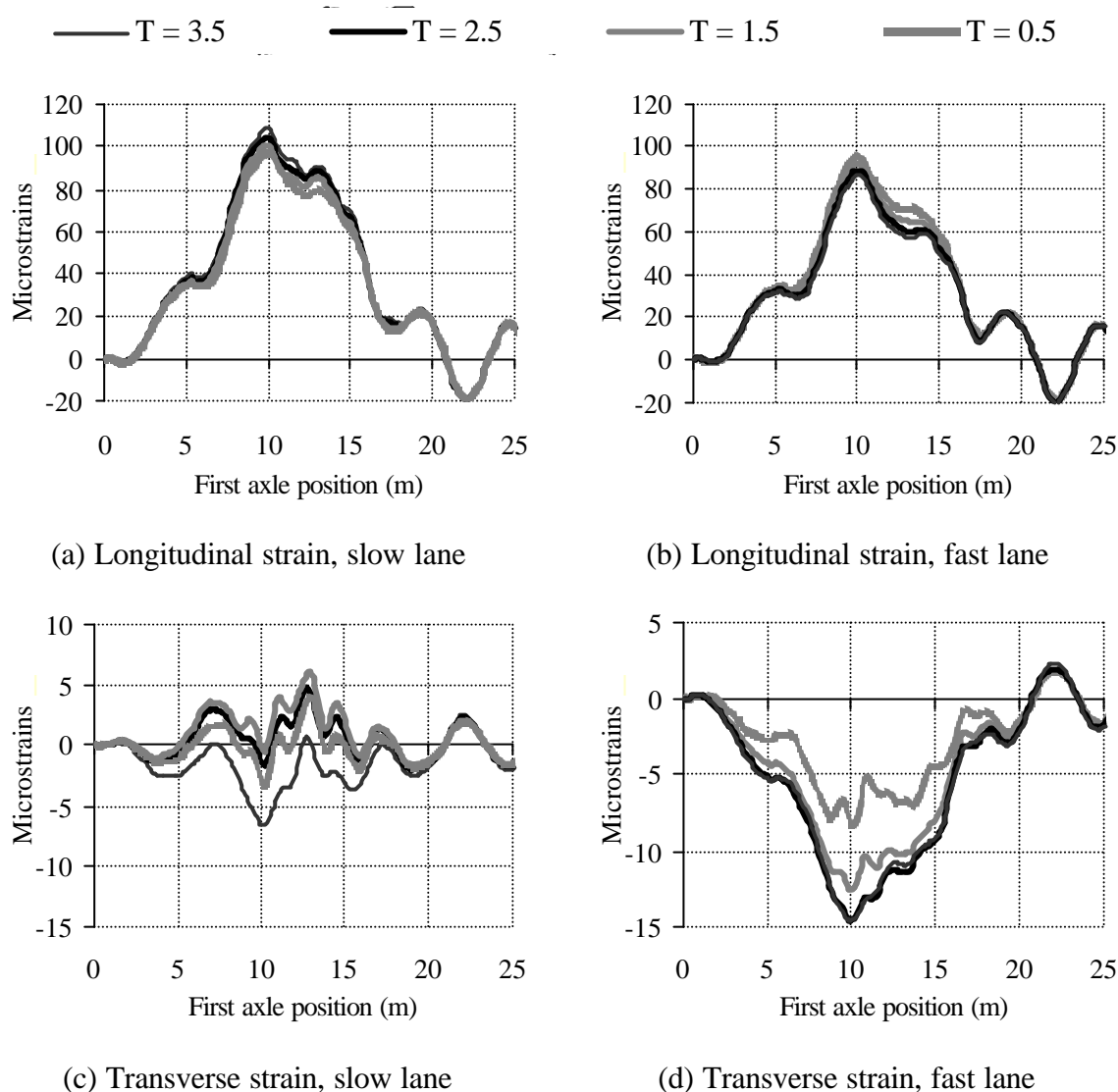


Figure 6.37 – Total strain at midspan (longitudinal distance of the sensor from start of the bridge: 8 m; T : Transverse location from bridge centreline)

The bridge response at 8 m from the bridge start and 2.5 m from the centreline (approximately centre of slow lane) when a two-axle truck travels over the slow lane at different speeds and weights is represented in Figure 6.38. Figures 6.38(b), (d) and (f) illustrate the importance of the dynamic component in the total transverse strain, especially at the highest speed. The dynamic component of longitudinal strain (Figures 6.38(a), (c) and (e)) is more significant at 70 and 85 km/h than at 55 km/h. The two heaviest vehicles (Figures 6.38(c) and (e)) follow a very similar strain pattern, though different in magnitude.

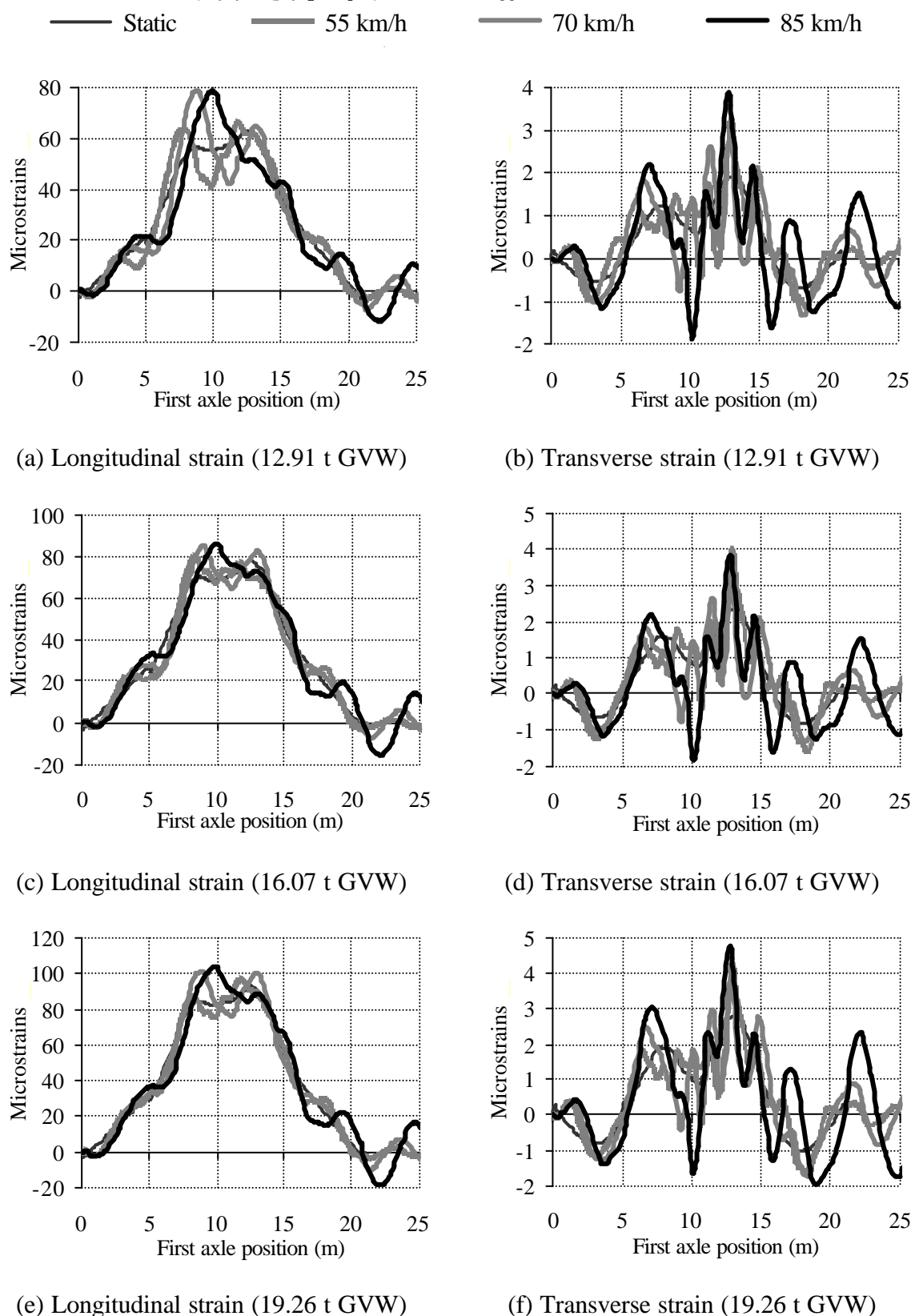


Figure 6.38 – Strain at midspan for different speeds and weights (sensor approx. in centre of slow lane) (GVW = gross vehicle weight)

The longitudinal and transverse strain caused by the lightest two-axle truck (12.91 t) travelling at 70 km/h is represented in the frequency domain in Figure 6.39. The spectrum of the total response reveal the presence of this dynamic component below 5 Hz. The spectrum of the static response have a significant component at frequencies close to 4.5 Hz (first natural frequency of the bridge), which is likely to cause interference with the dynamic response of the bridge.

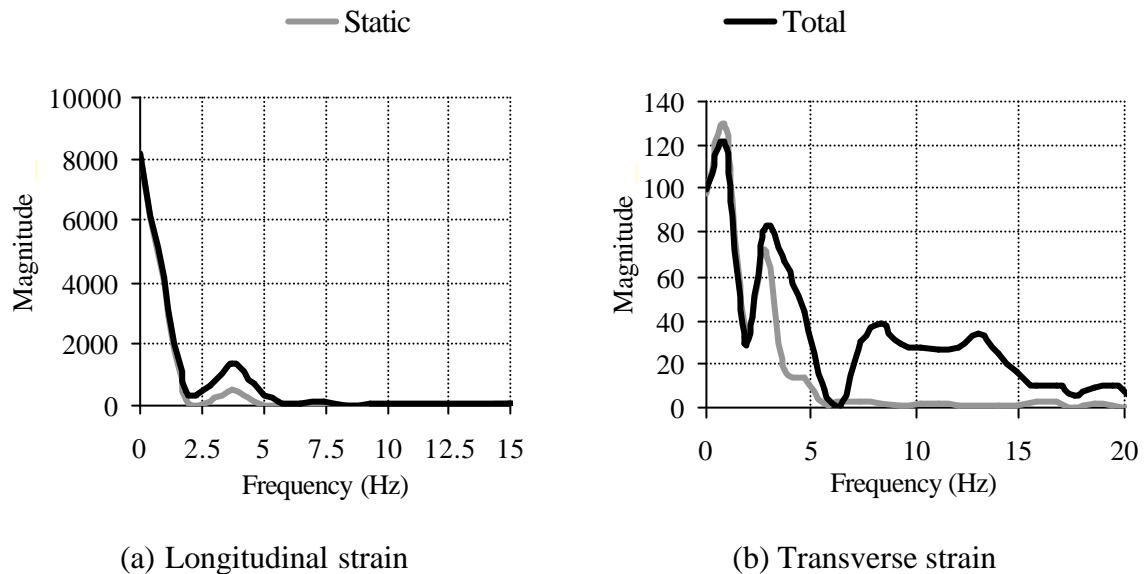


Figure 6.39 – Spectra of strain at midspan (sensor approx. in centre of slow lane)

For vehicles travelling at speed lower than 70 km/h, the spectra of the static response will be defined for lower frequency components (as more time will be necessary to cross the bridge), and the dynamic interference will decrease.

Different Truck Transverse Locations

B-WIM systems normally add all strains transversely at each longitudinal location to compensate for the deviations introduced by different truck transverse positions. However, the bridge bends more at some particular transverse locations and the added strain is also bigger. This effect is shown in Figure 6.40. The inner wheels of the two-axle truck (16.07 t) are driven at 0, 1 and 2 m from the centreline. Four different measurements equally spaced along the bridge section are added together in Figure 6.40. It can be observed that the magnitudes differ for the same speed when the truck moves just 1 m laterally, and B-WIM systems might require further consideration of the truck transverse location.

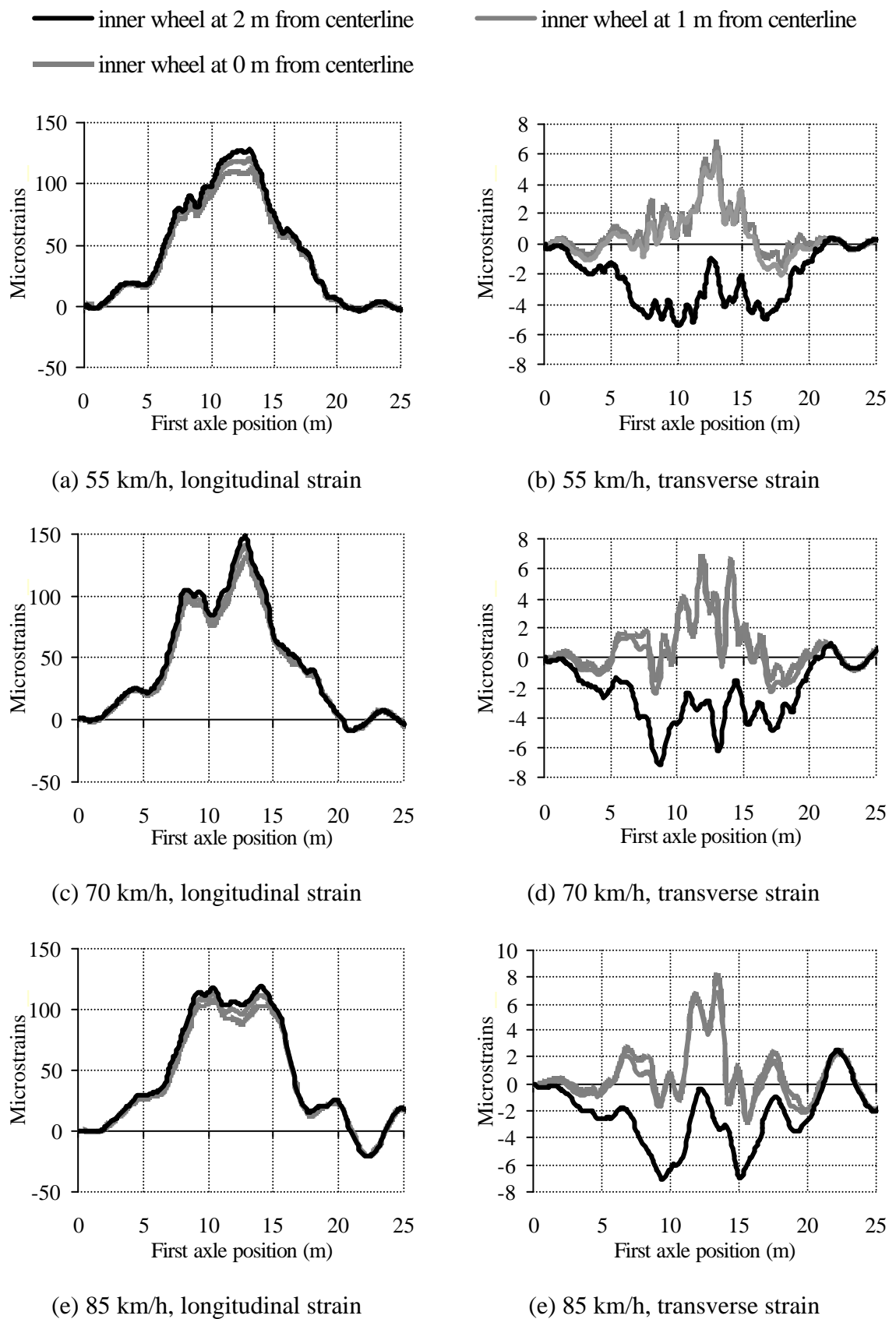
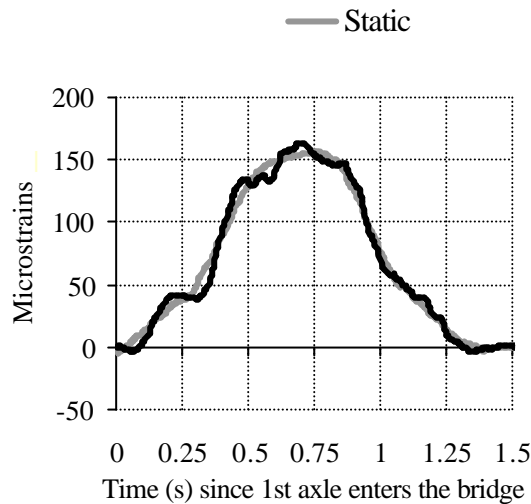


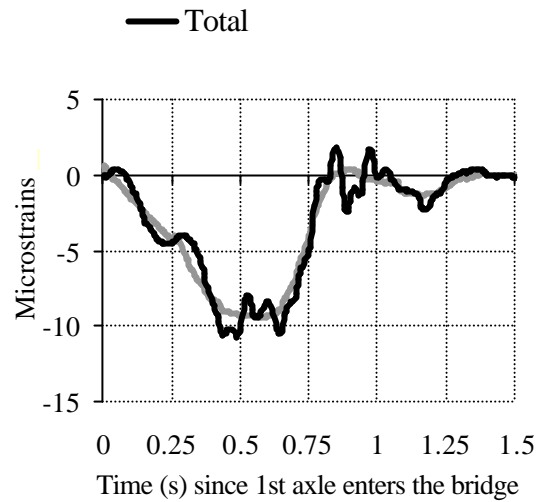
Figure 6.40 – Strain at midspan due to a two-axle (16.07 t) truck at different truck distances from centreline

Simultaneous Traffic Events

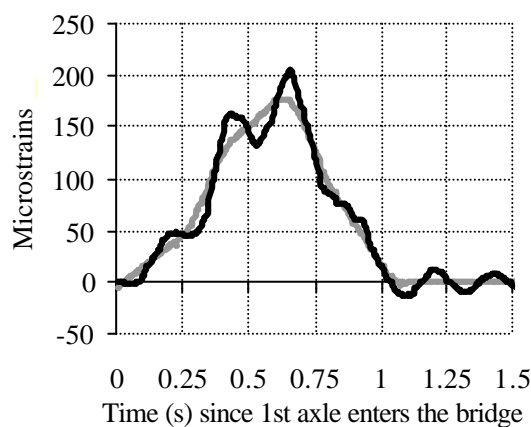
Figure 6.41 show the bridge response for different combinations of two-axle (16.07 t) and three-axle (22 t) trucks running in opposite directions (Figure 6.31(b)).



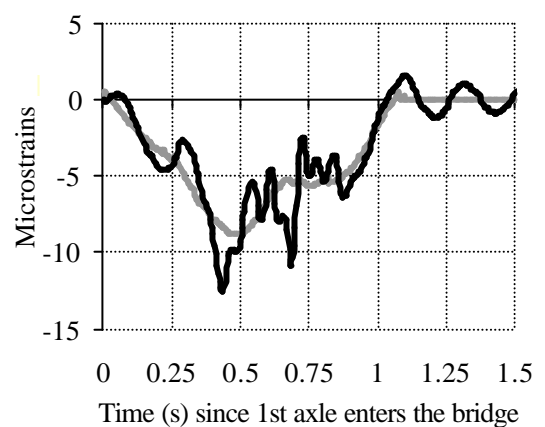
(a) 3-axle at 55 km/h and 2-axle at 70 km/h,
longitudinal strain



(b) 3-axle at 55 km/h and 2-axle at 70 km/h,
transverse strain

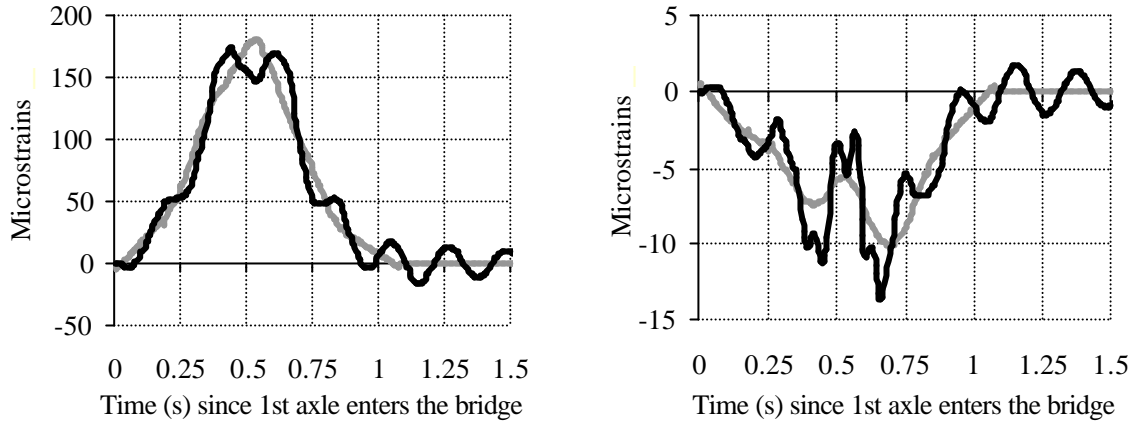


(c) 3-axle and 2-axle at 70 km/h,
longitudinal strain



(c) 3-axle and 2-axle at 70 km/h,
transverse strain

Figure 6.41 (continued on following page)



(e) 3-axle at 85 km/h and 2-axle at 70 km/h, longitudinal strain
(f) 3-axle at 85 km/h and 2-axle at 70 km/h, transverse strain

Figure 6.41 – Longitudinal strain at midspan (sensor approx. in centre of slow lane)

B-WIM measurements are generally restricted to only one truck being on the bridge (Section 3.2). In the cases of Figure 6.41, the total response vibrates around the static response and it is more favourable at lower speeds from the point of view of B-WIM measurements (less amplitude and more oscillations).

6.5.2 Two-Span Isotropic Slab

A two-span isotropic bridge model is illustrated in Figure 6.42. The bridge has a uniform rectangular cross-section of 0.8 m depth. The deck is supported on four bearings at either end and on two bearings at the centre. Supports are spaced longitudinally at 18 m and horizontal translation is prevented at one end. The length of the elements along the span was chosen as 1.2 m and their width 1 m, except for the rows of elements at each edge which are 0.9 m wide and the elements at each end which are 0.5 m long.

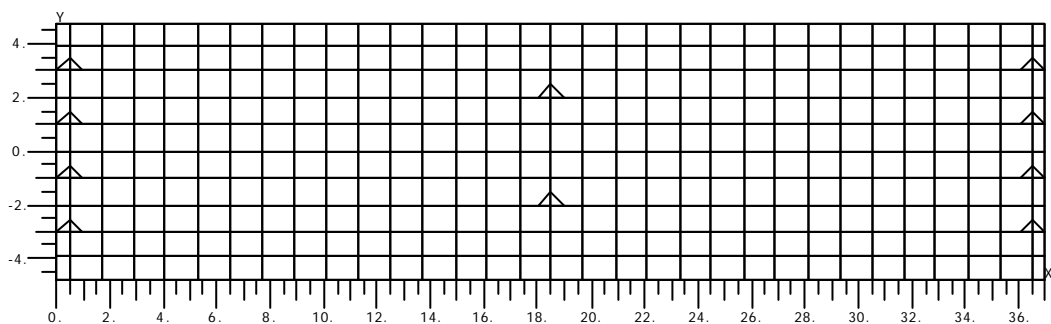


Figure 6.42 – Two-Span Slab Finite Element Model

Influence lines of longitudinal and transverse bending due to a unit axle load travelling on the slow lane are represented in Figure 6.43.

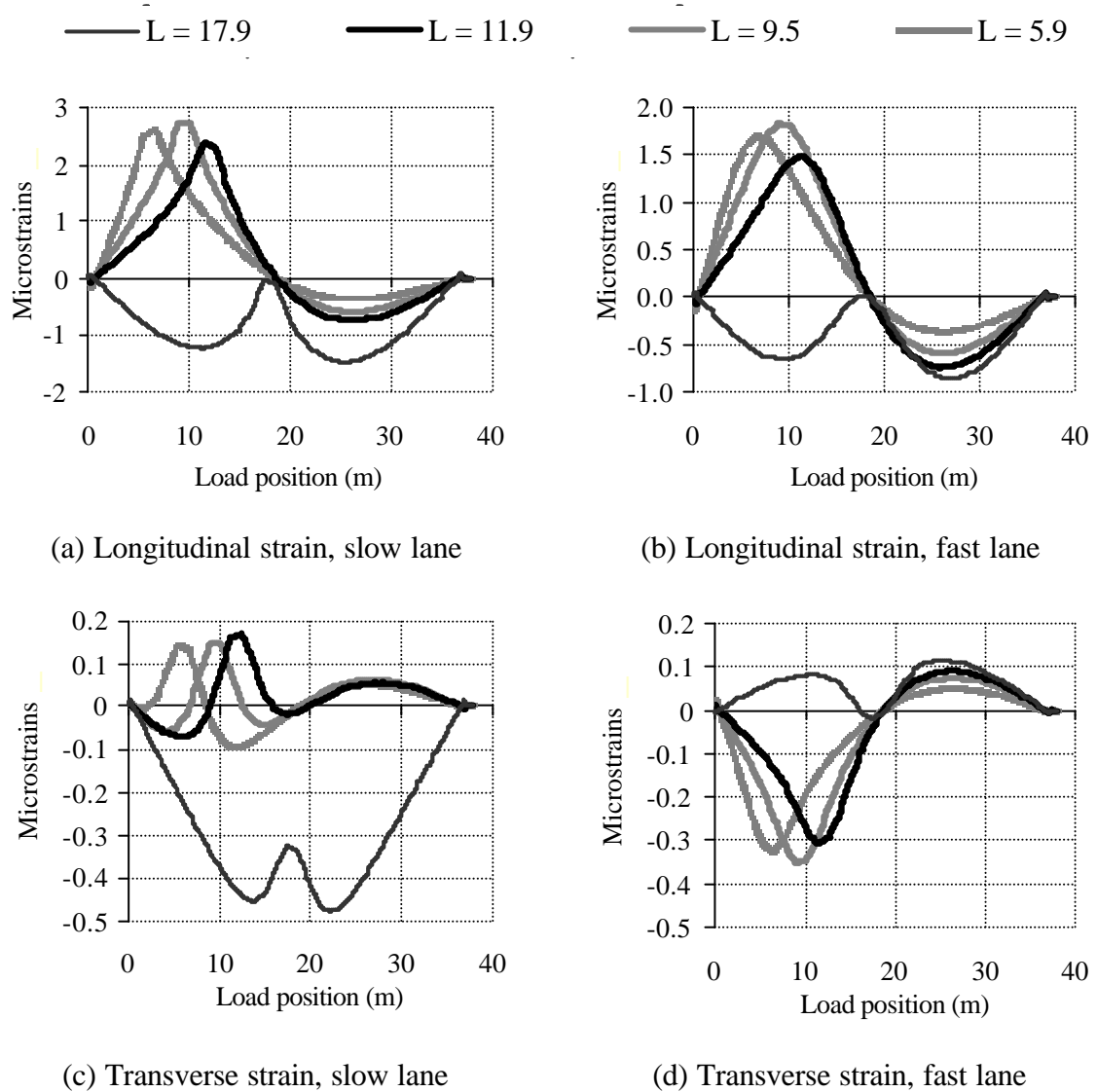


Figure 6.43 – Influence line of strain at different locations in first span (L : longitudinal distance of the sensor from start of the bridge; Transverse location from bridge centreline: 2.5 m)

Figure 6.44 shows the main six modes of vibration of this structure.

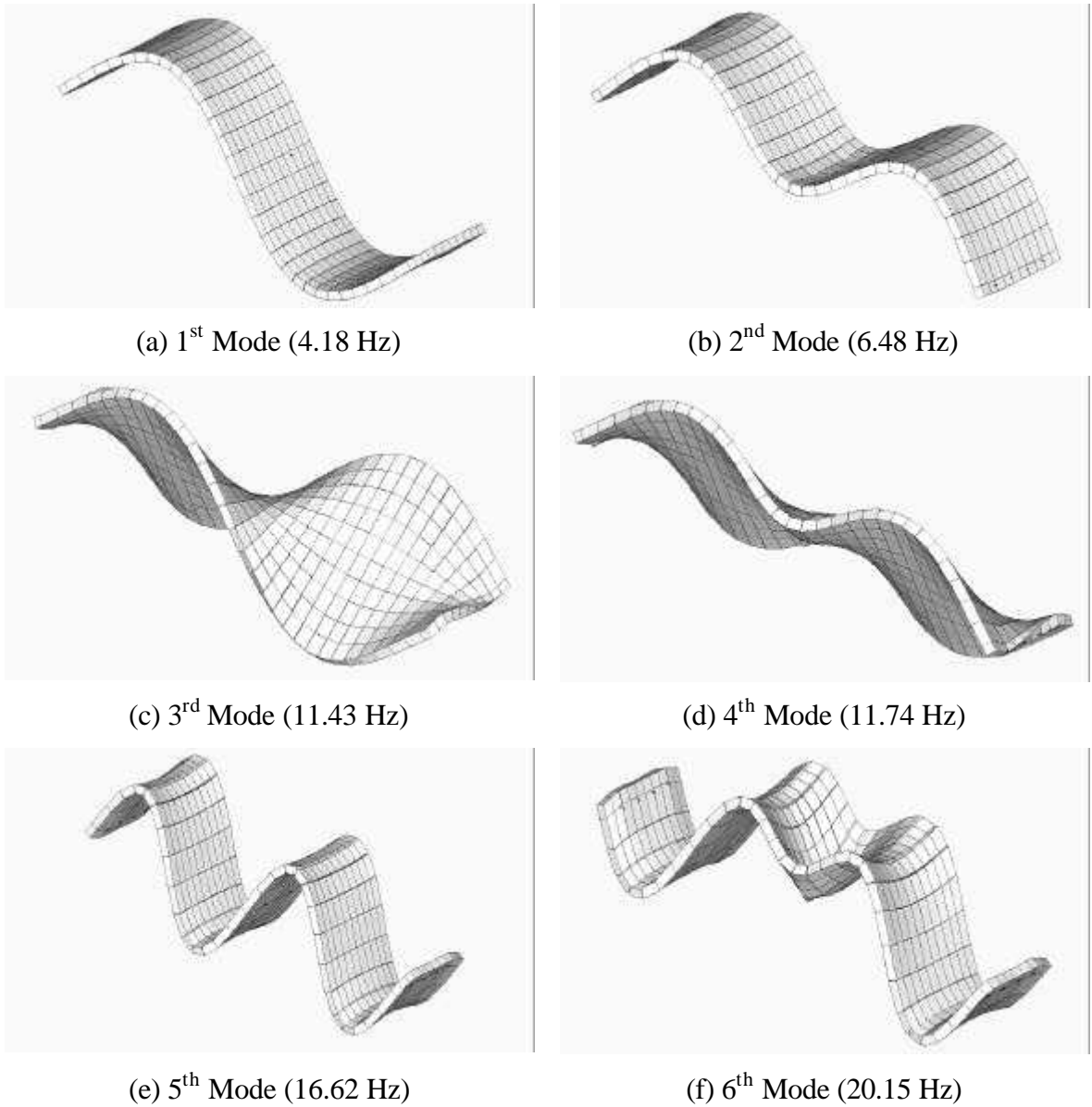
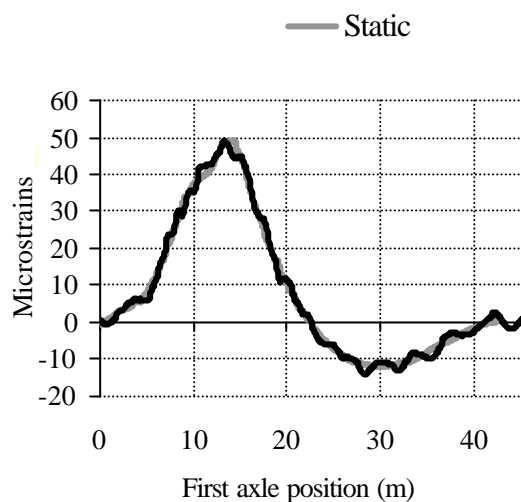
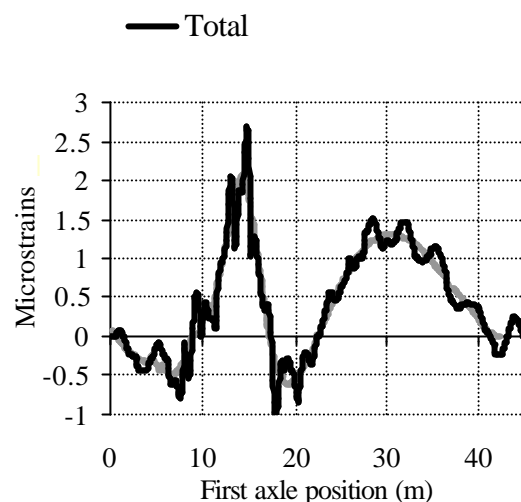


Figure 6.44 - Modes of vibration of the Two-Span Slab

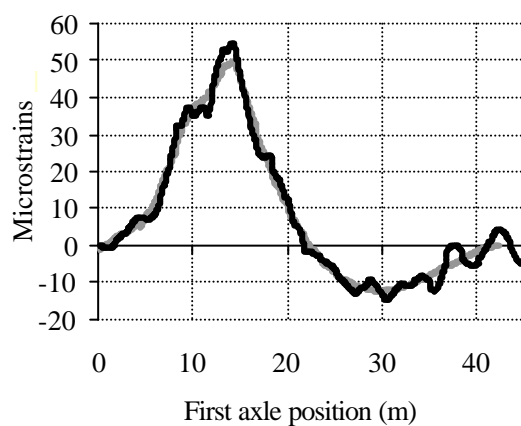
Results of simulations performed for a three-axle truck (22 t GVW) are illustrated in Figure 6.45.



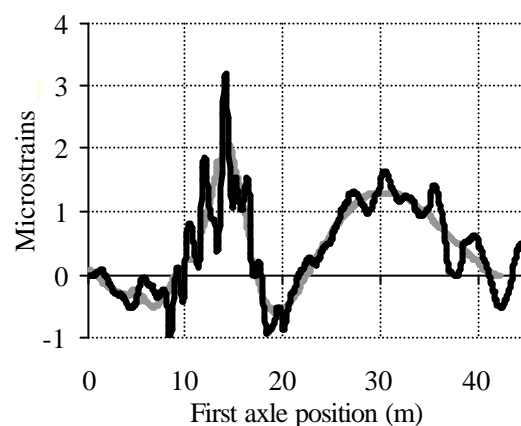
(a) 55 km/h, longitudinal strain



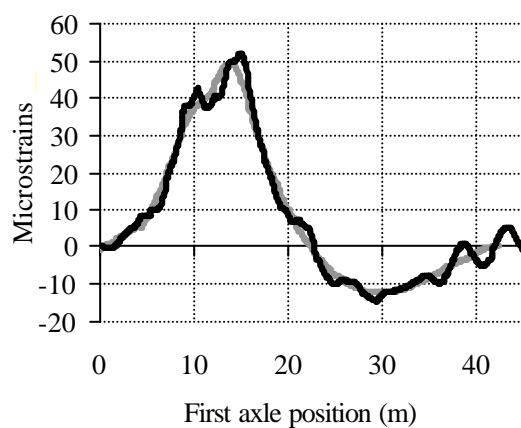
(b) 55 km/h, transverse strain



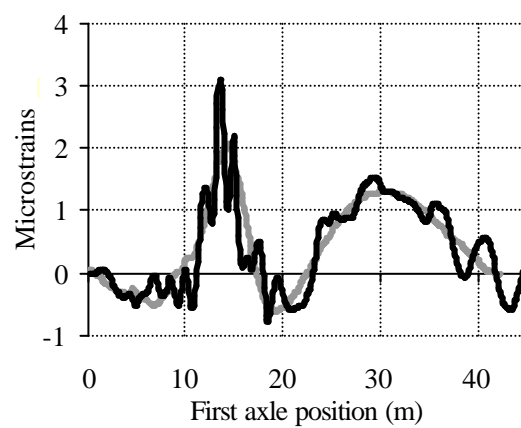
(c) 70 km/h, longitudinal strain



(d) 70 km/h, transverse strain



(e) 85 km/h, longitudinal strain



(f) 85 km/h, transverse strain

Figure 6.45 – Strain at midspan of first span (sensor approx. in centre of slow lane)

The results at 70 km/h are represented in the frequency domain in Figure 6.46. Though there are also significant dynamic components below 5 Hz, unlike the response of the

single span bridge, the highest component of the spectrum takes place over the zero frequency component for the longitudinal strain and it is maximum for the zero frequency component in the case of transverse bending.

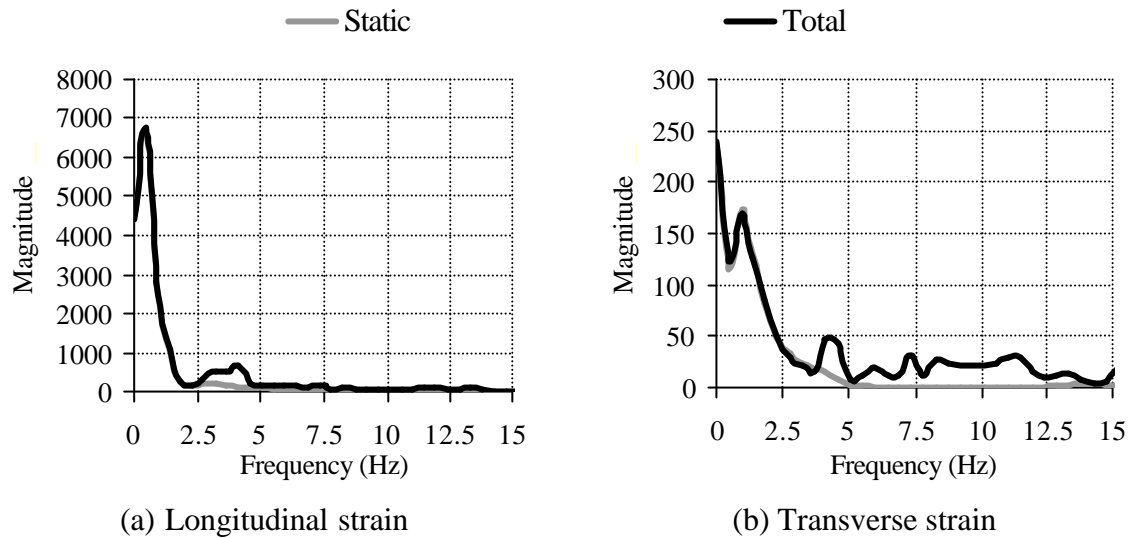


Figure 6.46 – Spectra of strain at midspan (sensor approx. in centre of slow lane)

Sensors are less sensitive to low frequency dynamics in certain locations, i.e., near the central support. The response at this location under the slow lane is given in Figure 6.47. Figure 6.48 shows the spectra of this response for a speed of 70 km/h. Compared to the spectra in Figure 6.46, it can be seen the difference between static and total response below 5 Hz is greatly reduced.

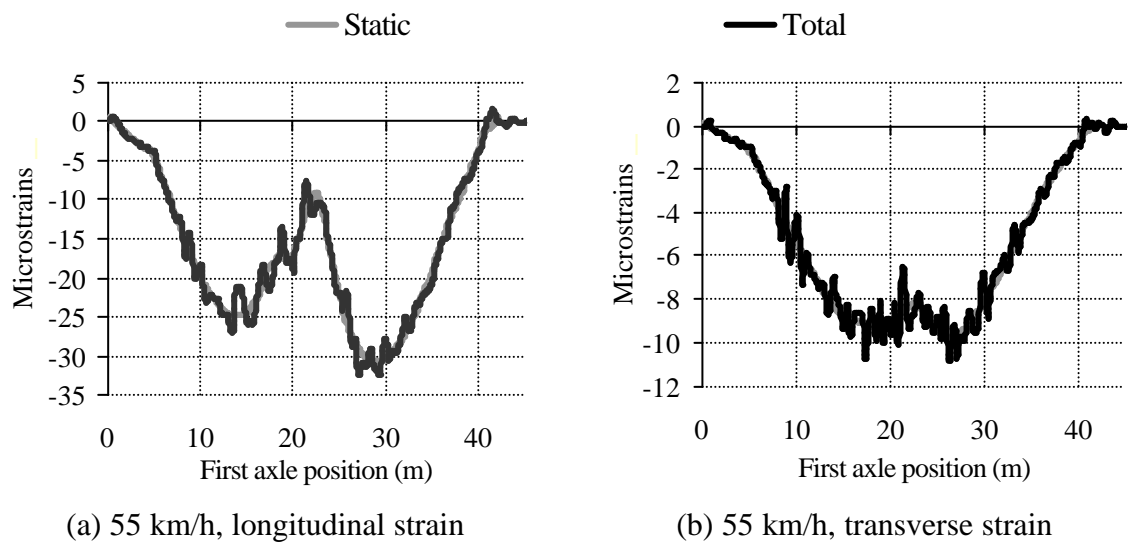
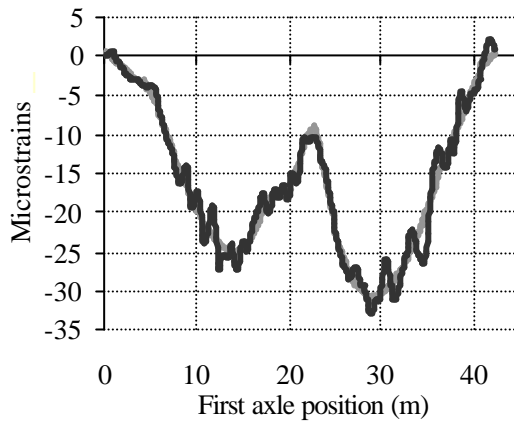
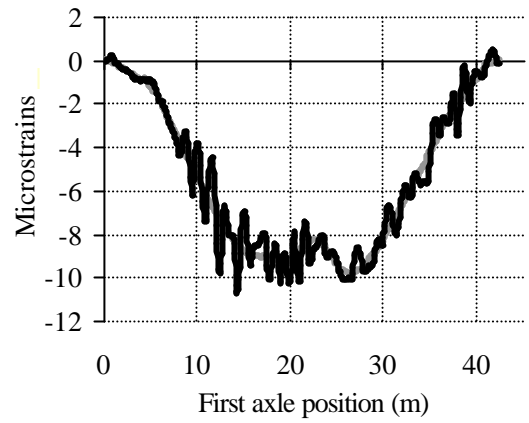


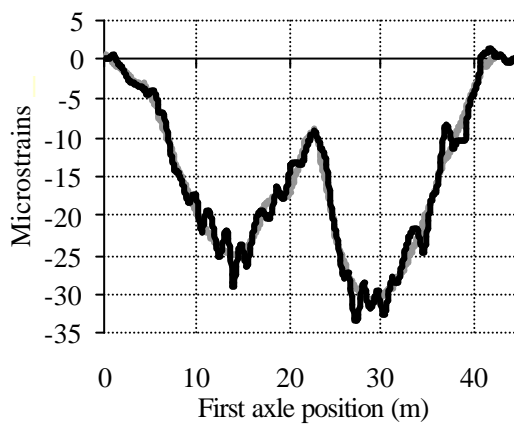
Figure 6.47 (continued on following page)



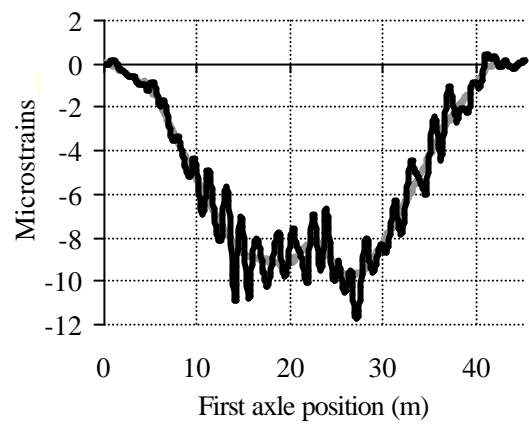
(c) 70 km/h, longitudinal strain



(d) 70 km/h, transverse strain

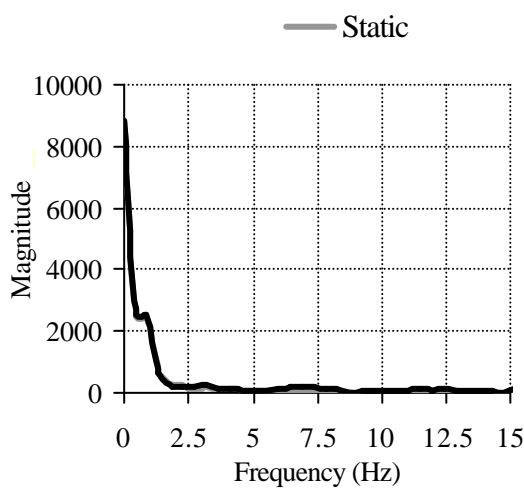


(e) 85 km/h, longitudinal strain

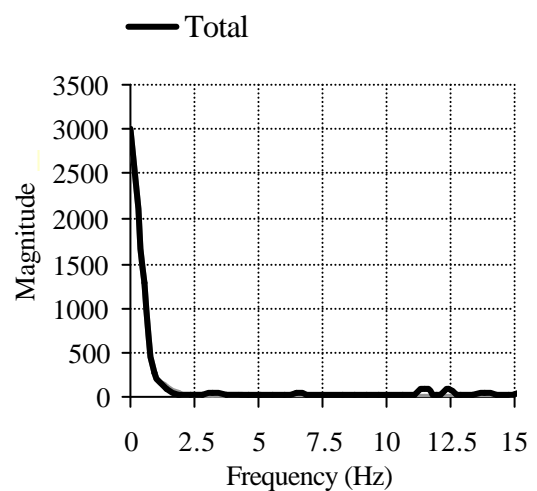


(f) 85 km/h, transverse strain

Figure 6.47 – Strain at central support (sensor approx. in centre of slow lane)



(a) Longitudinal strain



(b) Transverse strain

Figure 6.48 – Spectra of strain at central support (sensor approx. in centre of slow lane)

6.5.3 Slab with Edge Cantilever

A planar model as shown in Figure 6.37, is used to represent a bridge with edge cantilever, simply supported on three bearings at each end. The cross-section is divided into four different types of element. Three rows of plate elements are used to model each edge cantilever (element type numbers 2, 3 and 4 in Figure 6.49). The depth of these elements is calculated according to the real second moment of area and their density is also adjusted to achieve equal mass per unit length in the longitudinal direction. All elements are 1 m long. Two different elastic moduli are specified for each element type to allow for the variation of second moment of area in the two directions.

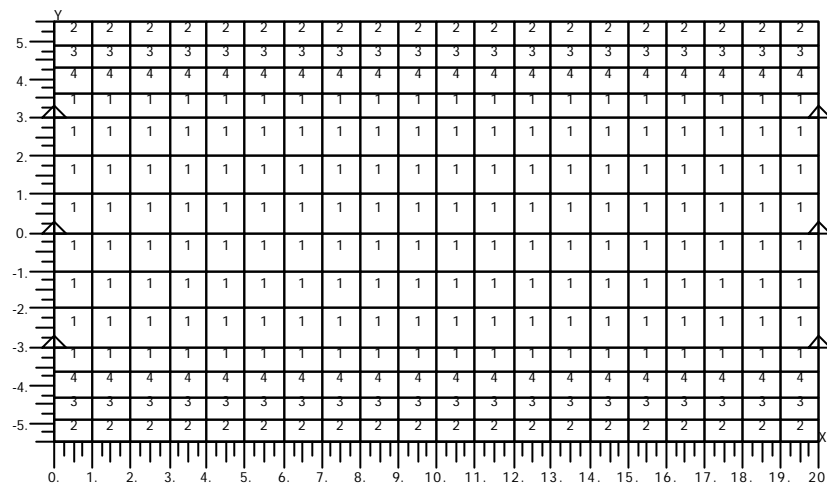


Figure 6.49 – Finite element model of slab with edge cantilever

Figure 6.50 illustrates the static response, at different bridge locations, to the passing of a unit axle load along the slow lane. Figure 6.51 shows the modes of vibration of this structure.

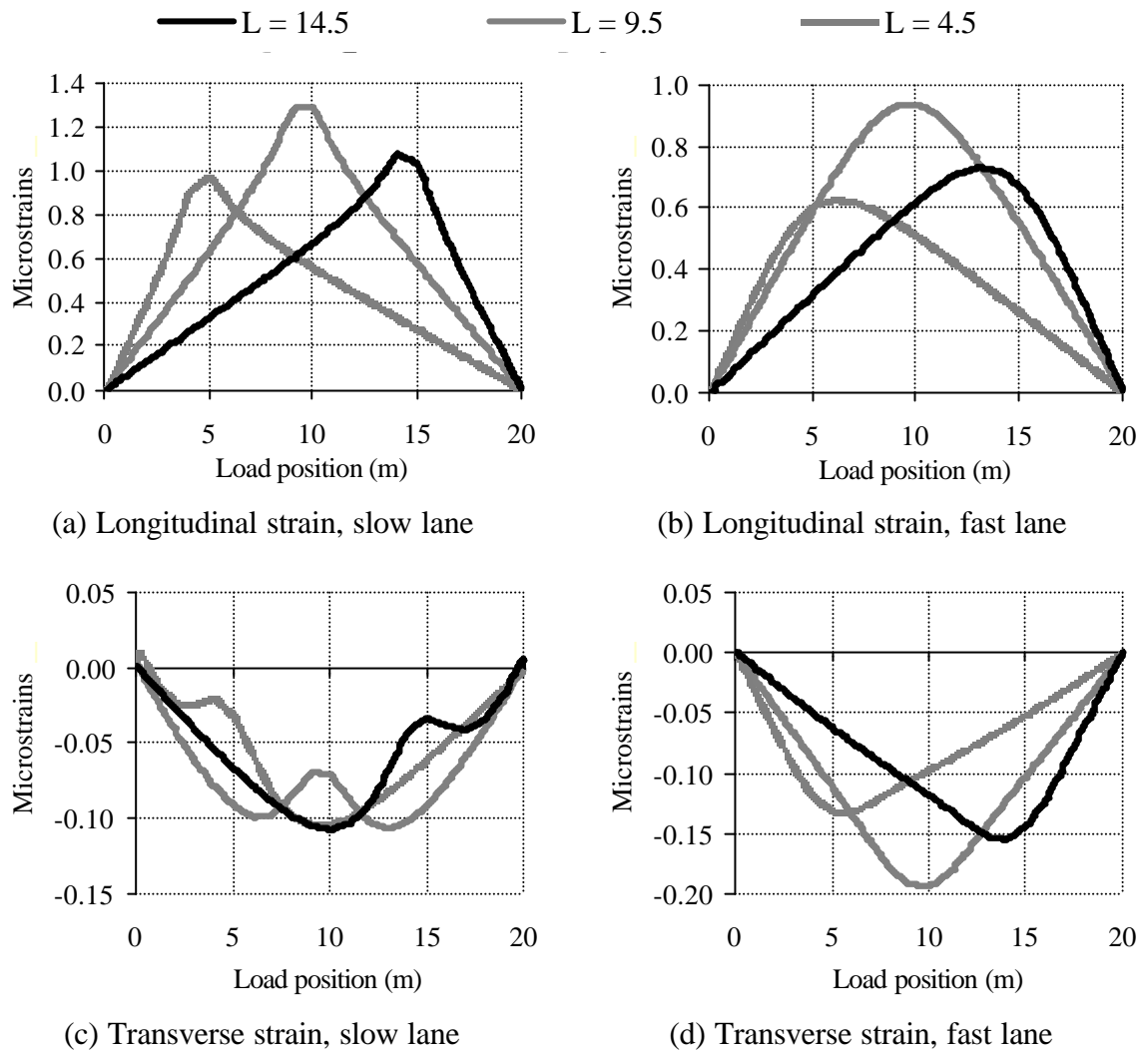


Figure 6.50 – Influence line of strain (L : longitudinal distance of the sensor from start of the bridge; transverse location from bridge centreline: 2.5 m)

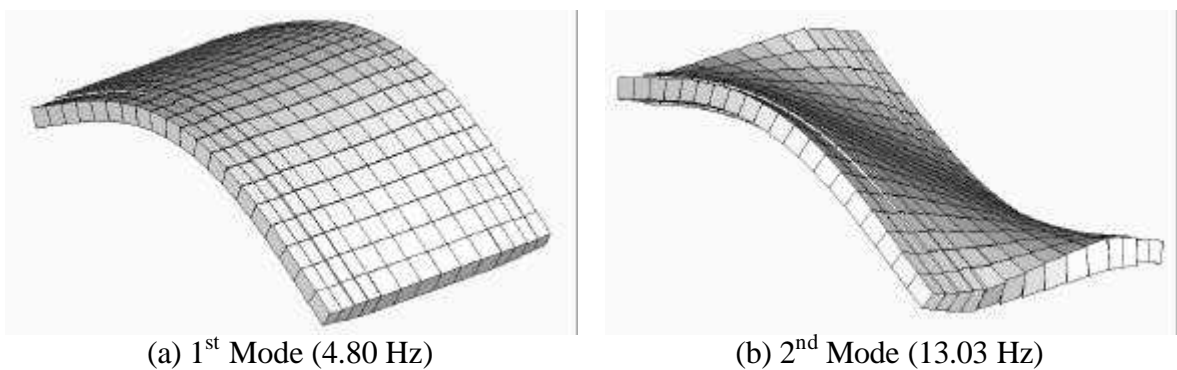


Figure 6.51 (continued on following page)

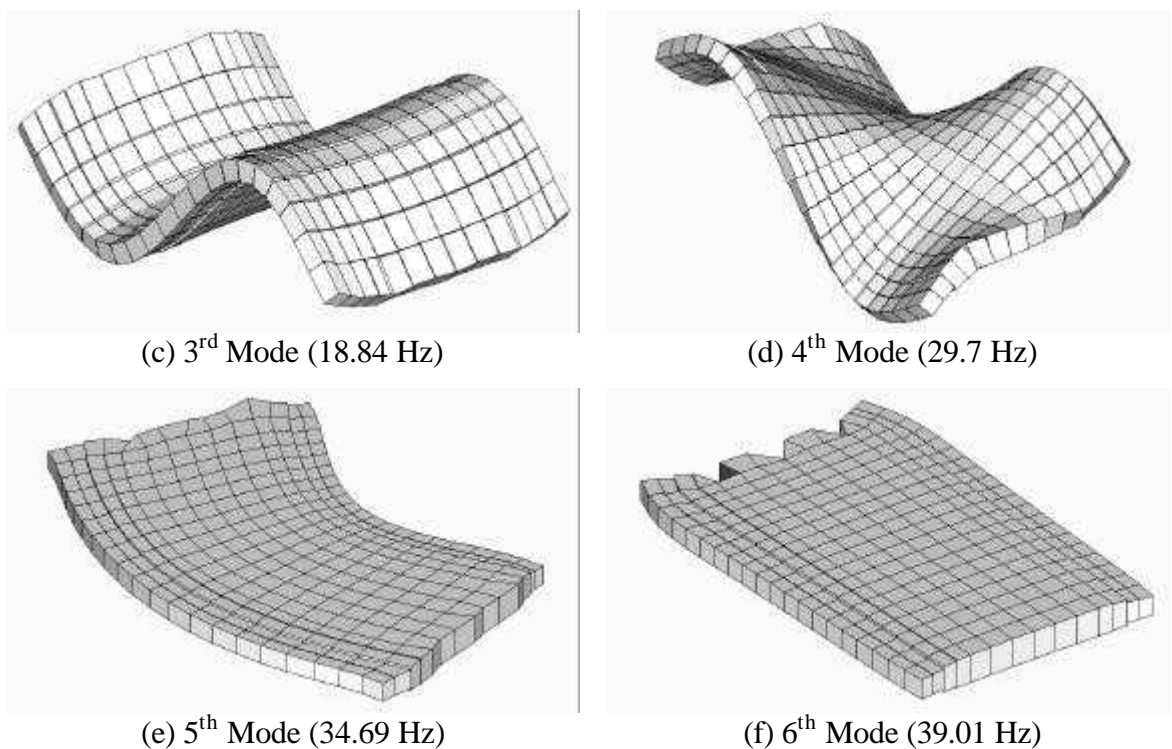


Figure 6.51 - Modes of vibration of a Slab with Edge Cantilever

Results of simulations performed for the lightest three-axle truck (22 t) are illustrated in Figure 6.52. The spectra of the response at 70 km/h are represented in Figure 6.53. Differences between total and static are noticeable below 5 Hz due to the influence of the first natural frequency of the bridge (4.8 Hz).

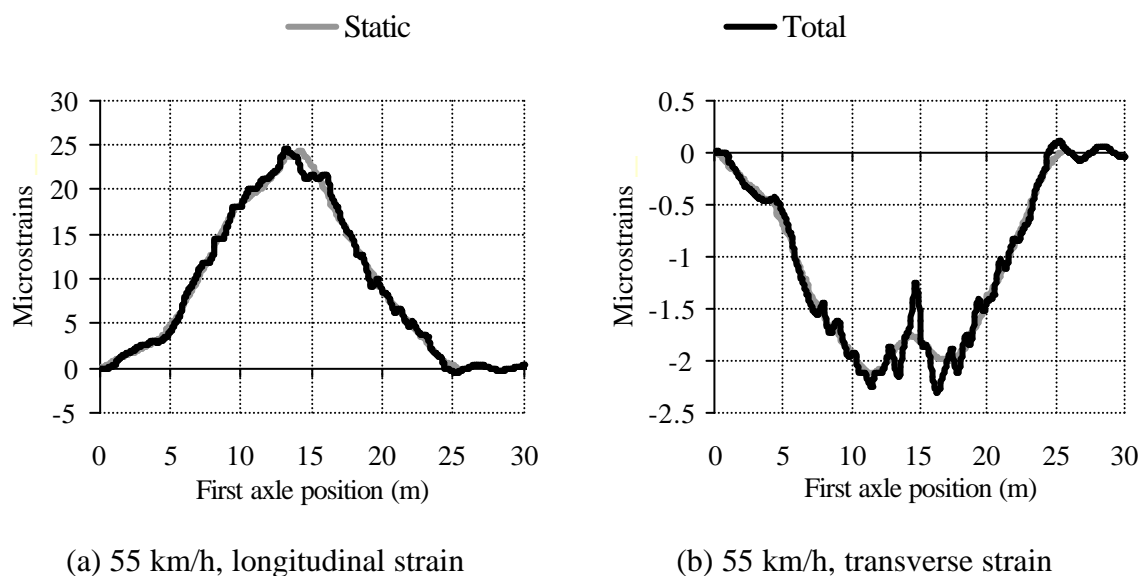
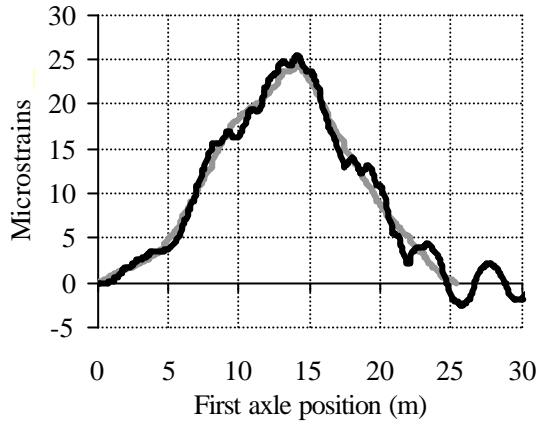
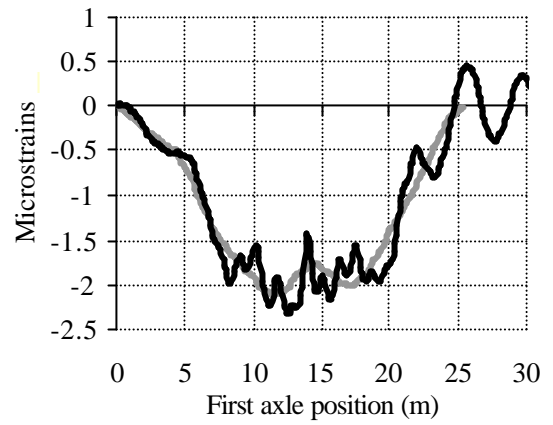


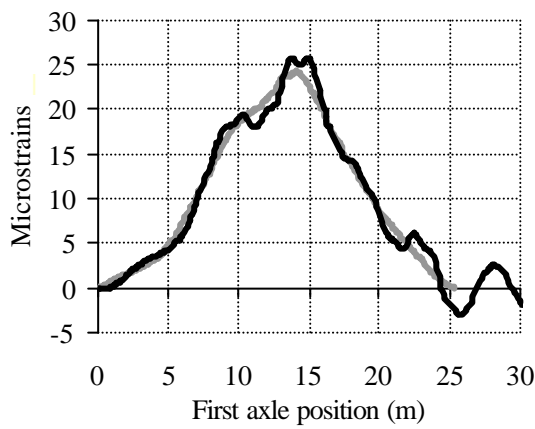
Figure 6.52 (continued on following page)



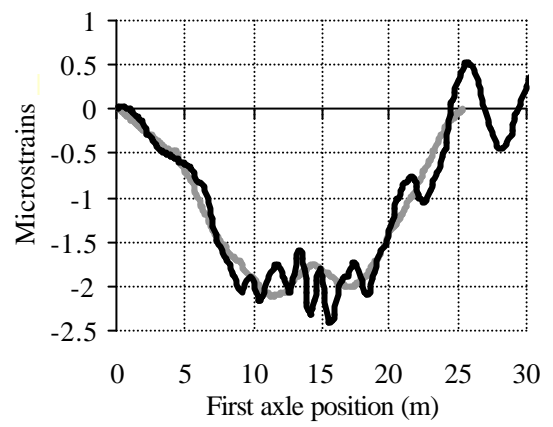
(b) 70 km/h, longitudinal strain



(c) 70 km/h, transverse strain

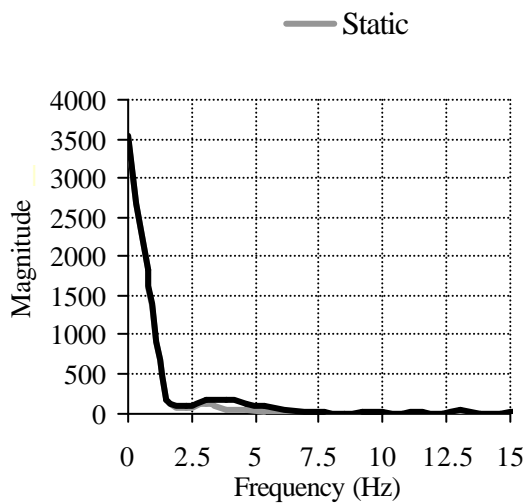


(c) 85 km/h, longitudinal strain

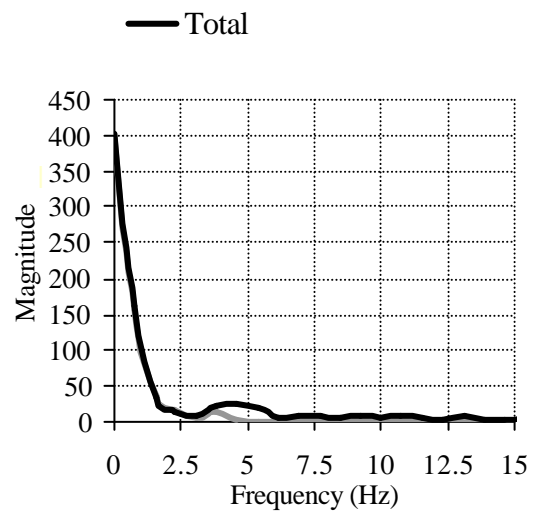


(c) 85 km/h, transverse strain

Figure 6.52 – Strain at midspan (sensor approx. in centre of slow lane)



(a) Longitudinal strain



(b) Transverse strain

Figure 6.53 – Spectra of strain at midspan (sensor approx. in centre of slow lane)

6.5.4 Voided Slab Bridge

A 25 m voided slab deck, supported on four bearings at either end, is illustrated in Figure 6.54. The void stops short at each end forming solid diaphragm beams 1 m wide over the supports. The orthotropic geometry of the voided slab (different second moment of area in x and y directions) is modelled by selecting a different modulus of elasticity in the longitudinal and transverse directions (element type 1 in Figure 6.54) as recommended by O'Brien & Keogh (1999). The diaphragm beams are solid, and thus, they have the same modulus of elasticity in both directions (element type 2 in Figure 6.54).

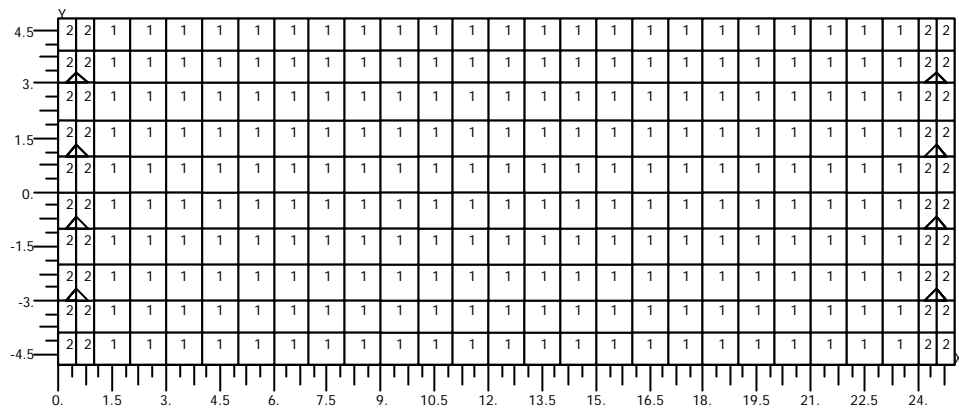


Figure 6.54 – Voided Slab Finite Element Model

Influence lines are shown in Figure 6.55.

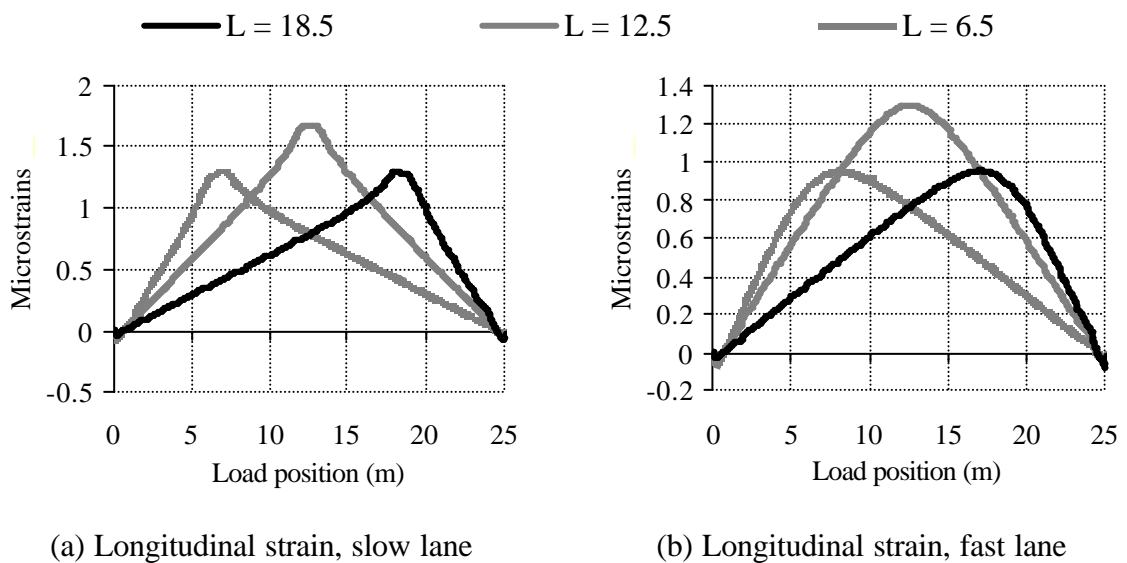
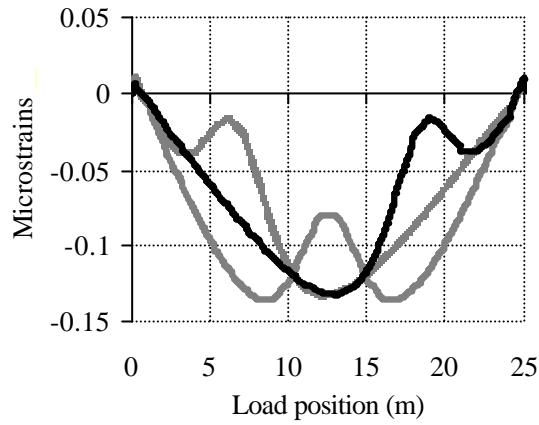
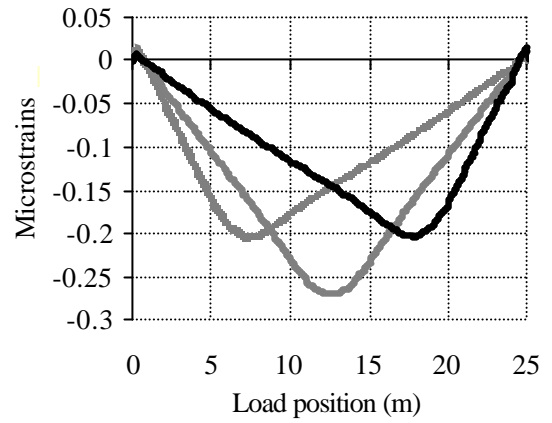


Figure 6.55 (continued on following page)



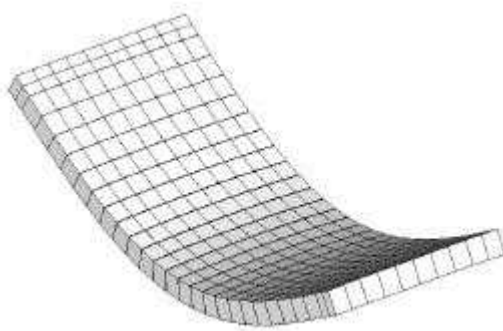
(c) Transverse strain, slow lane



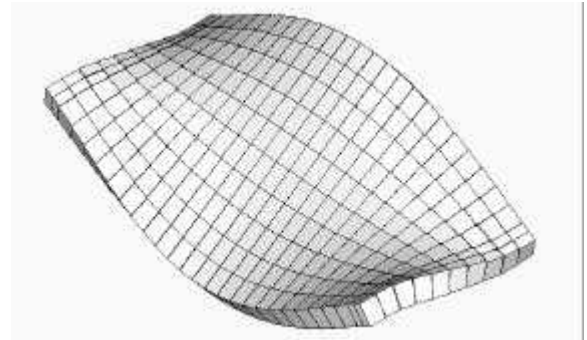
(d) Transverse strain, fast lane

Figure 6.55 – Influence line of strain (L : longitudinal distance of the sensor from start of the bridge; transverse location from bridge centreline: 2.5 m)

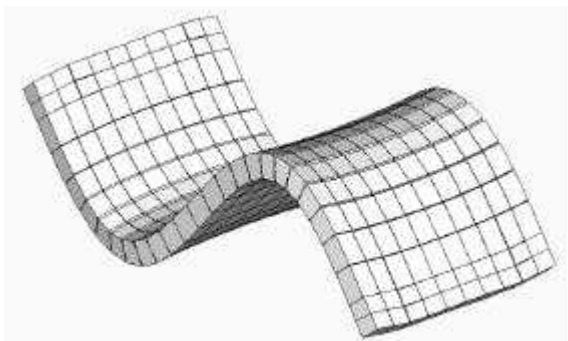
The main modes of vibration are represented in Figure 6.56.



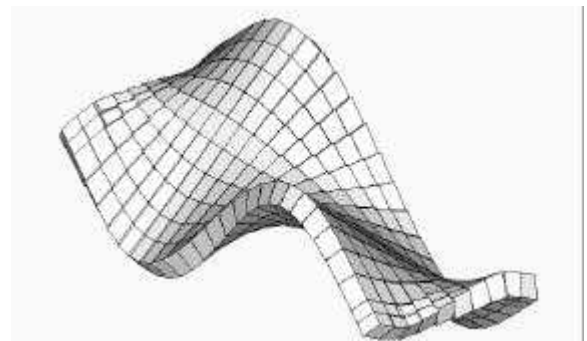
(a) 1st Mode (3.80 Hz)



(b) 2nd Mode (12.73 Hz)

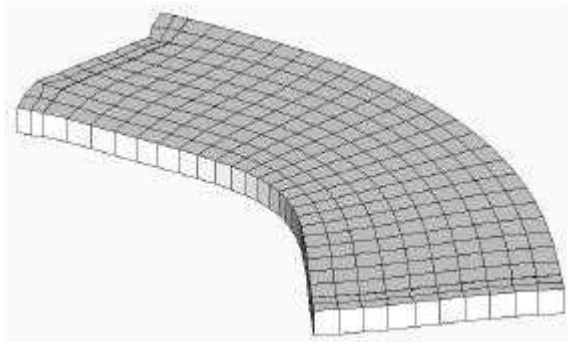


(c) 3rd Mode (15.08 Hz)

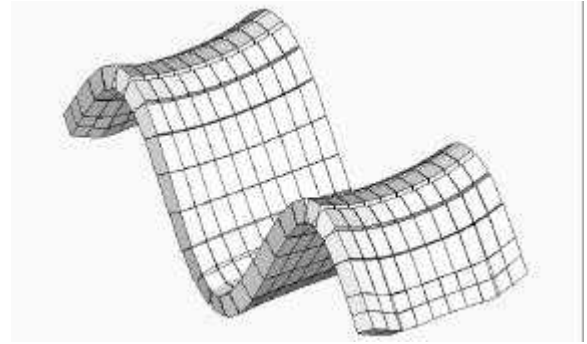


(d) 4th Mode (27.96 Hz)

Figure 6.56 (continued on following page)



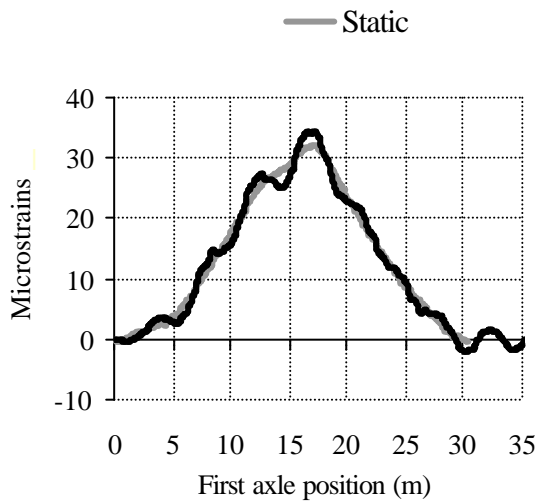
(d) 5th Mode (30.36 Hz)



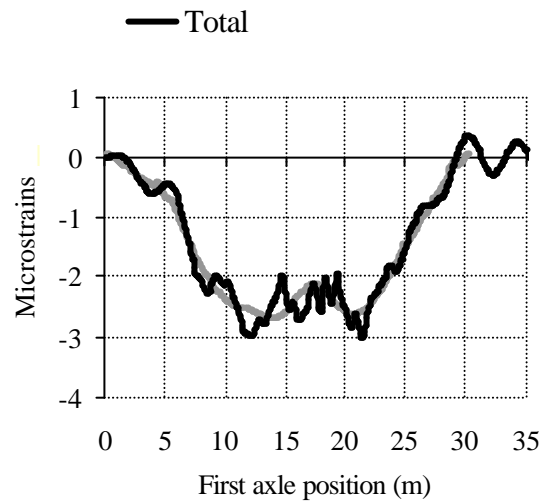
(e) 6th Mode (33.38 Hz)

Figure 6.56 - Modes of vibration of a Voided Slab

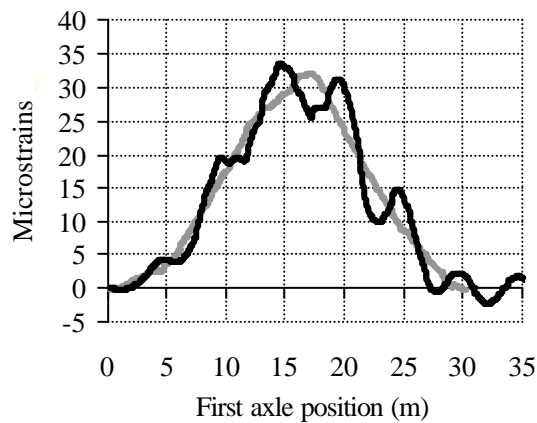
A three-axle truck (22 t) causes the response illustrated in Figure 6.57.



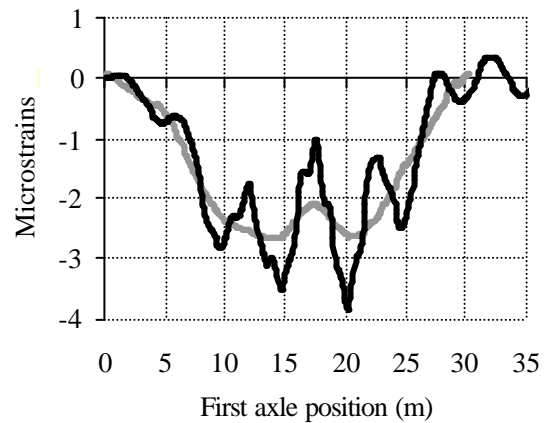
(a) 55 km/h, longitudinal strain



(b) 55 km/h, transverse strain

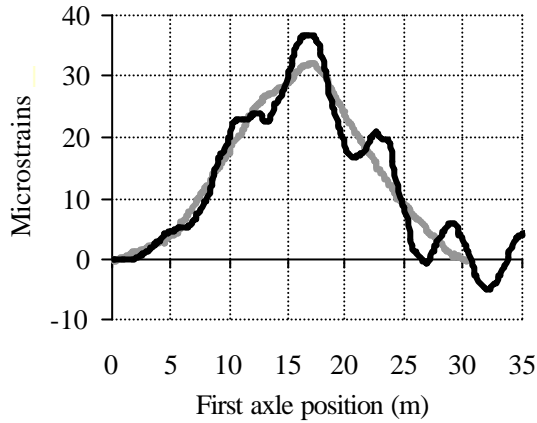


(c) 70 km/h, longitudinal strain

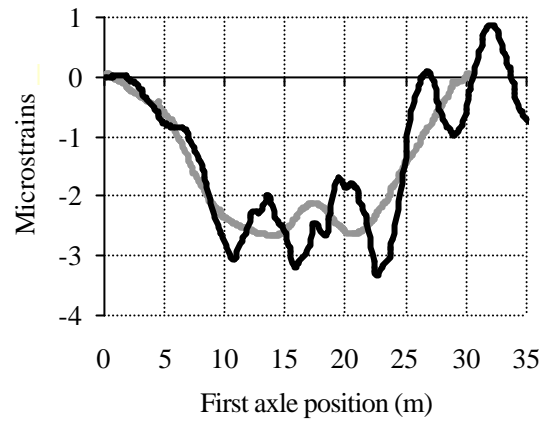


(d) 70 km/h, transverse strain

Figure 6.57 (continued on following page)



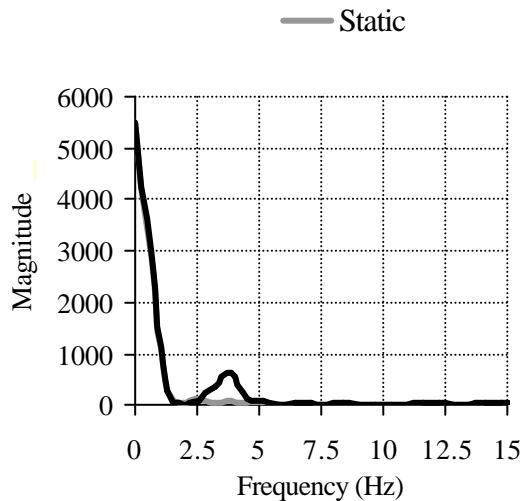
(e) 85 km/h, longitudinal strain



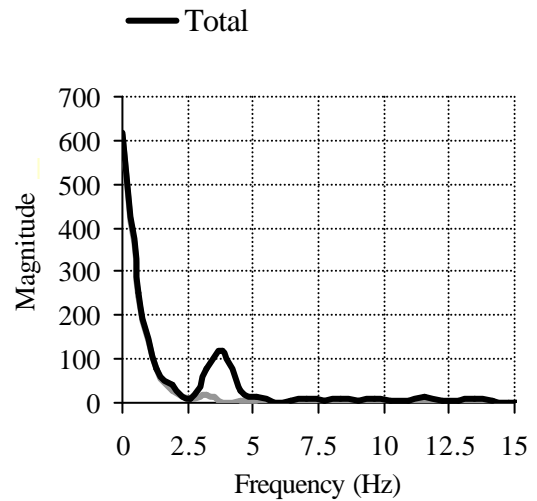
(f) 85 km/h, transverse strain

Figure 6.57 – Strain at midspan (sensor approx. in centre of slow lane)

The frequency domain representation of the response at 70 km/h shows a significant dynamic component below 5 Hz again (Figure 6.58). However, the dynamic component does not interfere as much as in previous cases (i.e. single span slab bridge). The bridge is longer, the vehicle takes more time in crossing and the static response is defined with lower frequency components than in shorter bridges.



(a) Longitudinal strain



(b) Transverse strain

Figure 6.58 – Spectra of strain at midspan (sensor approx. in centre of slow lane)

6.5.5 Beam and Slab

A beam and slab deck consists of a number of longitudinal beams connected across their tops by a thin continuous structural slab. In transfer of the load longitudinally to the supports, the slab acts in concert with the beams as their top flanges. In addition it acts to ensure sharing of load between beams. Figure 6.59 shows a plan-view of the model used for the simulations. The model consists of 8 precast concrete beams supported on bearings at each end. Solid diaphragm beams are extended 1 m over the supports. The elastic modulus of the precast beams is 34 kN/mm^2 and the in-situ slab is 31 kN/mm^2 . The plate elements are assigned a thickness of 0.16 m which is equal to the depth of the slab. In Figure 6.59, element type 1 represents the beam elements, element type 2 the diaphragm and element type 3 the slab elements.

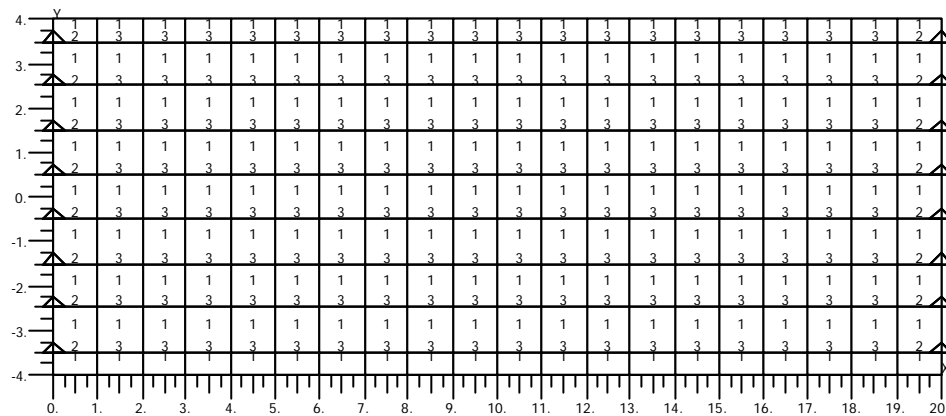


Figure 6.59 – Beam and Slab Bridge Finite Element Model

Figures 6.60 and 6.61 give influence lines for strain in plate elements and stress in beam elements respectively.

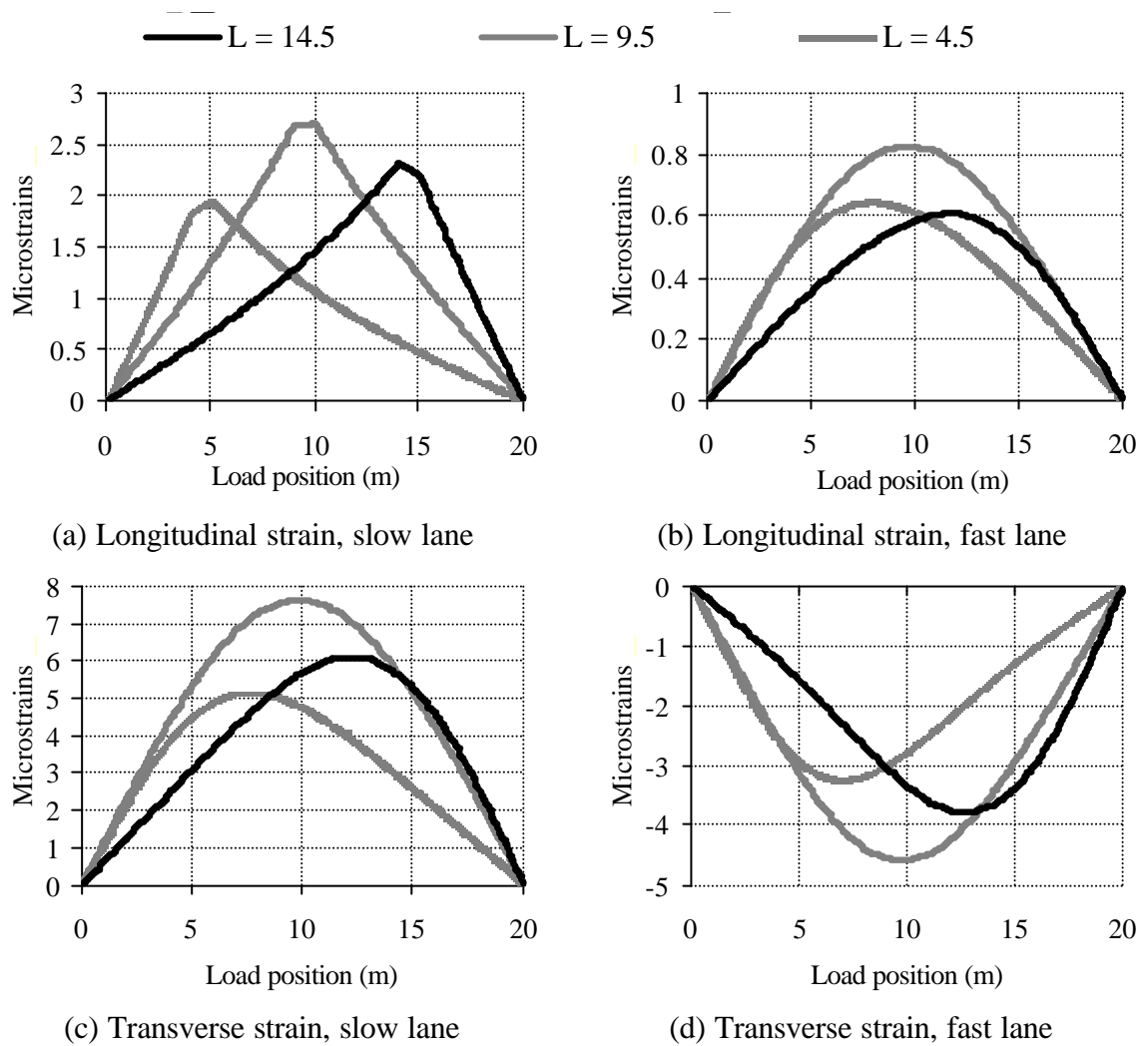


Figure 6.60 – Influence line of strain in plate elements (L : longitudinal distance of the sensor from start of the bridge; transverse location from bridge centreline: 2.0 m)

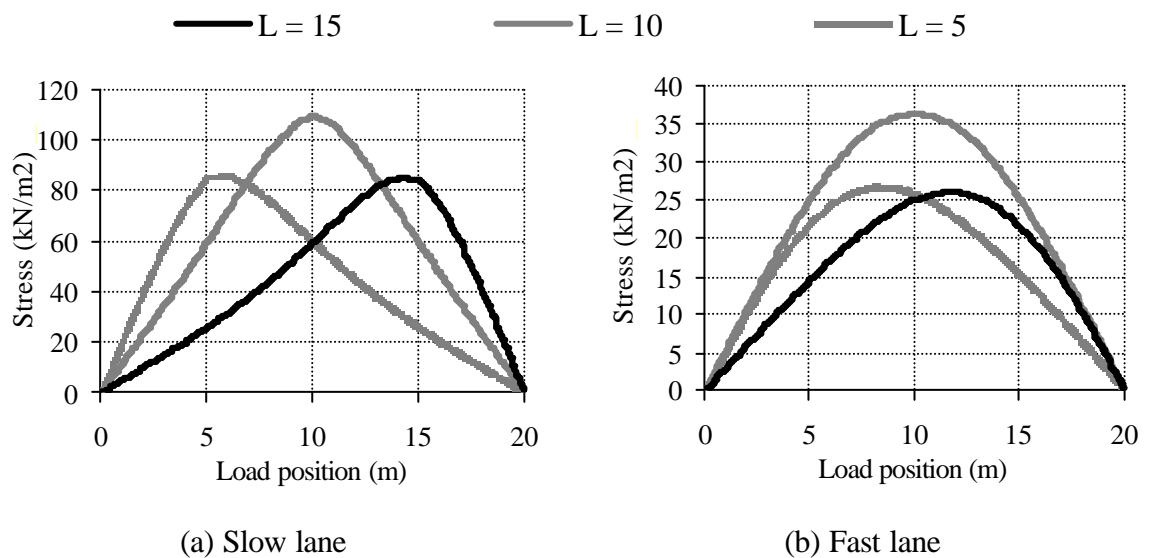


Figure 6.61 – Influence line of stress in beam elements (L : longitudinal distance of the sensor from start of the bridge; transverse location from bridge centreline: 1.5 m)

The modes of vibration of this beam and slab model are given in Figure 6.62.

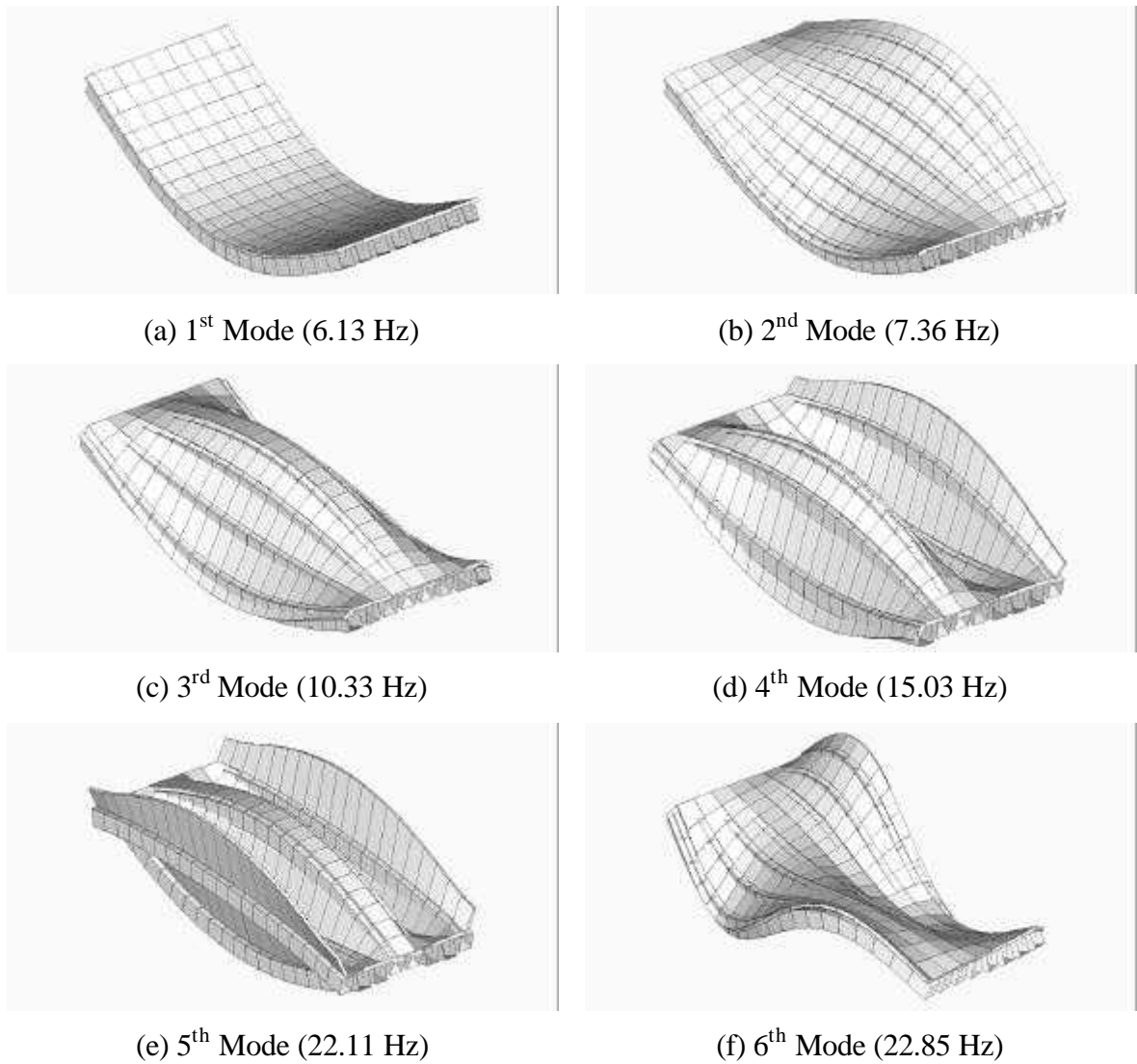
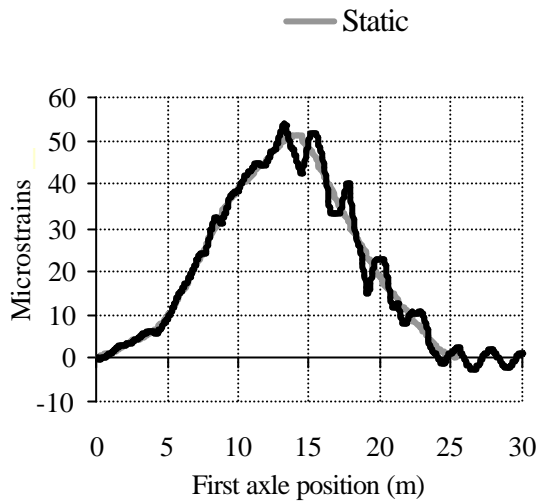
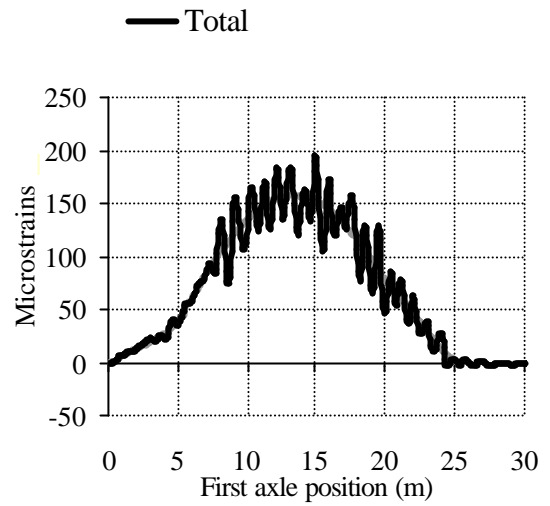


Figure 6.62 - Modes of vibration of a Beam and Slab Bridge

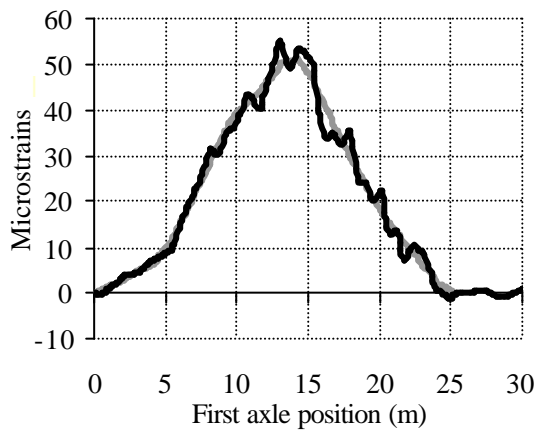
Figure 6.63 illustrates the results of the simulation for the lightest three-axle truck. In this model, transverse bending is more significant than longitudinal bending.



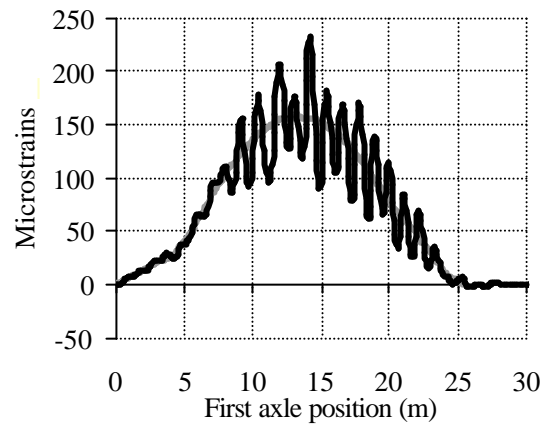
(a) 55 km/h, longitudinal strain



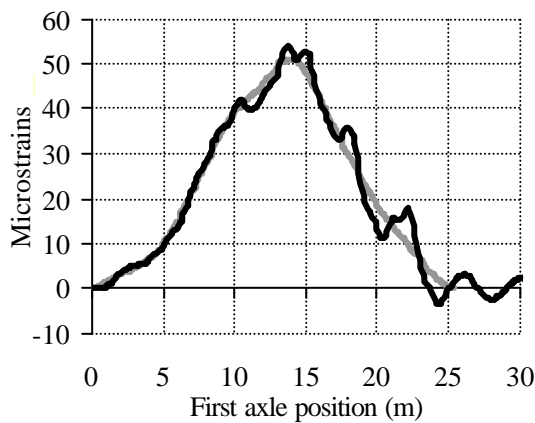
(b) 55 km/h, transverse strain



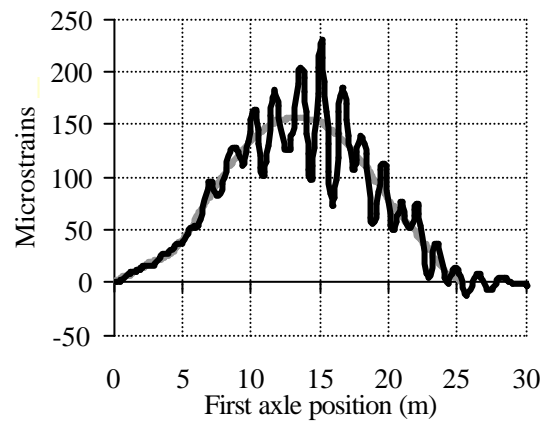
(c) 70 km/h, longitudinal strain



(d) 70 km/h, transverse strain



(e) 85 km/h, longitudinal strain



(f) 85 km/h, transverse strain

Figure 6.63 – Strain at midspan (sensor approx. in centre of slow lane)

Figure 6.64 represents the stress in a beam in a sensor located at 0.5 m from the plate element whose strain is shown in Figure 6.63. As expected, the longitudinal strain of Figure 6.63 and the stress in Figure 6.64 follow very similar patterns.

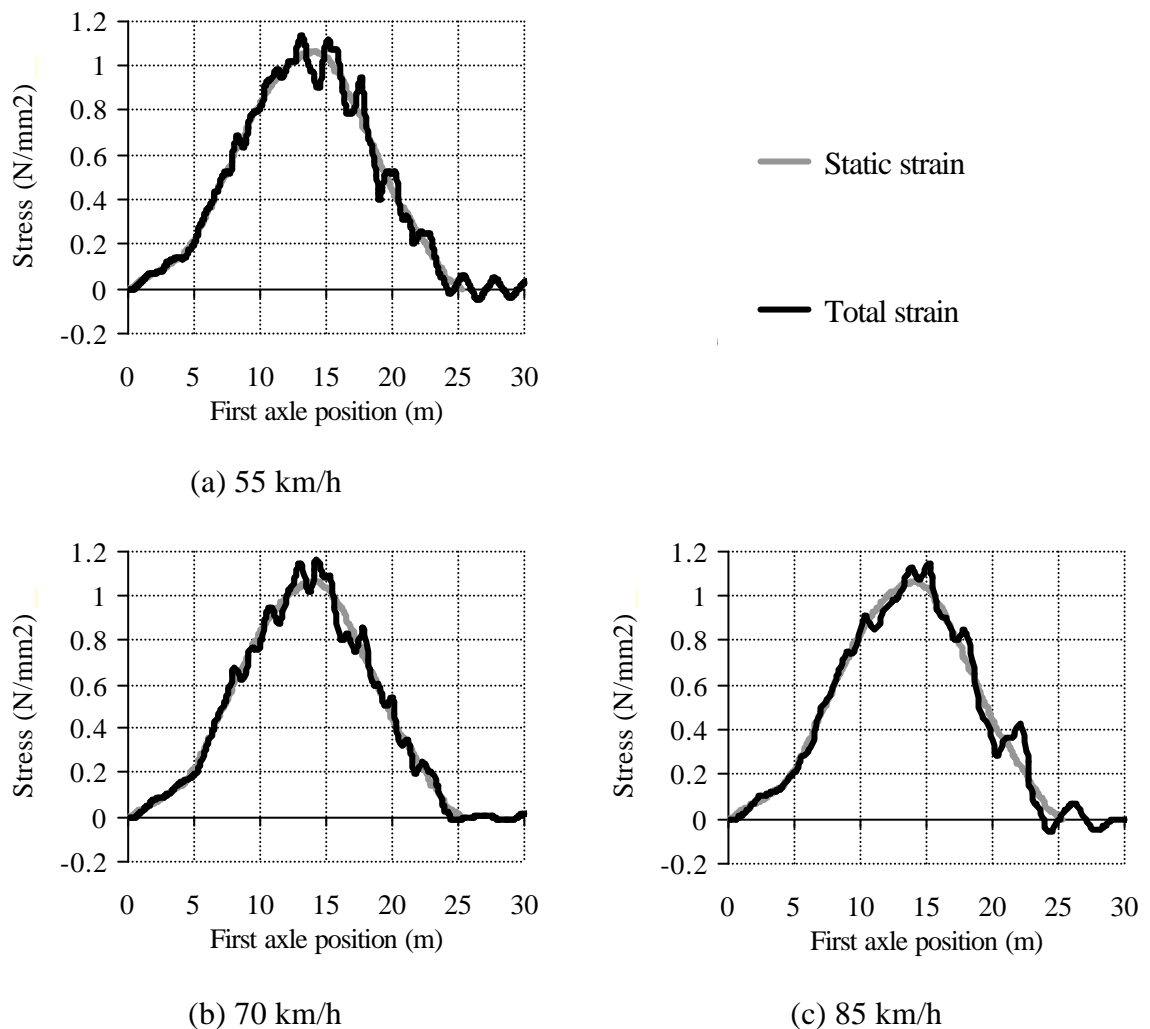


Figure 6.64 – Stress in beam at midspan (sensor in 2nd beam from section centre)

Figure 6.65 shows the spectra of Figure 6.63 for the case of 70 km/h speed. The differences between total and static are less in the case of transverse bending for frequencies below 5 Hz. The frequency components of the static response are more scattered in the case of longitudinal bending due to the ‘sharper’ shape of the influence line.

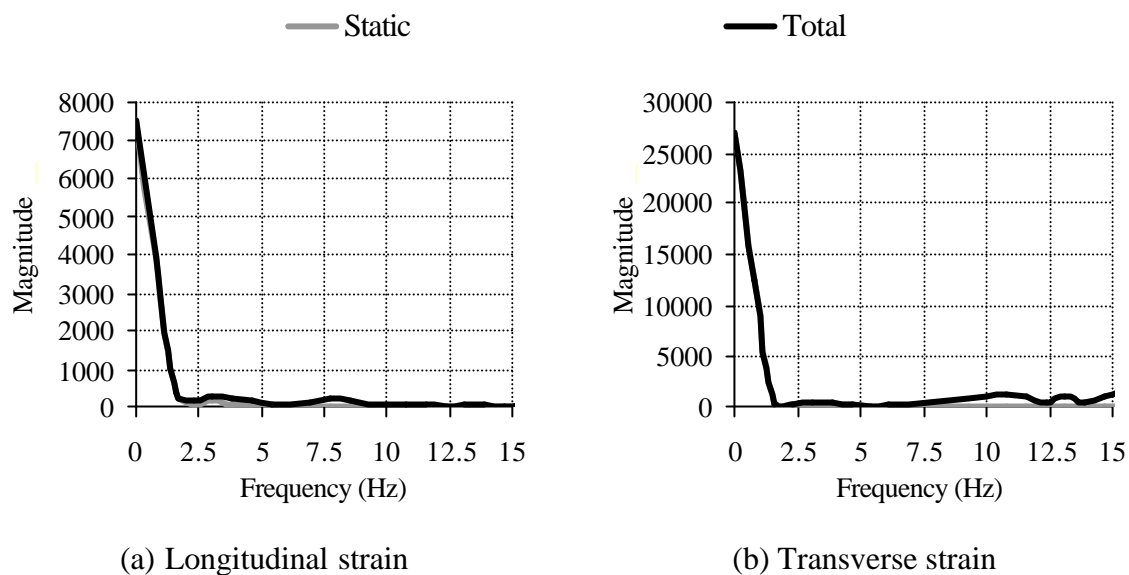


Figure 6.65 - Spectra of strain at midspan (sensor approx. in centre of slow lane)

6.5.6 Skew

Most of bridge decks built recently are likely to have some form of skew. These bridges are subjected to considerable torsion and the direction of maximum strain changes across the width from near parallel to span at the edge to near perpendicular to the abutment in central regions. A 45° skew model as shown in Figure 6.54 was analysed. The slab deck is 0.6 m in depth.

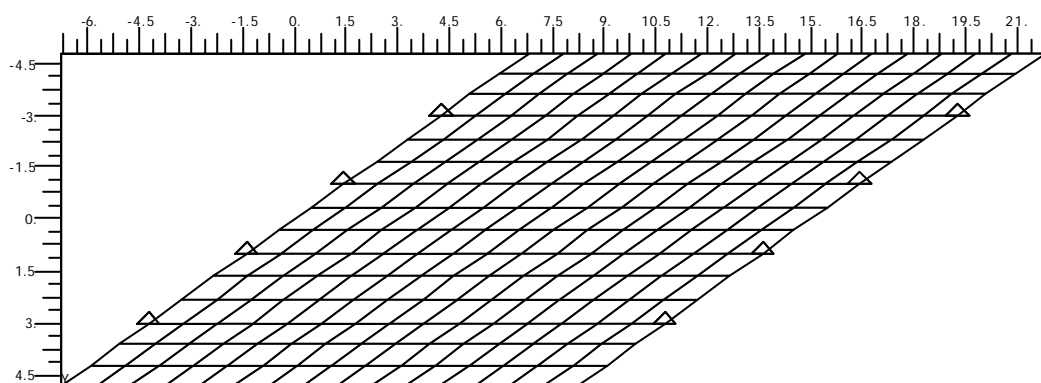


Figure 6.66 – Skew Bridge

The influence lines due to a unit axle on the slow lane are represented in Figure 6.67.

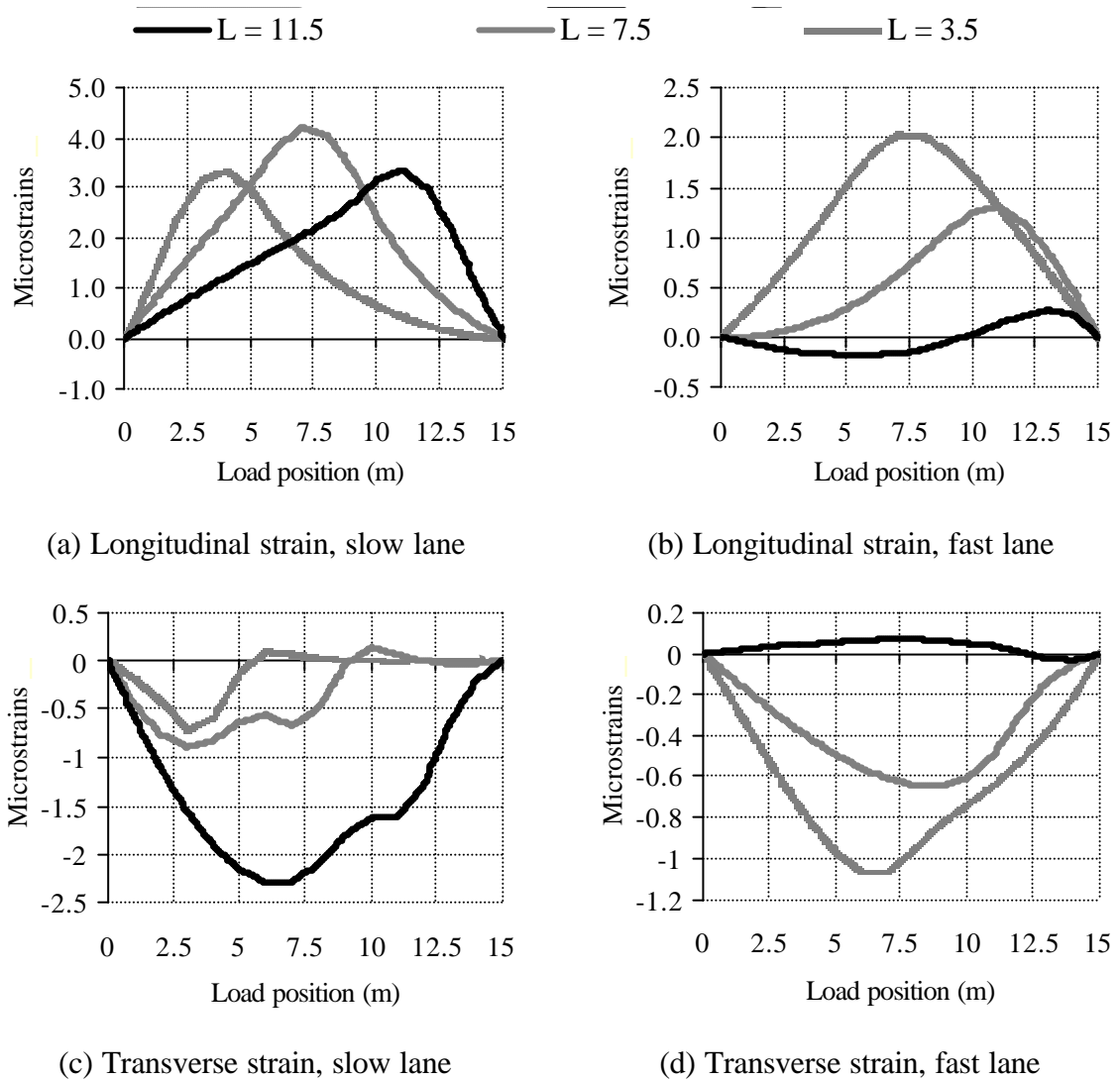


Figure 6.67 – Influence line of strain (L : longitudinal distance of the sensor from start of the bridge; transverse location from bridge centreline: 2.0 m)

The main modes of vibration are represented in Figure 6.68. The model was tested with a mesh based on triangular elements which gave the same modes of vibration.

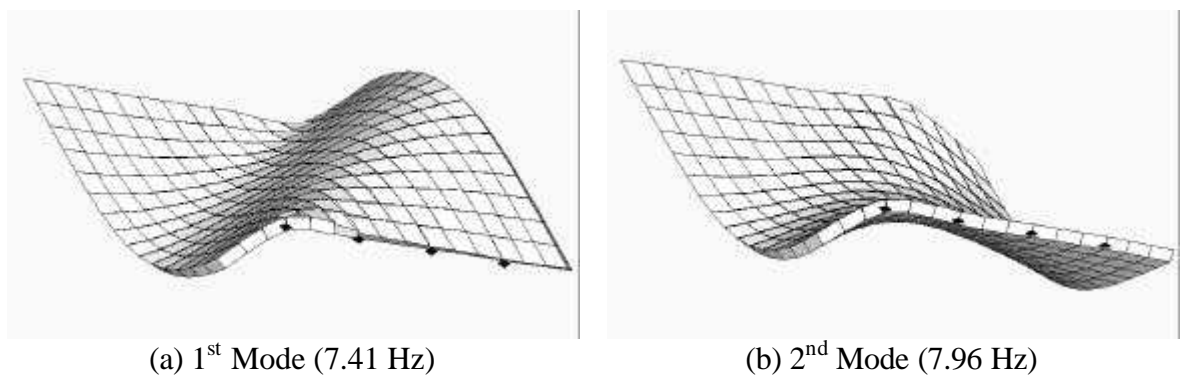
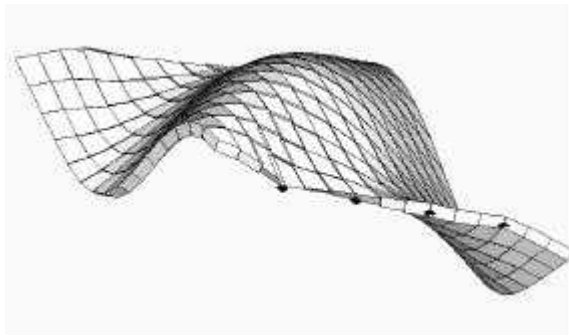
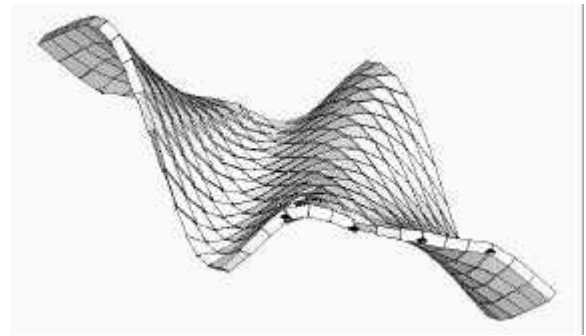


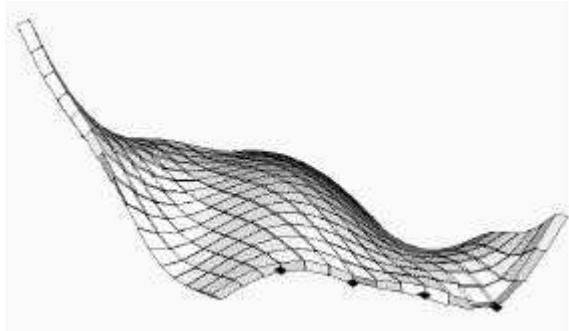
Figure 6.68 (continued on following page)



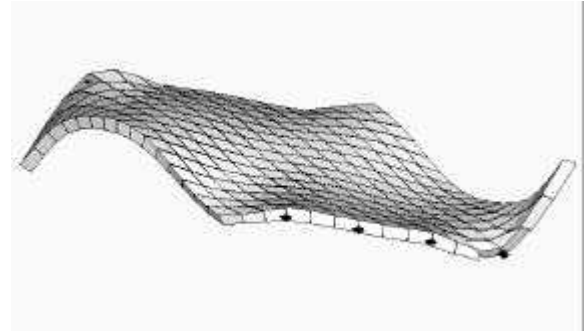
(c) 3rd Mode (19 Hz)



(d) 4th Mode (23.27 Hz)



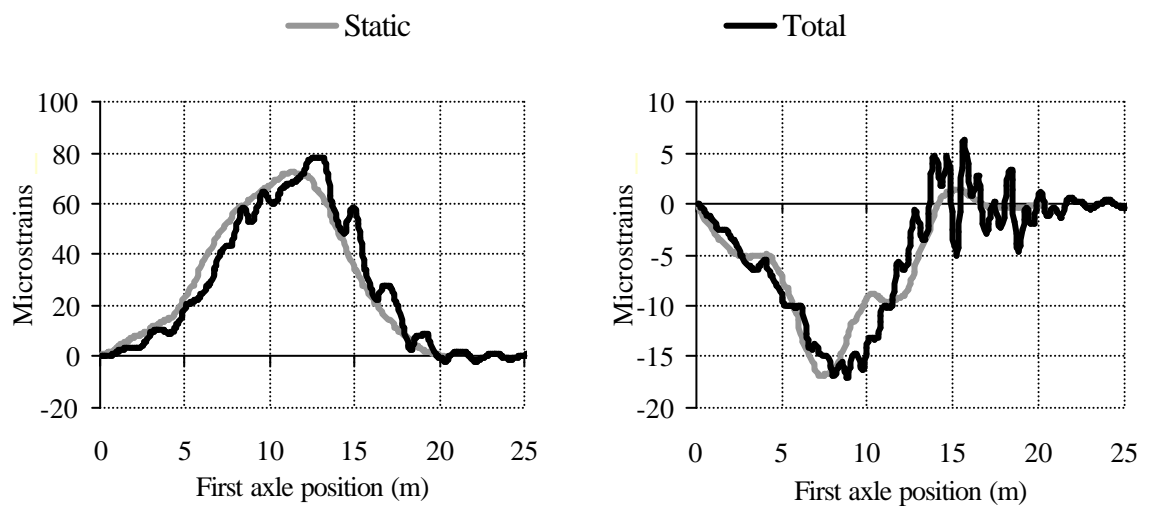
(c) 5th Mode (33.33 Hz)



(d) 6th Mode (35.34 Hz)

Figure 6.68 – Modes of Vibration of a Skew Bridge

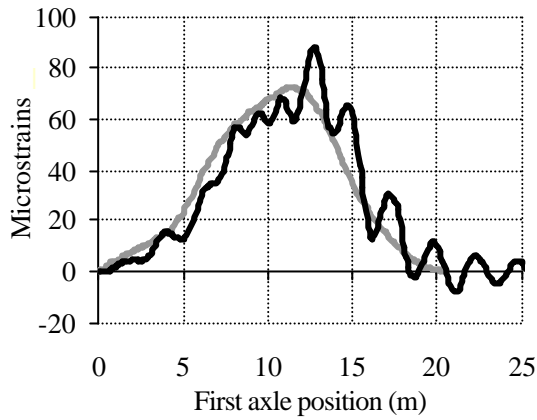
Results of simulations performed for a three-axle truck (22 t GVW) crossing the slow lane are illustrated in Figure 6.69.



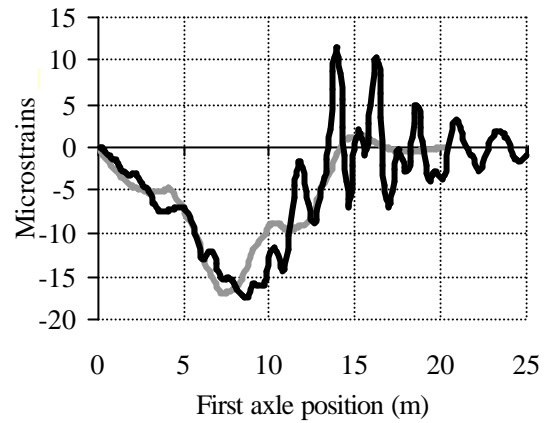
(a) 55 km/h, longitudinal strain

(b) 55 km/h, transverse strain

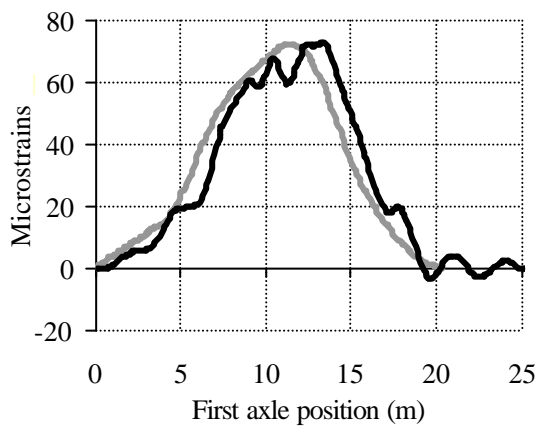
Figure 6.69 (continued on following page)



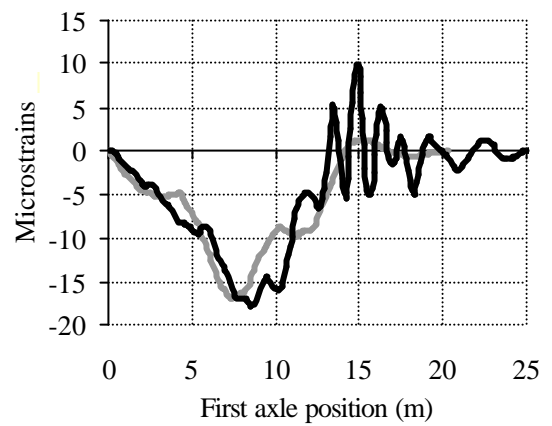
(c) 70 km/h, longitudinal strain



(d) 70 km/h, transverse strain



(e) 85 km/h, longitudinal strain



(f) 85 km/h, transverse strain

Figure 6.69 – Strain at midspan (sensor approx. in centre of slow lane)

The spectra of the previous figure are represented in Figure 6.70 for the 70-km/h run. The static response concentrates around a few harmonics of low frequency which interfere with dynamics below 5 Hz.

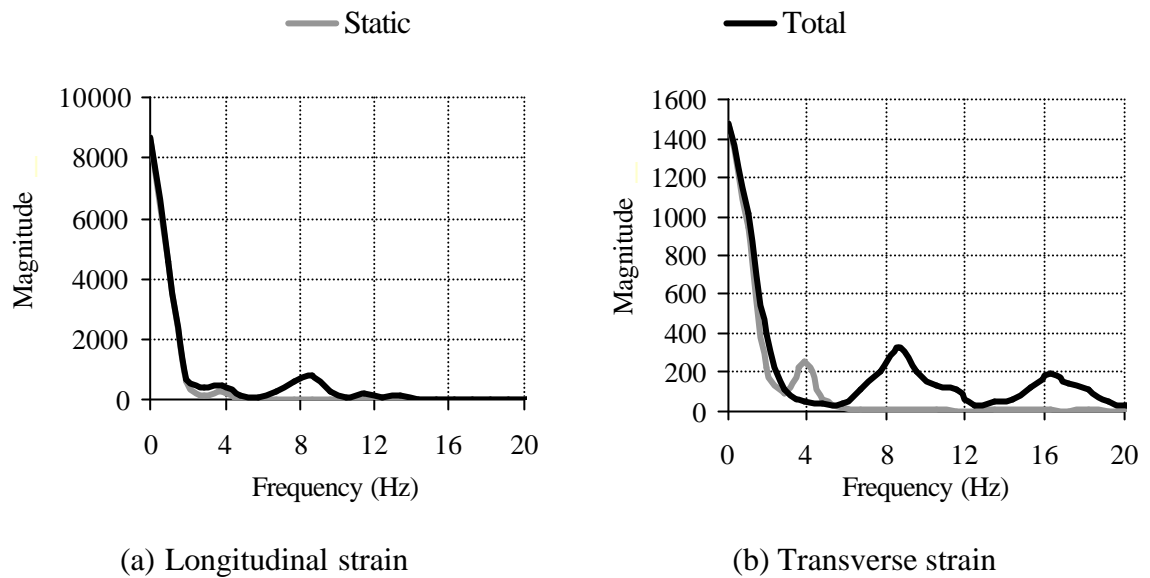


Figure 6.70 – Spectra of strain at midspan (sensor approx. in centre of slow lane)

6.5.7 Cellular

The cross-section of a cellular or box deck is made up of a number of thin slabs and thin or thick webs which totally enclose a number of cells. These complicated structural forms are commonly used in preference to beam and slab decks for spans in excess of about 30 m because, in addition to the low material content, low weight and high longitudinal bending stiffness, they have high torsional stiffnesses which gives them better stability and load distribution characteristics (Hambly 1991). A spatial model is used to represent a two-span, three-cell bridge deck with edge cantilevers. The cross-section is represented in Figure 6.71(a) and a general overview is given in Figure 6.71(b). Solid diaphragms 2 m thick are located at the end and central supports.

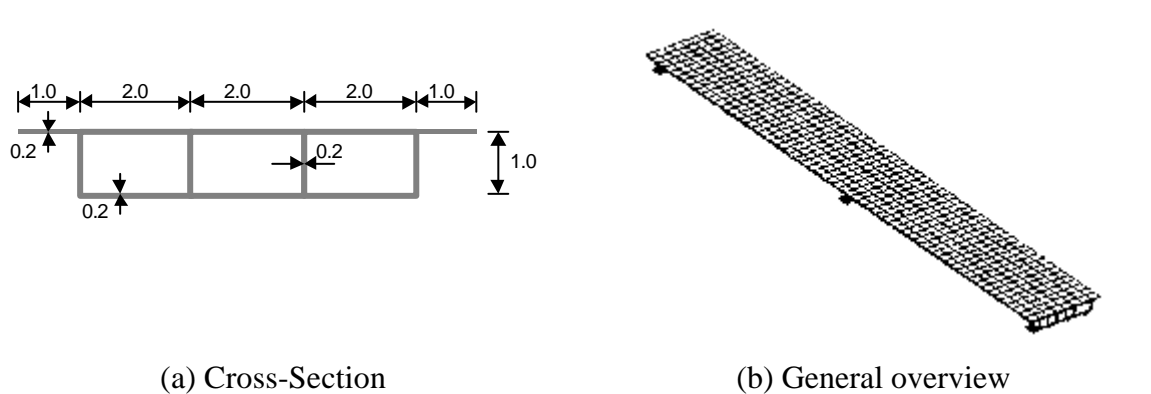
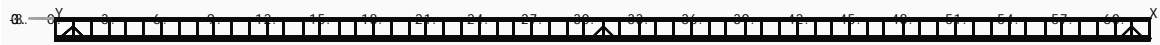
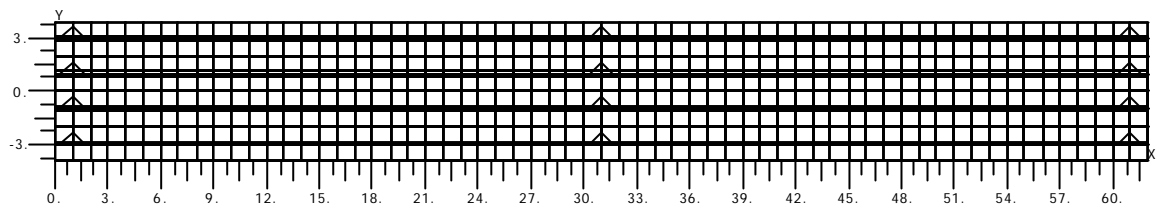


Figure 6.71 – Box Girder

The deck is supported transversely on a support under each. Dimensions and element composition are given in Figures 6.72(a) and (b).



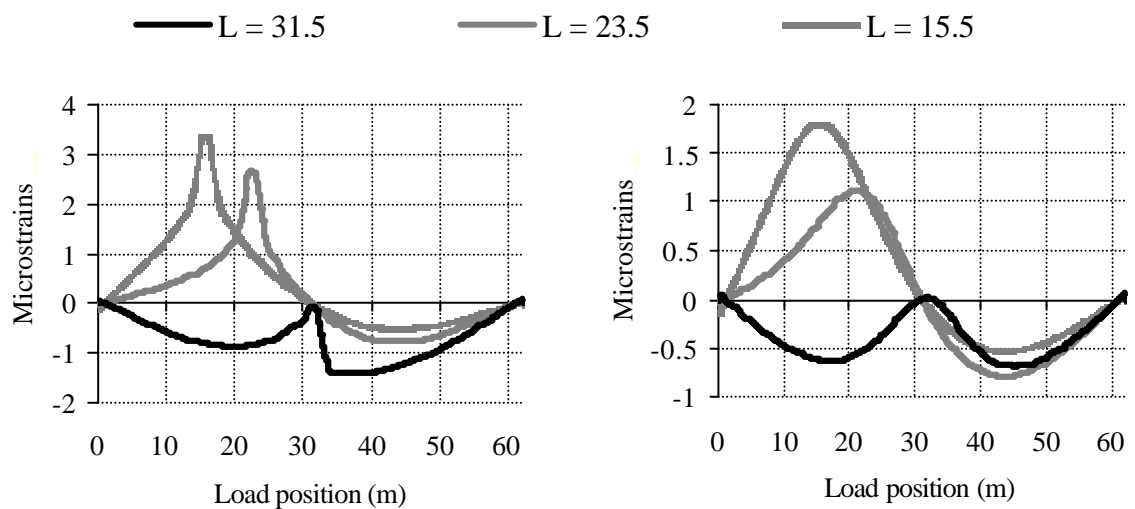
(a) Side view



(b) Plan view

Figure 6.72 – Finite element model of cellular bridge finite element

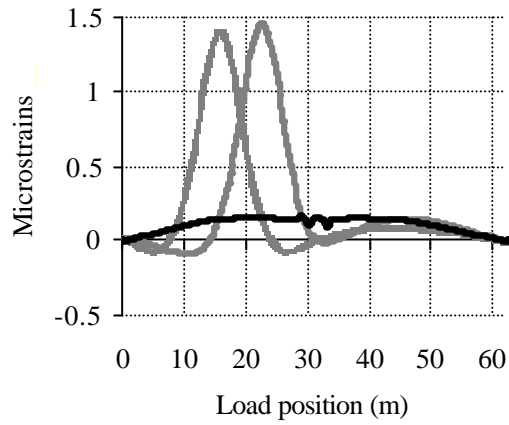
Influence lines are given in Figure 6.73 and dynamic characteristics in Figure 6.74.



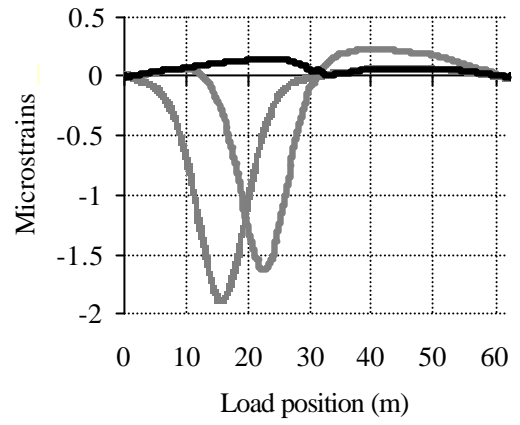
(a) Longitudinal strain, slow lane

(b) Longitudinal strain, fast lane

Figure 6.73 (continued on following page)

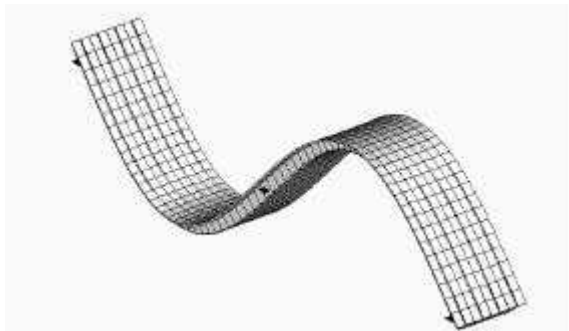


(c) Transverse strain, slow lane

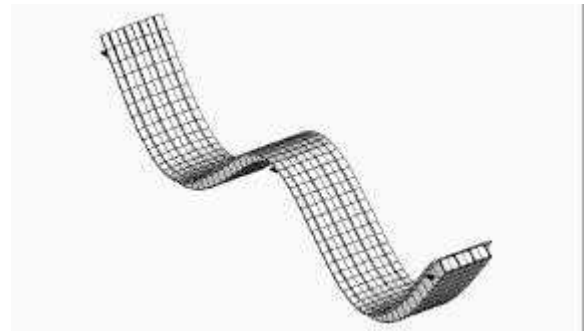


(d) Transverse strain, fast lane

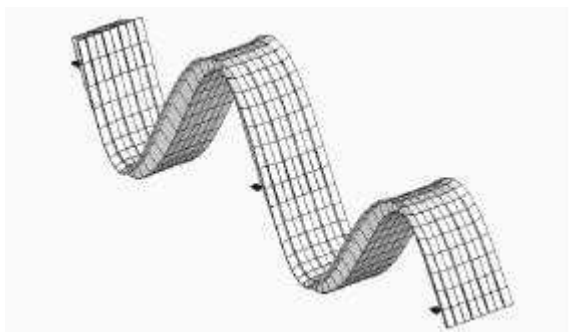
Figure 6.73 – Influence line of strain at the bottom plate (L : longitudinal distance of the sensor from start of the bridge; transverse location from bridge centreline: 2.5 m)



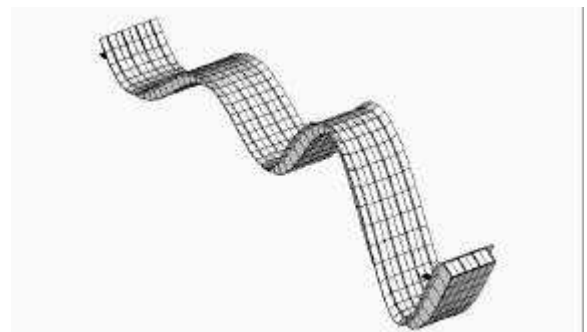
(a) 1st Mode (2.95 Hz)



(b) 2nd Mode (4.60 Hz)



(c) 3rd Mode (10.98 Hz)



(d) 4th Model (13.14 Hz)

Figure 6.74 (continued on following page)

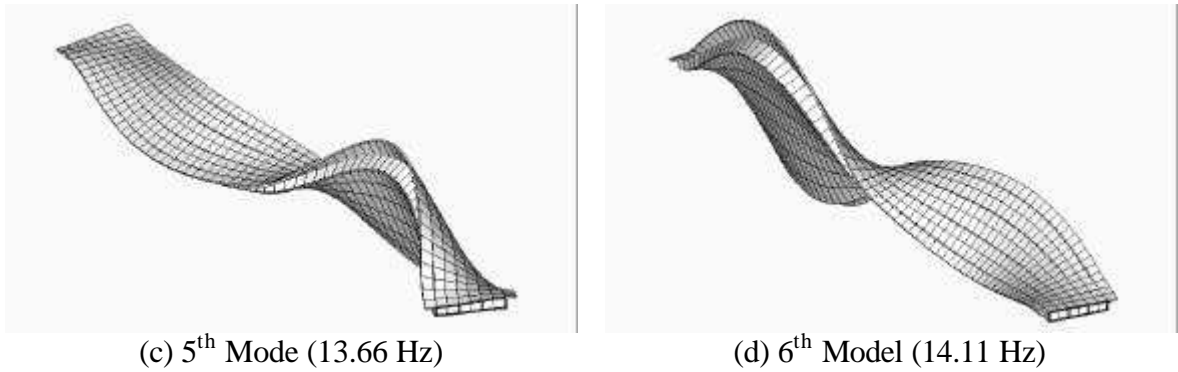


Figure 6.74 - Modes of vibration of Cellular Bridge

The dominant modes of vibration are in the longitudinal direction as shown in Figure 6.62. The longitudinal and transverse strain responses of the bridge under the crossing of a three-axle truck (22 t) over the slow lane are shown in Figure 6.75.

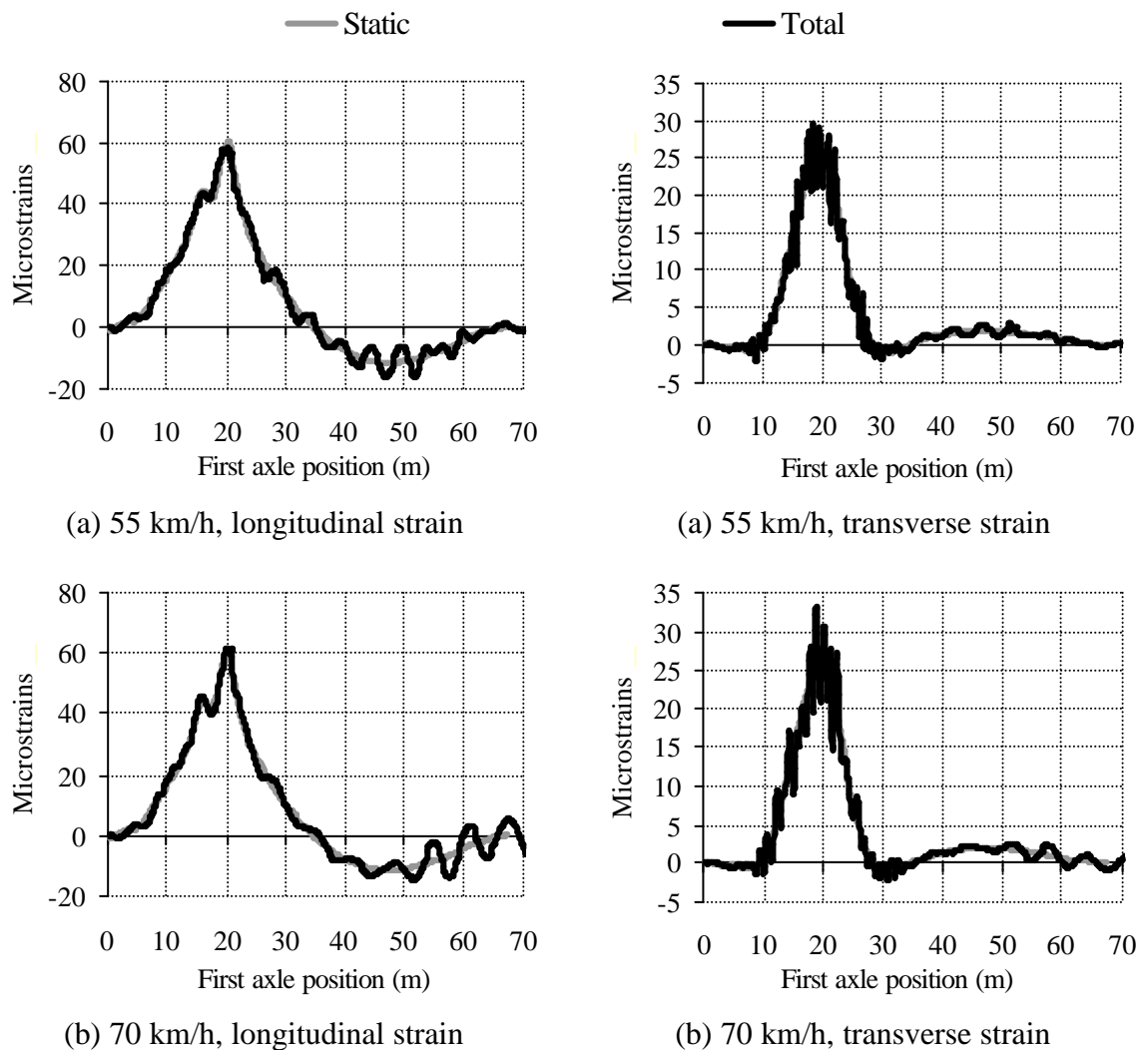
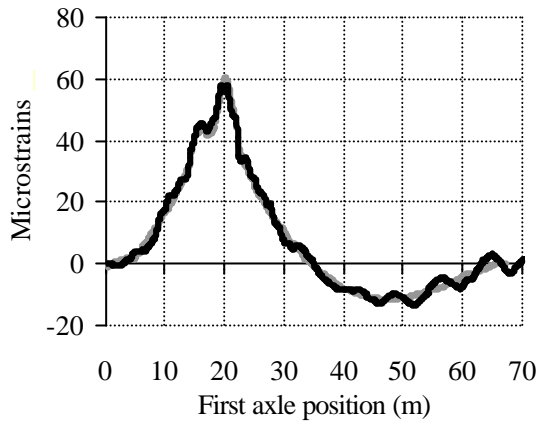
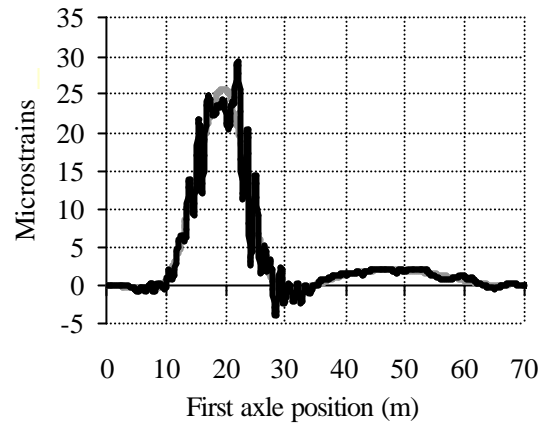


Figure 6.75 (continued on following page)



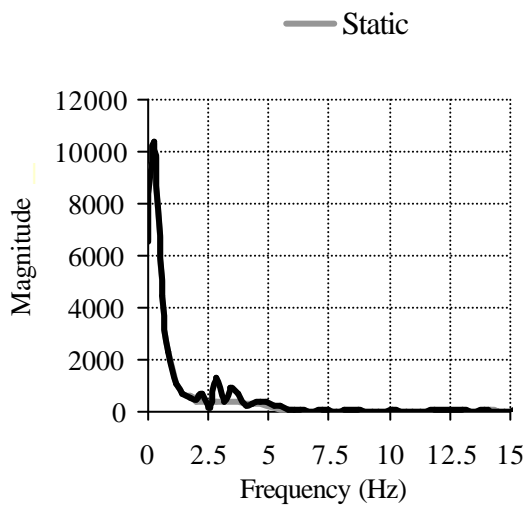
(c) 85 km/h, longitudinal strain



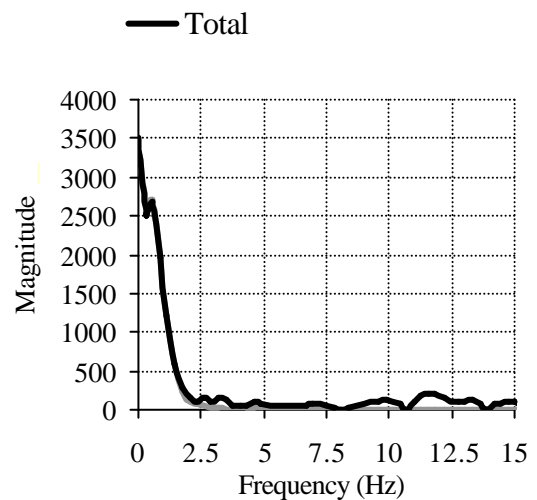
(c) 85 km/h, transverse strain

Figure 6.75 – Strain at midspan of first span (sensor approx. in centre of slow lane)

The spectra in Figure 6.76 correspond to the 70 km/h run of the previous figure. There are different dynamic frequency components interfering with the static response below 5 Hz (the first two modes of vibration of the bridge are below this frequency).



(a) Longitudinal strain

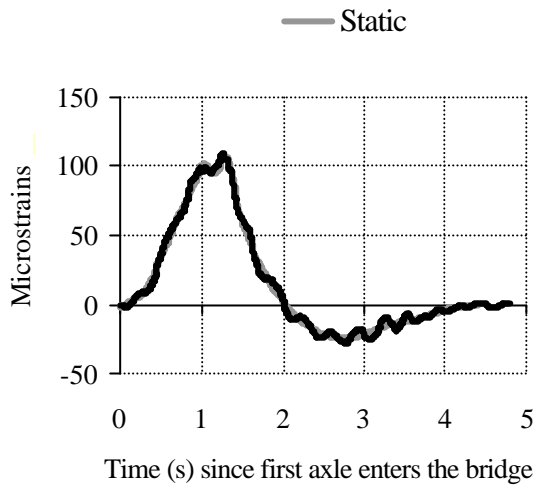


(b) Transverse strain

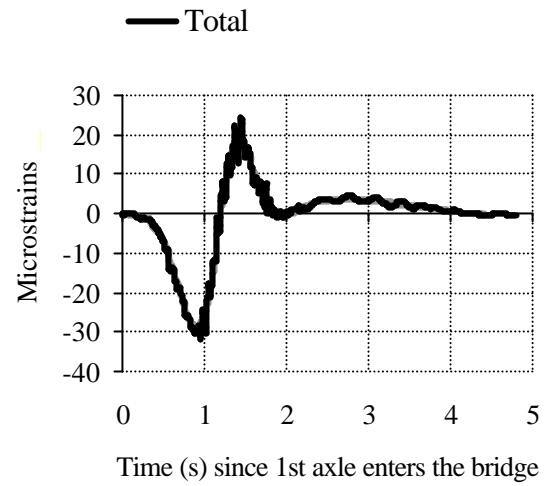
Figure 6.76 – Spectra of strain at midspan of first span (sensor approx. in centre of slow lane)

Simultaneous Traffic Events

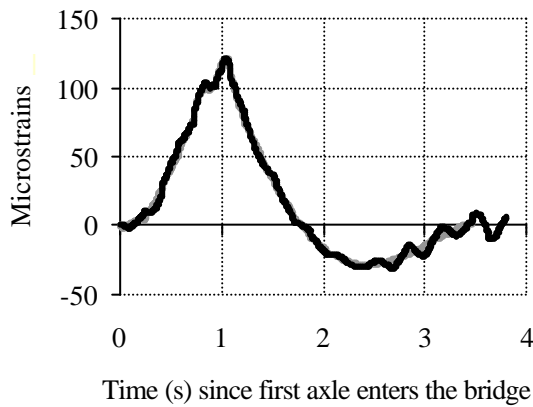
Figure 6.77 shows the bridge response for different speed combinations of a pair of three-axle trucks (27.43 t) running in the same direction but in different lanes.



(a) 55 (slow lane) and 70 km/h (fast lane),
longitudinal strain



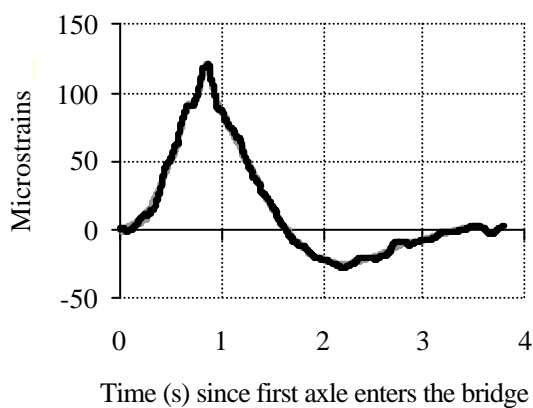
(b) 55 (slow lane) and 70 km/h (fast lane),
transverse strain



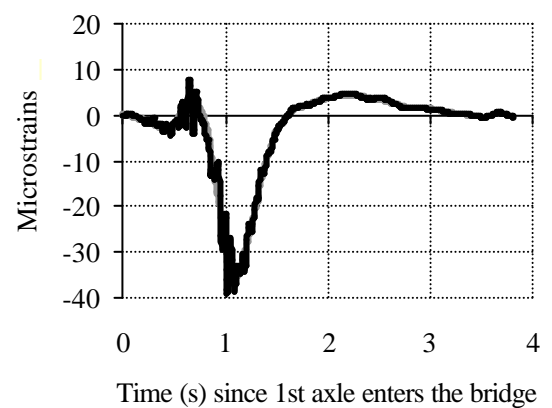
(c) Both at 70 km/h, longitudinal strain



(d) Both at 70 km/h, transverse strain



(e) 85 (slow lane) and 70 km/h (fast lane),
longitudinal strain



(f) 85 (slow lane) and 70 km/h (fast lane),
transverse strain

Figure 6.77 – Strain at midspan of first span (sensor approx. in centre of slow lane)

Long bridges are likely to have two or more heavy vehicles crossing at the same time and BWIM accuracy might decrease considerably. In the case of Figure 6.77, the longitudinal strain is quite close to the static, though the magnitude of the dynamic oscillation increases with time. Higher frequency components can be detected in the transverse direction due to the smaller stiffness.

6.6 CONCLUSIONS

There is a need to determine the influence of bridge and vehicle dynamics on B-WIM accuracy. Test trials can only measure a small number of parameters in the field and cover a small sample of bridges and vehicles. Accurate modelling of the bridge-truck dynamic interaction is required for further testing. In this chapter, a Lagrange multiplier technique has been used for the simulation of a vehicle passing over a bridge using finite element models. The formulation used by the author for the implementation of this technique has been described. An example has also been given of how to carry out the simulation in the MSc/NASTRAN environment.

Different bridge and truck finite element models have been built that will be used to test a number of B-WIM algorithms in Chapter 9. Road profile has been generated stochastically from a power spectral density function for ‘good’ conditions. Trucks are modelled as rigid frame bodies. Frame twist, body pitch, bounce and roll, axle hop and roll are taken into account. Two types of truck configuration (two- and three-axle) with three different loading conditions and three different speeds are used in simulations (limited reproducibility conditions – Appendix B).

Longitudinal and transverse strain has been calculated at different locations in seven bridges:

- Single span isotropic slab (16 m): Transverse bending is not significant. Longitudinal bending is sharper and higher in the lane crossed by the vehicle and more suitable for B-WIM purposes. The first natural frequency is 4.51 Hz (longitudinal) and dynamic oscillations around the static response are important, especially at higher speeds. The strain response at different transverse locations of the same section differs slightly. Strain has also been calculated for different transverse locations of the truck path (0, 1

and 2 m from bridge centreline). Strain results are higher at 70 km/h and at 2 m from the bridge centreline. When running two trucks simultaneously on the bridge, total strain does not exhibit high deviations from the static response.

- Two-span isotropic slab (37 m): Transverse strain is much smaller than longitudinal strain. Unlike the influence line for longitudinal bending of a location near midspan, the influence line at the central support has the same sign regardless of the truck location. Therefore, dynamics, only noticeable when the truck is in the second span, are less significant in the central support location than in other locations.
- Slab with edge cantilever (20 m): The shape of the influence lines is very similar to the isotropic single slab, except for transverse bending in the driving lane. However, vibrations are less significant than in the isotropic slab due to the greater bridge mass.
- Voided slab deck (25 m): Static response is similar to the preceding slab with edge cantilever, but the mass per unit length is much smaller. The first natural frequency is 3.80 Hz and the total strain oscillates around the static component with significant amplitude.
- Beam and slab (20 m): The same level of dynamics appears for beam and longitudinal bending of the slab. A new possibility arises for this type of structural system: the measurement of transverse bending of the slab, of higher magnitude than the corresponding longitudinal bending. Dynamics of transverse strain have high amplitudes, but they oscillate with a higher frequency than longitudinal strain.
- Skew (15 m): In this 45° skew bridge, though the first natural frequency is relatively high (7.41 Hz), total strain shows a significant deviation from the expected static response.
- Cellular (62 m): This two-span continuous bridge is the longest and has the smallest first natural frequency (2.95 Hz) of all models being analysed. The influence line for longitudinal strain is less pronounced than for transverse bending. The first two mode shapes are longitudinal (unlike for the single span bridges under study, while the second mode of vibration is torsional), but these low frequency dynamic components have little importance in the total longitudinal strain until the vehicle reaches the second span. When calculating strain due to two trucks crossing the bridge simultaneously, the dynamic component is negligible compared to the static component.